COMPUTATIONAL STUDIES ON GROUP 14 ELEMENTS (C, Si AND Ge) IN ORGANOMETALLIC AND BIOLOGICAL COMPOUNDS

Liwen Yu, B.S., M.S.

Dissertation Prepared for the Degree of

DOCTOR OF PHILOSOPHY

UNIVERSITY OF NORTH TEXAS

May 2007

APPROVED:

Martin Schwartz, Major Professor
Paul Marshall, Committee Member
Thomas Cundari, Committee Member
Mohammad Omary, Committee Member
Bill Poirier, Committee Member
Ruthanne Thomas, Chair of the Department of Chemistry
Sandra L. Terrell, Dean of the Robert B. Toulouse School of Graduate Studies

Yu, Liwen. Computational studies on Group 14 elements (C, Si and Ge) in organometallic and biological compounds. Doctor of Philosophy (Physical Chemistry), May 2007, 117 pp., 22 tables, 33 illustrations, references, 183 titles.

A series of computational studies were carried out on Group 14 (C, Si and Ge) elements in organometallic and biological compounds. Theoretical studies on classical and H-bridged $A_3H_3^+$ (A=C, Si and Ge) as π ligands with different organometallic fragments at B3LYP and B3P86 level reveal a reverse charge transfer from ligand to metal in Si and Ge complexes whereas in C complexes there is a small charge transfer from metal to ligand. The H-bridged complexes are more stable than the complexes based on $Si_3H_3^+$ and $Ge_3H_3^+$ ligands with terminal hydrogens. The stability of the bridged systems increases from Si to Ge. Corrective scale factors for computed harmonic C≡O vibrational frequencies for 31 organometallic complexes have been determined at the HF and B3LYP levels. The scaled B3LYP frequencies exhibit a greater reliability than do HF frequencies. Experimental data have shown that Si/Ge-substituted decapeptides are advantageous over their C analog *in vitro* and *in vivo* studies in modern hormone therapy. A computational investigation was carried out on the synthesized decapeptides focusing on position 5 containing Si and Ge. The results have shown that there are some differences in C, Si and Ge-containing analogs. However, further investigations are needed to elucidate the observed advantages of Si/Ge over C analogs.

ACKNOWLEDGMENTS

I would like to thank Dr. Martin Schwartz and Dr. Gantasala Srinivas for their kind and enormous help to make this work possible. I also would like to thank Welch Foundation for the funding.

TABLE OF CONTENTS

LIST OF TABLES

Page

LIST OF ILLUSTRATIONS

Page

CHAPTER 1

INTRODUCTION

In this study, a series of computational investigations were carried out on Group 14 (C, Si and Ge) elements in organometallic and biological compounds. The results of three different projects were presented in this writing and some of the results have already been published in journal publications. The projects include:

1. (Chapter 3) Theoretical studies on classical and H-bridged $A_3H_3^+$ (A=C, Si and Ge) as π ligands in organometallic chemistry.

η^3 π complexes of $A_3H_3^+$ (A=C, Si and Ge) with different organometallic fragments have been studied at B3LYP and B3P86 levels. In Si and Ge complexes there is a ligand to metal charge transfer whereas in C complexes there is a small charge transfer from metal to ligand. These remarkable differences in electronic structure between C and its heavier analogs are explained using molecular orbitals and natural charges. All the π complexes for Si and Ge are considered viable target for synthetic pursuit [1]. Organometallic complexes based on H-bridged $Si_3H_3^+$ and $Ge_3H_3^+$ were also studied with different organometallic fragments at B3LYP and B3P86 levels. The H-bridged complexes are more stable than the complexes based on $Si_3H_3^+$ and $Ge_3H_3^+$ ligands with terminal hydrogens. The stability of the bridged systems increases from Si to Ge [2].

2. (Chapter 4 and 5) Scale factors for C≡O vibrational frequencies in organometallic complexes [3].

Corrective scale factors for computed harmonic C≡O vibrational frequencies for 31 organometallic complexes have been determined at the HF and B3LYP levels.

Although the generic scale factor available in the literature [4] for B3LYP/6-31G(d) worked well for metal carbonyl frequencies, the HF scale factors are substantially lower than earlier proposed general values. The scaled B3LYP frequencies exhibit a greater reliability than do HF frequencies. Both of these features can be attributed to the ability of the former method to account for the high degree of electron correlation in triply bonded CO and its variation with bonding environment.

3. (Chapter 6) A computational study on C/Si/Ge bioisosterism.

Si- and Ge-substituted decapeptides have shown some biological and pharmacological advantages over their C analogs in *vitro* and *in vivo* studies in modern hormone therapy. A computational investigation was carried on the synthesized decapeptides focusing on the Si/Ge-containing residue at position 5 of decapeptides. The results have shown that there are some differences in C, Si and Ge-containing analogs, however, no definitive conclusions can be drawn at this point. Further investigations including molecular mechanics (MM) and molecular dynamic (MD) need to be carried out for explanation.

Chapter References

1. Srinivas G. N., Yu L., Schwartz M., *Organometallics* 2001, *20*, 5200
2. Srinivas G. N., Yu L., Schwartz M., J*. Chem. Soc. Dalton Trans.* 2002, 1857
3. Yu L, Srinivas G. N., Schwartz M., *J. Mol. Struct. (Theochem)* 2003, *625*, 215
4. Scott A. P., Radom L., *J. Phys. Chem.* 1996, *100*, 16502

CHAPTER 2

THEORETICAL BACKGROUND

Introduction

Two types of electronic structure computational methods were used in this study: Ab Initio [1-2] and density functional theory (DFT) [3-5] calculations. These methods have been widely used in chemistry and have proven to be competitive with experimental chemistry to predict the structures and properties of chemical systems [6-10].

Electronic structure methods use the laws of quantum mechanics as the basis for their computations [11-13]. Quantum mechanics states that the energy and other related properties of a molecule may be obtained by solving the Schrödinger equation [14]:

$$H\Psi = E\Psi \tag{1.1}$$

Here H is the Hamiltonian operator representing the total energy. E is the numerical value of the energy of the state, that is, the energy relative to a state in which the constituent particles (nuclei and electrons) are infinitely separated and at rest. Ψ is the wavefunction that completely describes the corresponding system. A wavefunction depends on the Cartesian coordinates of all particles and on the spin coordinates. Ψ^2 (or $|\Psi|^2$ if Ψ is complex) is interpreted as the probability distribution of the particles within the molecule. Once the wavefunction is known for a particular state of a system then any physical observable, such as energy and electron density, etc, may in principle be determined [5].

The Hamiltonian operator H is made up of kinetic and potential energy terms:

$$H = T + V \tag{1.2}$$

The kinetic operator T is a sum of differential operators:

$$T = - \frac{-h^2}{8\pi^2} \sum_i \frac{1}{m_i} \left(\frac{\partial^2}{\partial x_i^2} + \frac{\partial^2}{\partial y_i^2} + \frac{\partial^2}{\partial z_i^2} \right) \tag{1.3}$$

The sum is over all particles i (nuclei+ electrons) and m_i is the mass of particle i, and *h* is Planck's constant. The potential operator is the Coulomb repulsion between each pair of charged entities:

$$V = \sum_{i<j} \sum \left(\frac{e_i e_j}{r_{ij}} \right) \tag{1.4}$$

The sum is over distinct pairs of particles (i, j) with electric charges e_i, e_j separated by a distance r_{ij}.

In order to solve the Schrödinger equation, one has to use two approximations without, hopefully, significantly changing the results. The Born-Oppenheimer approximation [11] is the first one to simplify the general molecular problem by separating nuclear and electronic motions. It has been proved valid since the mass of a typical nucleus is thousands of times greater than that of an electron, therefore the nuclei move very slowly relative to the electrons. This approximation implies that the electron distribution depends only on the instantaneous positions of the nuclei and not on their velocities. This allows chemists to solve the wavefunction for electron motion in the field of "fixed" nuclei first, leading to an effective electronic energy called the "potential surface" [12] of the molecule. This effective energy is then used as potential energy for a subsequent study of the nuclear motion, thus, yielding the total energy of the system and the final solution to the wavefunction. The wavefunction can now be expressed as in the form

$$\Psi = \Psi_{el}\Psi_{nucl.} \quad (1.5)$$

Thus the wavefunction of electrons and nuclei can be solved separately:

$$H_{el}\Psi_{el} = E_{el}\Psi_{el} \quad (1.6)$$

$$H_{nucl}\Psi_{nucl} = E_{nucl}\Psi_{nucl} \quad (1.7)$$

However, introduction of the Born-Oppenheimer approximation alone does not permit exact analytical solution of equation (1.7) exactly except for the hydrogen molecule ion, H_2^+. In order to obtain reliable information about the electronic structure of molecules with the use of much less computational effort, another approximation, called the one-electron function (or orbital [13]) has been introduced. A one-electron orbital, χ (x, y, z, ξ) is a mathematical function of the Cartesian coordinates x, y, z and spin coordinate of a single electron. Functions containing both the cartesian and spin coordinates are also called spin orbitals. The combination of two one-electron spin orbitals with the same Cartesian coordinates but different spin coordinates is called a molecular orbital, φ. The wavefunction for a many electron system can now be simulated using one-electron orbitals according to molecular orbital theory in the following form:

$$\psi_{el} = \chi_1(1)\,\chi_2(2)\chi_3(3)\ldots\,\chi_n(n) \quad (1.8)$$

or $$\psi_{el} = \varphi_1\alpha(1)\beta(2)\varphi_2\alpha(3)\beta(4)\ldots\varphi_{n/2}\alpha(n-1)\beta(n) \quad (1.9)$$

α and β are two spin functions defined as follows [15]:

$$\alpha(\uparrow) = 1 \qquad \alpha(\downarrow) = 0$$

$$\beta(\uparrow) = 0 \qquad \beta(\downarrow) = 1 \quad (1.10)$$

The α function is 1 for a spin up electron, and the β function is 1 when the electron is spin down. In order to ensure the exclusion principle requirements for the wavefunction,

it is necessary to arrange the spin orbitals in some other more complicated way such as a Slater determinant [16]. For the general case of N electrons and N spin orbitals, a Slater determinant is given as

$$\Phi_{SD} = \frac{1}{\sqrt{n!}} \begin{vmatrix} \phi_1(1)\, \phi_2(1) \ldots\ldots \phi_n(1) \\ \phi_1(2)\, \phi_2(2) \ldots\ldots \phi_n(2) \\ \ldots\ldots \quad \ldots\ldots \quad \ldots\ldots \quad \ldots\ldots \\ \phi_1(n)\, \phi_2(n) \ldots\ldots \phi_n(n) \end{vmatrix} \tag{1.11}$$

In the one-electron approximation, the trial wavefunction is assumed to consist of a single Slater determinant. Such approximation implies the electron correlation is neglected or the electron-electron repulsion is only included as an averaged effect; as will be discussed in the following pages (Computational Methods).

Computational Methods

Hartree-Fock Theory

In the Hartree-Fock (HF) [17-18] method, the many electron wavefunction is assumed to have the form of a Slater determinant. It does not adequately take account of the correlation between motions of electrons. In particular, single-determinant wavefunctions take no account of correlation between electrons with opposite spin. Correlation of the motions of electrons with the same spin is partially, but not completely, accounted for by virtue of the determinant form of the wavefunction. These limitations lead to calculated energies above the exact values. The difference between the Hartree-Fock energy and the exact non-relativistic energy is the correlation energy,

E(exact) = E (Hartree-Fock) + E (correlation)

Thus, the accuracy of a Hartree-Fock result is limited by neglect of the correlation energy, and computational results using Hartree-Fock theory can not explain some chemical phenomena for which correlation effects are significant. Using a complete configuration interaction (CI) method can usually solve the problem. If the Hartree-Fock solution wavefunction is

$$\psi_o = (n!)^{-1/2} |\varphi_1\varphi_2\ldots\varphi_n| \tag{2.1}$$

then by mixing virtual orbitals with occupied orbitals, a complete wavefunction can be generated:

$$\psi = a_o\phi_o + \sum a_s\phi_s \tag{2.2}$$

The new wavefunctions φ_s are made from substituting virtual orbitals for occupied orbitals and "s" represents all the possible orbital substitutions. Full CI is the best representation of a wavefunction, but it is usually not practical because of the large number of determinants.

Møller-Plesset perturbation theory (MP) [19] is one of the practical approaches for incorporating electron correlation. In this method, the total Hamiltonian operator is treated as the sum of two parts, the second a perturbation of the first:

$$H_\lambda = H_0 + \lambda V \tag{2.3}$$

Here, H_0 is an operator such that the matrix representation is diagonal.

$$\int\ldots\int\psi_s H_0 \psi_t d\tau_1 d\tau_2 \ldots d\tau_n \tag{2.4}$$

The assumption that V is a small perturbation to H_0 suggests that the perturbed wavefunction and energy can be expressed as a power series in V. The usual way to do so is in terms of the parameter λ:

$$\psi = \psi^{(0)} + \lambda\psi^{(1)} + \lambda\psi^{(2)} + \lambda\psi^{(3)}\ldots \tag{2.5}$$

$$E = E^{(0)} + \lambda^1 E^{(1)} + \lambda^2 E^{(2)} + \lambda^3 E^{(3)} \ldots \quad (2.6)$$

Practical correlation methods can now be formulated by setting the parameter λ equal to 1, and by truncation of the series to various orders. These methods are referred to as MP2, MP3, MP4 and so on corresponding to the order of truncation of the energy terms.

Density Functional Theory

Density functional theory (DFT) is also a member of the series of electronic structure methods. The basis of DFT theory was proved by Hohenberg and Kohn [20] about three decades ago. It states that there exists a one-to-one relationship between the electron density and the energy of a system. The goal of DFT methods is to design the functional, which connects the energy with the electron density, ρ [21].

The DFT functional divides the electronic energy into several terms:

$$E = E^T + E^V + E^J + E^{XC} \quad (2.7)$$

E^T - Kinetic energy term, arising from the motions of electrons.

E^V - Potential energy term, arising from nuclear-electron attraction and nuclear-nuclear repulsion.

E^J - Electron-electron repulsion term, also described as the Coulomb self-interaction of the electron density.

E^{XC} - Exchange-correlation term, describing the remaining part of the electron-electron interaction.

All the terms above are functions of the electron density, ρ, except for nuclear - nuclear repulsion. E^{XC} is a unique term. It replaces the exact exchange for a single

determinant in HF with a more general expression, the exchange-correlation functional E^{XC}, which includes the electron correlation to account for both exchange energy (E^x) and the electron correlation (E^c) that is omitted in HF theory (Ec=0). The E^{XC} term is usually separated into two parts, the exchange part, E^x, and the correlation part, E^c, corresponding to same-spin and mixed-spin interactions, respectively.

$$E^{XC}(\rho) = E^x(\rho, \nabla\rho) + E^C(\rho, \nabla\rho) \tag{2.8}$$

Both the exchange part E^x and the correlation part E^c can be of two distinct types: local functionals, which depends only on the electron density, ρ, and gradient-corrected functionals, which depends on both the electron density, ρ, and its gradient, $\nabla\rho$, respectively. The specific correlation energy is not known analytically. However, approximations of increasing accuracy have been developed [22,23]. Recently Vosko, Wilk and Nusair (VWN) constructed the results from Monte Carlo methods to make them suitable for the DFT calculations [24].

Pure DFT methods are defined as pairing an exchange functional with a correlation functional. For example, BLYP is a well-known pure DFT method, which pairs Becke's gradient-corrected exchange functional with the gradient-corrected correlation functional of Lee, Yang and Parr (LYP). Hybrid DFT methods are a counterpart of pure DFT methods. They makes an exact connection between the exchange-correlation energy and the corresponding potential, which connects the non-interacting reference and the actual system.

In the past few years, DFT methods have gained steadily popularity and have been applied extensively to many problems which were previously solved by ab initio Hartree-Fock methods. In practice, a DFT calculation involves similar efforts to those

required for an ab initio Hartree-Fock (HF) calculation, whose computational efforts both scale as N^4 (N stands for the number of basis functions). Just like HF methods, increasing the size of the basis set allows for better results for DFT. Despite the similarities between DFT and HF methods, DFT methods can possibly achieve greater accuracy than HF methods at almost the same cost. Such an advantage is due to the fact that DFT methods include some effects of electron correlation, ignored in HF calculation, at a much lower computational cost than traditional correlated methods, such as MP2 and QCISD, do. The advantage of DFT methods to traditional methods is more obvious when used on larger molecular systems and heavy-atom molecules.

However, DFT is a comparatively new method to the field of computational chemistry. It only has about a 30-year-history so far, while the conventional quantum methods have been used for 70 years. Various new functionals and methodologies need to be developed. Currently, there is no known systematic way to judge the quality of new functionals, and the calibration system for DFT methods is less developed. Therefore, certain cautions should be taken to judge the performance of DFT methods. The results need to be compared with experimental data or higher level ab initio methods to evaluate the calculation quality.

Basis Sets

Introduction

Almost all theoretical calculations use a basis set expansion to express the unknown molecular orbital (MO) in terms of a set of known functions to solve the Schrödinger equation. A basis set is a mathematical description of the orbitals within a

system (which in turn combine to approximate the total electronic wavefunction) to perform the theoretical calculation. The molecular orbitals Ψ_i can be expressed as a linear combination of N nuclear-centered basis functions χ_μ (μ=1,2,…,N) (also referred to as atomic orbitals, AO),

$$\Psi_i = \sum_{\mu}^{N} c_{\mu i} \chi_\mu \qquad (3.1)$$

Eq. 3.1 can be an exact relationship if the basis set is complete, which means that an infinite number of basis functions are being used. This is entirely impossible in actual calculations. Larger basis sets give more accurate approximations of the orbitals but require greater computational efforts, and smaller basis sets lead to poorer representations at lower expense. It implies that some compromises need to be made between computational cost and accuracy. It is important to make the basis sets as small as possible while not sacrificing the accuracy in calculations. The type of basis function also influences the accuracy. The functions should be physically meaningful and with integrals which are easy to calculate.

There are two major types of basis functions: Slater type orbitals (STO) [16] and Gaussian type orbitals (GTO) [25]. Comparing these two, GTOs are less satisfactory than STOs because GTOs represent improper behavior near the nucleus. However STOs are much more complicated in numerical computations, which make them unsuitable for practical calculations, while all integrals in the computations of GTOs can be evaluated easily.

Therefore a procedure that has come into wide use is to fit a STO to a linear combination of primitive Gaussian functions, which couples the ease of calculation of integrals involving GTOs with the improved physical behavior of STOs.

$$\chi_\mu = \sum_p d_{\mu p} g_p \qquad (3.2)$$

where $d_{\mu p}$'s are fixed constants and g_p's are primitives.

Basis functions which have the above form are referred to as "contracted functions." A basis function consisting only of a single Gaussian function is defined as uncontracted.

Different Types of Basis Sets

Minimal Basis Sets

Minimal basis sets use fixed-size atomic-type orbitals and only employ the minimum number of functions to contain all the electrons in the neutral atoms.

STO-3G is a minimal basis set. A minimal basis set only contains a single valence function of each symmetry type; therefore it's unable to expand and contract in response to different molecular environments. For example, Li contains 3 electrons and F contains 9 electrons but the number of basis functions assigned to them is both 5. It's likely to give a poor description, especially with anisotropic molecules and polar molecules.

Split Valence Basis Sets

Split valence basis sets allow for more than one single basis function for each valence orbital. 3-21G is an often seen split-valence basis set. 6-31G is a larger split-valence basis set and 6-311G is a triply split-valence basis set.

The basis sets described above are comprised of functions centered at the nuclear positions and are suitable for molecules whose electrons are tightly held to the

nuclear center. Additional adjustments need to be made to add more flexibility to the basis sets to account for exceptional molecules.

Polarized and Diffused Basis Sets

The addition of polarized functions allows orbitals to change size. This change helps calculations on polar molecules, small strained ring molecules, etc. Polarization functions are important for obtaining a bonding description in many molecules. 6-31G(d), also known as 6-31G*, is a common polarized basis set, which means adding additional d functions to heavy atoms (non-H atoms). Another popular polarized basis set is 6-31G(d, p), which also referred to as 6-31G**. It adds sets of d functions on non-H atoms and p functions to H atoms. The addition of diffuse functions, which are normally s- and p- functions, allows orbitals to occupy a larger region of space. Basis sets with diffuse functions are essential for systems where the electron density is far away from the nucleus, such as anions, molecules with lone pairs or excited states. Diffuse functions help greatly in the calculation of electron affinities, proton affinities and inversion barriers. Diffuse functions are denoted as "+". For example, in 6-31++G (d) or 6-31++G* notation, the first + means adding a set of diffuse s- and p- function in addition to a d polarized function to heavy atoms and the second + indicates to adding a diffuse s- function to H atom and He atom.

Effective Core Potentials and Associated Basis Sets

The elements beyond the third row of the periodic table are more difficult to model than the elements in the lower rows. There are two reasons for this:

1. Large number of core electrons in those elements.

2. Relativistic effects in those elements are often non-negligible

Therefore basis sets for systems with those heavy elements are often handled somewhat differently. The core electrons need to be treated differently from valence shell electrons to account for the relativistic effects and the effects of core electrons on the valence shell electrons. The problem is solved by introducing an effective core potential (ECP) (also referred to as “pseudo-potential”) to represent all the core electrons [26,27]. The ECPs include all electron shells except for the outermost one, valence shell. The core electrons are replaced by a linear combination of Gaussian functions while the valence electrons are treated explicitly with proper basis sets.

There are four major steps in designing ECP type basis sets. First a good quality all-electron wavefunction is generated for the atom. Then the valence orbitals are replaced by a set of pseudo-orbitals. This set of pseudo-orbitals is designed to be nodeless so that the outer part will behave correctly but will not have nodal structure in the core region to be orthogonal to the core orbitals. Then the core electrons are replaced by a numerical potential so that the solution to the Schrödinger equation produces valence orbitals matching the pseudo-orbitals. Lastly, this numerical potential is fitted to a suitable set of Gaussian functions, Eq. 3.3 [28]

$$U_{ECP}(r) = \sum_i a_i r^{n_i} e^{-\alpha_i r^2} \qquad (3.3)$$

The parameters a_i, n_i and α_i depend on the angular momentum (s-, p-, d-, etc.).

The Lanl2DZ basis set is one such ECP. This basis set uses the valence double-ζ (DZ) basis set on light elements and effective core potentials plus DZ on heavy elements [29]. The SBKJC-21G (The Stevens-Basch-Krauss-Jansien-Cundari set) is

another example of ECPs with the associated basis sets ([4211/4211/411]) [30]. Another set of ECPs used in this study are relatively small core Stuttgart-RSC relativistic effective core potentials and their associated basis sets [31-33]. In these effective core potentials, the core consists of all but the outermost electrons. The performance of most ECPs agrees with the experimental results [34].

Natural Bond Orbitals (NBO)

Natural bond orbital (NBO) analysis was originated as a technique for studying hybridization and covalent effects in polyatomic wavefunctions [35]. It is useful for understanding bonding in molecules. The NBO method extracts the information in the first-order density matrix of the ab initio calculations. Then a unique set of atomic hybrids and bond orbitals is developed for a given molecule, thereby leading to a "Lewis structure" which is easy to understand.

The general procedure consists of a sequence of transformations from the input basis set $\{\chi_i\}$ to various localized basis sets (natural atomic orbitals (NAOs), hybrid orbitals (NHOs), bond orbitals (NBOs), and localized molecular orbitals (NLMOs)) [36].

$$\text{Input basis} \rightarrow \text{NAOs} \rightarrow \text{NHOs} \rightarrow \text{NBOs} \rightarrow \text{NLMOs}$$

The NLMOs may be subsequently transformed to delocalized natural orbitals (NOs) or molecular orbitals (MOs). The above steps are automated by the NBO computer programs [37].

A NAO is a valence-shell atomic orbital whose derivation involves diagonalizing the localized block of the full density matrix of a given molecule associated with input basis function $\chi_i(A)$ on that atom. In a polyatomic molecule, the NAOs mostly retain

one-center character, and thus are optimal for describing the molecular electron density around each atomic center. The resulting atomic charge on each atom corresponds to natural atomic charge.

The NBO is formed from NHOs. For a localized σ-bond between atoms A and B, the NBO is:

$$\sigma_{AB} = c_A h_A + c_B h_B \qquad (3.4)$$

where h_A and h_B are the natural hybrids centered on atoms A and B. NBOs closely correspond to the picture of localized bonds and lone pairs as basic units of molecular structure, so that it is possible to conveniently interpret ab initio wavefunctions in terms of the classical Lewis structure concepts by transforming these functions to NBO form.

Chapter References

1. Hehre W.J., Radom L., Schleyer P.V.R., Pope J. A., Ab Initio Moecular Orbital Theory, Wiley-Interscience: New York, 1986
2. Richards W.G., Ab initio Molecular Orbital Calculations for Chemists, Oxford: Clarendon Press, 1983
3. Dreizler R.M., Gross E. K. V., Density Functional Theory, Springer, Berlliln, 1990
4. Becke A. D., *Phys. Rev. A* 1988, *38*, 3098
5. Becke A. D., *J. Chem. Phys*. 1993,*98* 5648
6. Jursic B.S., *Theochem*. 1998, *417*, 89
7. Davidson e.R., *Int. J. quantum Chem*. 1998, *69*, 241
8. Nwobi O., Higgins J., Zhou X., Liu R., *Chem. Phys. Lett.* 1997, *272*, 155
9. Kaupp M., Malkina O. L., Malkin V.G., *J. Chem. Phys*. 1997, *106*, 9201

10. Barone V., Bencini A., Totti F., Uytterhoeven M. G., *Int. J. Quantum. Chem.* 1997. *61*. 361

11. Mehra J.R., The discovery of Quantum Mechanics. New York: Springer-Verlag, c1982

12. Ziock K., Basic Quantum Mechanics, Wiley: New York, 1969

13. Kompaneyets A.S., Basic Concepts in Quantum Mechanics, New York, Reinhold Pub. Corp.: 1966

14. Schrödinger E., *Ann. Physik*, 1926, *79*, 361

15. Foresman J. B., *Exploring chemistry with electronic structure methods*, 2nd edition, Gaussian, Inc, 1996

16. Slater J.C., *Phys. Rev*. 1930, *36*, 57

17. Roothan C. C. J., *Rev. Mod. Phys*. 1951, *23*, 69

18. Pople J. A., Nesbet R. K., *J. Chem. Phys*. 1959, *22*, 571

19. Møller C., Plesset M. S., *Phys. Rev*. 1934, *46*, 618

20. Hohenberg P., Kohn W., *Phys. Rev*. 1964, *136*, B864

21. Parr R. G., Yang W., *Density Functional Theory*, Oxford University Press, 1989

22. Gunnarsson O., Lundquist I., *Phys. Rev*. 1976, *B13,* 4274

23. von Barth U., Hedin L., *Phys. Rev.* 1979, *A20*, 1693

24. Vosko S. J., Wilk L., Nusair M., Can. *J. Phys.* 1980,*58*, 1200

25. Boys S. F., *Proc. Roy. Soc. (London)*, 1950, *A200*, 542

26. Frenking G., Antes I., Böhme M., Dapprioh S., Ehlers A. W., Jonas V., Nauhaus A., Otto M., Stegmann R., Veldkamp A., Vyboishchikov S. F., *Rev. Comput. Chem.* 1996*, 8*, 63

27. Cundari T. R., Benson M. T., Lutz M. L. and Sommerer S. O., *Rev. Comput. Chem*. 1996, *8*, 145

28. Jensen F., *Introduction to Computational Chemistry*, Wiley, 1999

29. Hay P.J., Wadt W. R., *J. Chem. Phys*. 1982, *77*, 3654

30. Stevens W., Krauss J. M., Basch H., Jasien P.G., *Can. J. Chem*. 1992, *70,* 612

31. Basis sets were obtained from the extensible Computational Chemistry Environment Basis Set Database, Version 1.0, as developed and distributed by the Molecular Sciences Laboratory, which is part of the Pacific Northwest Laboratory, P.O.Box 999, Richland WA 99352, USA, and funded by the U.S. Department of Energy under contract DE-AC06-76RLO 1830. Contact David Feller, Karen Schuchardt, or Don Jones for additional information.

32. Dolg M., Wedi U., Stoll H., Preuss H., *J. Chem. Phys*., 1987, *86*, 866

33. Andrae D., Haeussermann U., Dolg M., Stolll H., Preuss H., *Theor. Chim. Acta,* 1990, *77*, 123

34. Dyall K., *J. Chem. Phys*. 1991, *96*, 1210

35. Foster J. P., Weinhold F., *J. Am. Chem. Soc*. 1980, *102,* 7211-7218

36. Reed A. E., Curtiss, L. A., Weinhold F., *Chem. Rev*. 1988, 899-926

37. Reed A. E., Weinhold F., *F. QCPE Bull*., 1985, *5*, 141

38. Gaussian 98, Revision A.9, Frisch M. J., Trucks G. W., Schlegel H. B., Scuseria G. E., Robb M. A., Cheeseman J. R., Zakrzewski V. G., Montgomery J. A., Stratmann Jr.,R.E., Burant, J. C., Dapprich S., Millam, J. M., Daniels, A. D., Kudin K. N., Strain M. C., Farkas O., Tomasi J., Barone V., Cossi M., Cammi R., Bennucci B., Pomelli C., Adamo C., Clifford S., Ochterski J., Petersson G. A., Ayala P. Y., Cui Q., Morokuma K., Malick D. K., Rubuck A. D., Raghavachari K., Foresman J. B., Cioslowski J. J., Ortiz V. A., Baboul G., Stefanov B. B., Liu G., Liashenko A., Piskorz P., Komaromi I., Gomperts R., Martin R. L., Fox D. J., Keith T., Al-Laham M. A., Peng C. Y., Nanayakkara A., Challacombe M. P., Gill M. W., Johnson B., Chen W., Wong M. W., Andres J. L., Gonzalez C., Head-Gordon M., Replogle E. S. and Pople J. A., Gaussian, Inc., Pittsburgh PA, 1998.

CHAPTER 3

CLASSICAL $A_3H_3^+$ (A=C, SI AND GE) AS π LIGANDS IN ORGANOMETALLICS

Properties of Classical $A_3H_3^+$ (A=Si and Ge) Ligands

Organometallics with Carbocyclic Ligands

Organometallic compounds are defined as materials which possess direct, more or less polar bonds $M^{\delta+}$–$C^{\delta-}$ between metal and non– and semi–metal elements [1]. It is convenient to classify organometallic compounds according to their respective ligands. Depending on the capability of the ligand to form multiple bonds, the pure bond (M–C single bond) can be supplemented by various degrees of interaction. The compounds with cyclic conjugated π ligand are known as π-complexes.

The organometallic chemistry based on the smallest aromatic carbocyclic 2π ligand, $C_3R_3^+$, has been well developed [2]. It has been proved to be a versatile ligand with transition metals [3]. The parent ion $C_3H_3^+$ appeared in 1967. The triphenylcyclopropenyl cation ($C_3Ph_3^+$) was found in many organometallic complexes, such as $(C_3Ph_3)Co(CO)_3$ [4], $(C_3Ph_3)Rh(CO)_3$ [5], $(C_3Ph_3)Ir(CO)_3$ [5], $[(C_3Ph_3)Ni(CH_3C(CH_2P(C_6H_5)_2)_3)]^+$[6], $(C_3Ph_3)NiCp$ [7], $(C_3(t\text{-}Bu)_2MeWCp(PMe_3)Cl_2$ [8] and $(C_3Ph_3)Mo(CO)_2(bipy)Br$ [9]. The three-membered carbocyclic ring bonds to the metal atom in a symmetrical η^3 fashion. Various theoretical analyses have been reported on these metallatetrahedrane complexes [10]. However, the number of η^3–cyclopropenyl complexes known to date is still relatively very small compared to the vast number of η^5–cyclopentadienyl complexes [2]. A question of significant interest is whether the η^3–coordination property will also be favored for the heavier analogs $Si_3R_3^+$ and $Ge_3R_3^+$?

Since Si and Ge of group 14 are more electropositive than C, cations involving these elements should be more stable than the corresponding carbocations. $Si_3H_3^+$, produced by ion-molecule reactions of silicon ions with silane, has been detected in the gas phase by ion cyclotron resonance (ICR) spectroscopy [11]. Its ring structure is calculated to the global minimum, and it has shown potential as a ligand in main-group pyramidal (Si_3H_3X, X=N, NH^+, PO, C_{3v}) and sandwich ($(Si_3H_3)_2X$, X= B^+, $C2^+$, D_{3h}) compounds [12-14]. Theoretical reports have also shown that the trigermacyclopropenium ion (D_{3h}) is a stable minimum on the potential energy surface of $Ge_3H_3^+$ [15]. The substituted analog $Ge_3R_3^+$ (R=*t*-Bu_3Si) has been prepared experimentally and characterized by X-ray analysis [16].

Comparison of ring sizes suggests that $Si_3H_3^+$ and $Ge_3H_3^+$ ligands may be more suitable π ligands than $C_3H_3^+$. The overlap of the small π–perimeter with the M(d) orbitals is unfavorable for $C_3H_3^+$. Cyclopentadienyl is an excellent η^5 ligand due to the ideal claw size of its π framework for a range of transition-metal fragments [17]. The cyclopropenyl cation, $C_3H_3^+$, provides a much smaller span of orbitals, which is compensated by the large out-of-plane bending of the ring substituents away from the metal [4-9]. The Si-Si and Ge-Ge bond lengths in $Si_3H_3^+$ and $Ge_3H_3^+$ should reduce this orbital mismatch considerably. A theoretical study on $(CO)_3Co(A_3H_3)$ (**1**, C_{3v}), $(CO)_3Rh(A_3H_3)$ (**2**, C_{3v}), $(CO)_3Ir(A_3H_3)$ (**3**, C_{3v}), $[(CO)_3Ni(A_3H_3)]^+$ (**4**, C_{3v}), $(PH_3)_3Co(A_3H_3)$ (**5**, C_{3v}) and $[(PH_3)_3Ni(A_3H_3)]^+$ (**6**, C_{3v}) (A= C, Si and Ge) complexes, which contain η^3 coordination between the metal and the π ligand A_3H_3, is presented here. The carbon compounds are included for comparison.

Results and Discussion

Computational Methods

All the molecular structures were optimized and characterized by using the B3LYP hybrid Hartree-Fock/DFT method [18]. Another DFT method, which combines Becke's exchange functional with Perdew's nonocal correlation functional method (B3P86) was also used for comparison [19]. For transition metals, the SBKJC-21G relativistic effective core potential and its associated basis set ([4211/4211/411]) was used [20, 21]. The standard 6-31G(d) basis set [22] was used for non-metallic elements. The combination of 6-31G(d) and SBKJC-21G is represented as basis set B1 throughout the text. Some structures (**1Si** and **4Si**) were also optimized using all-electron triple-ζ and one f polarization basis for metals and 6-311G(d) for non-metal elements (denoted as basis set B2) for comparison [23]. All the computations were carried out with the Gaussian-98 program package on an NCSA supercomputer [24, 25]. Natural atomic charges were obtained from NBO analysis. The results at the B3LYP/B1 level are used in the discussion unless specifically noted otherwise. For detailed descriptions of theoretical methods and basis sets, please refer to chapter 2 (Theoretical Background) in the text.

Molecular Geometries

All the complexes **1–6** (C_{3v}, Figure 1) are calculated to be minima, except **1Ge**, **2Ge** and **3Ge**, which are transition states. The imaginary frequency corresponds to a twist of the hydrogens on the Ge_3H_3 ring (Figure 2), which leads to a minimum with C_3 symmetry. However, the energies of the C_{3v} complexes are only ~ 0.1kcal/mol higher

than the twisted structures, which is negligible. The results at B3LYP/B2 level also have shown that **1Si** and **4Si** are minima.

The bond distances in **1–6** are calculated to be slightly shorter at the B3P86 level than at the B3LYP level. The differences in bond distances between B3LYP/B1 and B3LYP/B2 levels are very small (± 0.009 Å). On average the C-C, Si-Si and Ge-Ge distances are 1.421 ± 0.017, 2.240 ± 0.013 and 2.375 ± 0.027 Å, respectively at B3LYP/B1. The A-A distance is the longest in Ir complexes (**3**) and the shortest in Ni complexes (**4** and **6**). These findings are in accord with covalent radii of Ni (1.15 Å), Co (1.16 Å), Rh (1.25 Å) and Ir (1.27 Å) [26]. Similarly, the metal M–A distance is the longest in the Ir complexes and the shortest in the Co complexes. In general, the M–A distance is shorter in complexes containing PH_3 ligands than in complexes containing CO ligands (comparing **1**, **4**, **5** and **6**). The shortest M–A distance is found in Co complex **5**, 1.955 Å, 2.378 Å and 2.458 Å for C, Si and Ge, respectively. In comparison to the free ligand $A_3H_3^+$ ($C_3H_3^+$, 1.366 Å; $Si_3H_3^+$, 2.206 Å; $Ge_3H_3^+$, 2.300 Å, Figure 3(1)) [12, 15, 27], the A–A distance is elongated. The lengthening is found to be large in Ge (0.057 – 0.102 Å) and small in C complexes (0.038 – 0.037 Å) and Si complexes (0.025 – 0.047 Å). A comparison of the A-A bond length in typical cyclopropane–like structures A_3H_6 (C_3H_6, 1.509 Å; Si_3H_6, 2.345 Å; Ge_3H_6, 2.422 Å, Figure 3(2)) reveals a shortening of bond lengths in **1–6** [28]. Comparison with ethane-like structures A_2H_6 (C_2H_6, 1.531 Å; Si_2H_6, 2.350 Å; Ge_2H_6, 2.401 Å, Figure 3(3)) leads to similar conclusions [29]. The above bond length changes will be explained in later context.

The calculated C-C distances in **1C–6C** are very close to average C-C bond distances determined experimentally in $(C_3Ph_3)Co(CO)_3$ (1.42 Å), $(C_3Ph_3)Ir(CO)_3$ (1.43

Å), $[(C_3Ph_3)Ni(CH_3C(CH_2P(C_6H_5)_2)_3)]^+$ (1.41 Å) and $(C_3Ph_3)NiCp$ (1.43 Å) [4-7]. However, the Co-C, Ir-C, and Ni-C distances are shorter by 0.02, 0.03 and 0.04 Å in **1C**, **3C** and **6C** as compared to those in $(C_3Ph_3)Co(CO)_3$, $(C_3Ph_3)Ir(CO)_3$ and $[(C_3Ph_3)Ni(CH_3C(CH_2P(C_6H_5)_2)_3)]^+$. The Si-Si distances in **1–6** are shorter compared to that in Si_3H_3X (2.308 and 2.343 Å for N, NH^+ and PO, Figure 4 [13]). The Co-Si distance in **1Si** is slightly longer than the 2.25 Å value in $H_3SiCo(CO)_4$ [30] and 2.38 Å in $H_3SiCo(CO)_4$. Similarly, the Ni-Si distances in **4Si** and **6Si** are also longer than 2.15, 2.21 and 2.29 Å, found in $Ni(Silylene)_3$, $Ni\{(t\text{-}Bu)NCH{=}CHN(t\text{-}Bu)Si\}_2(CO)_2$ and $Ni(SIH_2C_6H_4SiH_2)_2(PMe_2C_2H_4PMe_2)$, respectively [31]. Such a lengthening of M-Si distances indicates the π bonding character.

Due to the differences in A_3H_3 ring size, a term, ω, is used to describe the nonplanarity of ring hydrogens in the A_3 ring. In other words, ω is the angle of A-H vector from the A_3 ring. The value is positive if hydrogens are tilted away from the metal, the ω will be negative if the hydrogens are tilted toward the metal (Figure 5). The bigger the value of ω is, the greater the tilt is; therefore the less planar the three-member ring is. The ω value is found to be much smaller in Si and Ge complexes than in C complexes. For C complexes, the ω values are greater than 20 degrees while they are less than 10 degrees for Si and Ge complexes. The exceptional case is **5**, in which all the C, Si and Ge rings have large positive ω (C: 26.9; Si: 14.6; Ge: 24.6 at B3LYP/B1 level). This is mainly due to the combination of short M–A distances and sterically large PH_3 ligand.

Electronic Structures

The electronic structures of the complexes **1–6** have been analyzed by the fragment molecular orbital (FMO) method [32]. The orbital interaction diagram of $[Co(CO)_3]^-$ with $C_3H_3^+$ and $Si_3H_3^+$ is shown in Figure 6 to illustrate the differences between C complexes and their heavier analogs. The frontier orbitals of $Co(CO)_3$ (ML_3 type) and $C_3H_3^+$ are well known in literature [10a, 32]. The valence molecular orbitals (MO) of $C_3H_3^+$ and those of $Co(CO)_3$ are from different electronic shells; therefore there are relatively big energy gaps between them in the interaction. The interaction between the higher lying $2a_1$ orbital of the $Co(CO)_3$ fragment and the $1a_1(\pi)$ orbital of $C_3H_3^+$ is found to be very weak due to the big energy difference. The HOMO of **1C**, 3e, shows the contributions from 2e (π^*), the LUMO of the ligand and 2e in $Co(CO)_3$, leading to a charge transfer from the metal center to the ligand ring. This charge transfer makes C_3H_3 an anionic ligand, as suggested by Collman *et al* [3]. The valence MOs of Si_3H_3 ligand are higher in energy than in C_3H_3, since they are formed from 3s and 3p orbitals. For example, the eigenvalues of the π MO are –18.05 and –12.30 eV for $C_3H_3^+$ and $Si_3H_3^+$, respectively, at B3LYP/6-31G(d) level. Because of these high-energy valence MOs of $Si_3H_3^+$, they match very well with the MOs of $Co(CO)_3$. The 2e, LUMO, orbital in $Co(CO)_3$ interacts with the 1e, LUMO-1, orbital on Si_3H_3. However, their bonding and antibonding (HOMO in **1Si**) combinations are filled. The HOMO-1 of **1Si** shows the contributions from $2a_1$, LUMO, in $Co(CO)_3$ and $1a_1$ (π), HOMO, in the Si_3H_3 ligand, leading to a charge transfer from ligand to metal, which is reversed flow compared to **1C** and cyclopentadienyl complexes. The electronic structure of **1Ge** is also found to be similar to that of **1Si**. The electronic structure analyses suggest that there is a charge

transfer from the metal to the ligand in C complexes, while for Si and Ge complexes, the charge transfer occurs from the ligand to the metal.

NBO Charges

The NBO charges of the complexes **1–6** are tabulated in Table 1. The NBO charge analysis confirms the electronic structure findings, which reveal that there is a charge transfer from the metal center to the ligand ring for **1C**. However, the NBO charges show this charge transfer to be very small for **1C**. For examples, the NBO charges are -0.06, -0.28 and 0.26e on Co, ring C and H, respectively. The electronic structure also reveals that there is a charge transfer from ligand to metal in Si and Ge complexes. The NBO charges –0.40, 0.23 and –0.10e on Co, Si and H for **1Si** respectively, and –0.35, 0.19 and –0.07e on Co, Ge and H for **1Ge** respectively, support this interpretation. Therefore, the bonding character of **1Si** and **1Ge** is remarkably different from that of **1C**. The lengthening of the A-A distances discussed previously when compared with free ligand $A_3H_3^+$ and the shortening of the A-A distances when compared with cyclopropane-like structures A_3H_6 can also be explained by the conclusion that there is charge transfer between the metal and ligand ring.

The electronic structures and NBO results of Si and Ge complexes **2–6** are found to be similar to that of **1Si**, and those of **2C–6C** are similar to that of **1C**.

Conclusions

Calculations at the B3LYP/B1 and B3P86/B2 levels show that the following: The complexes of A_3H_3 (A=C, Si and Ge) are minima. The electronic structure analysis

reveals that there is a charge transfer from the metal to the ligand in C complexes. Si and Ge complexes exhibit charge transfer from the ligand to the metal, which is a reversed electron flow compared both to C complexes and cyclopentadienyl complexes.

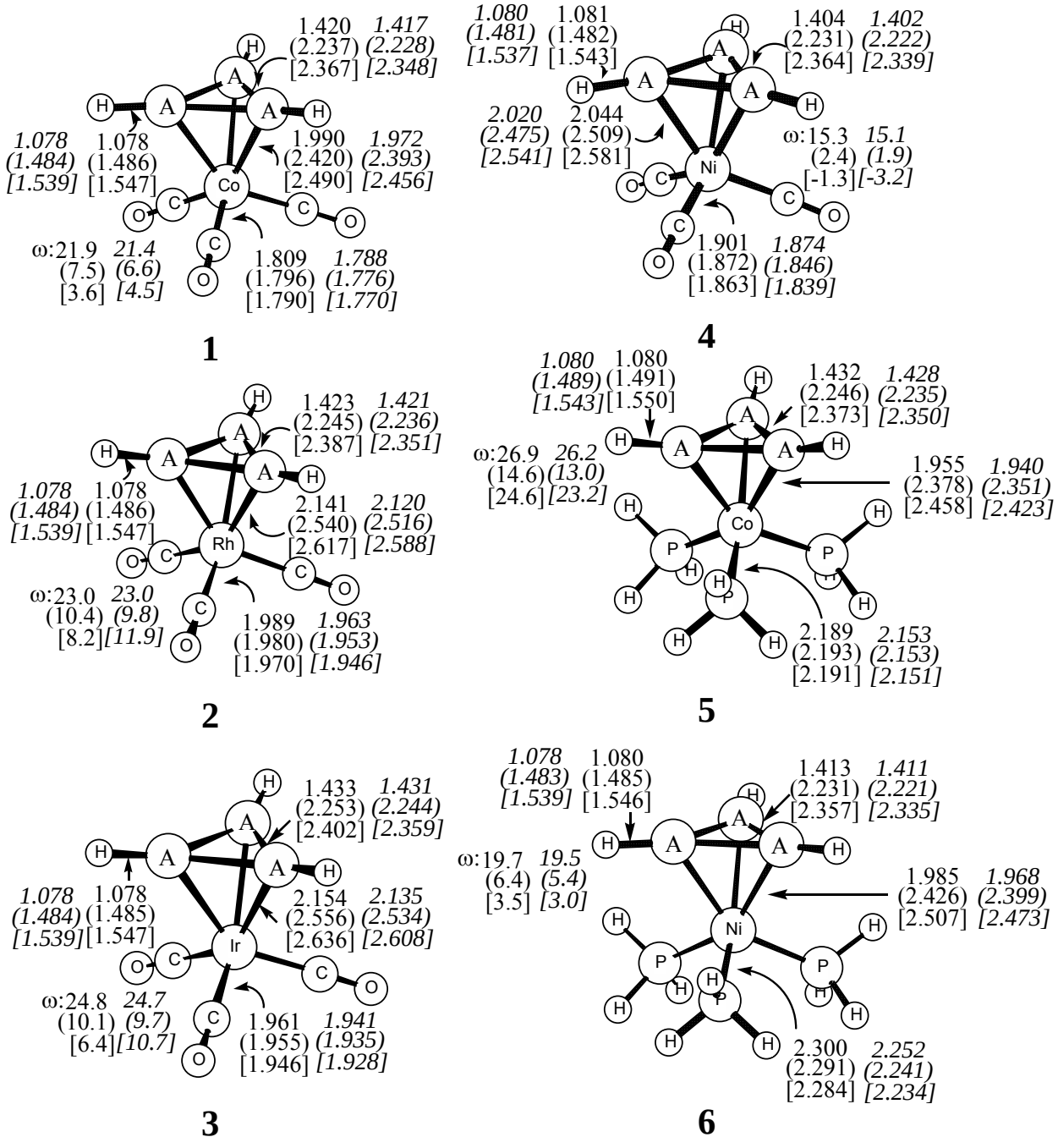

Figure 1. Optimized geometries and important bond distances for C, Si (in parentheses), and Ge (in brackets) complexes at B3LYP/B1 level. The values in italics are at the B3P86/B1 level. Refer to the text and Figure 5 for the definition of ω.

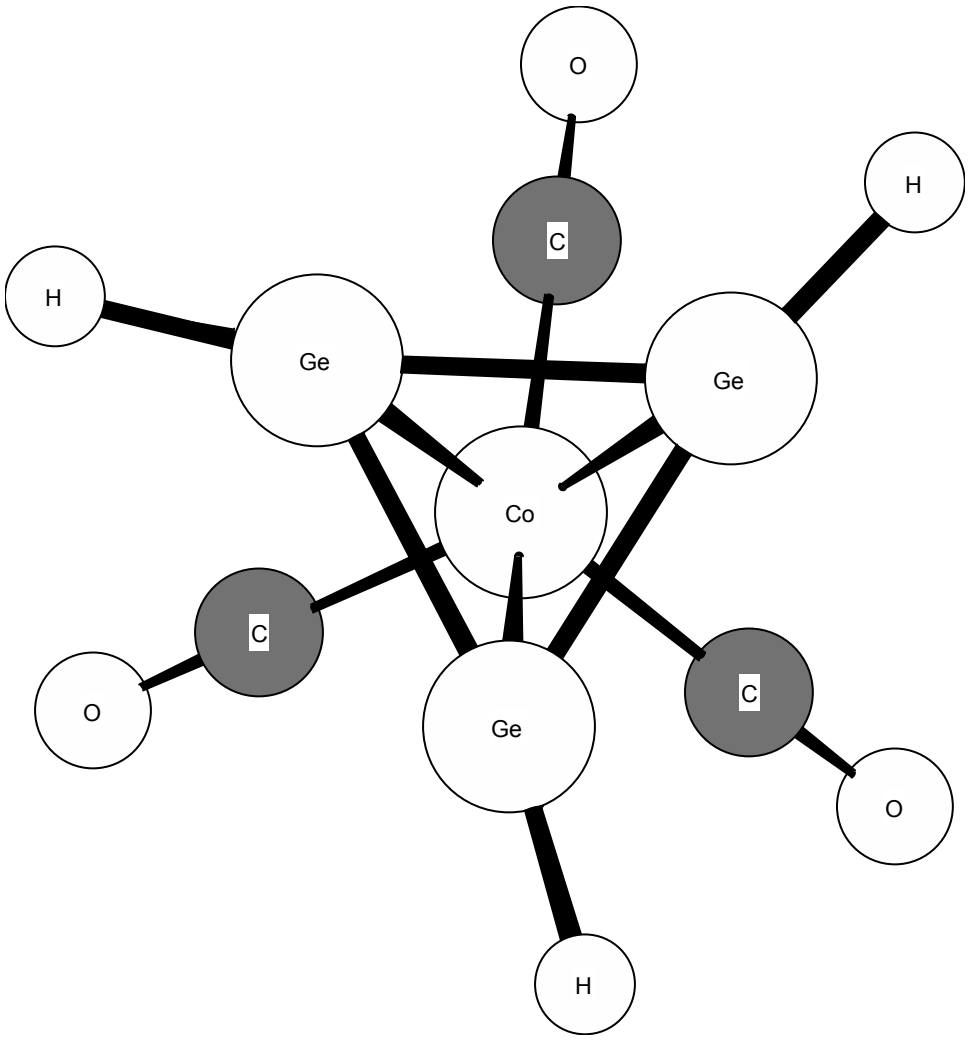

Figure 2. Top view of **1Ge** showing the twist of the hydrogens on the Ge_3 ring.

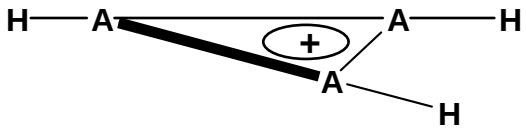

(1)

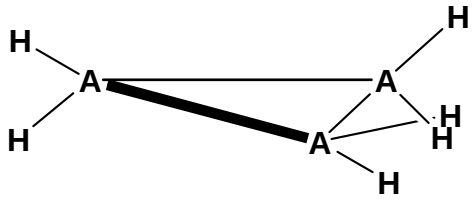

(2)

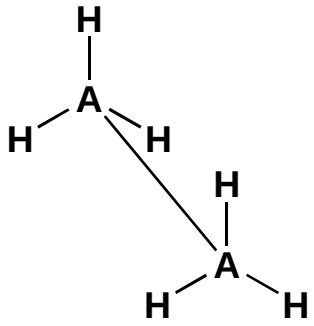

(3)

Figure 3. (1) Free ligand $A_3H_3^+$ (A=C, Si and Ge).
(2) Cyclopropane –like structure of A_3H_6 (A=C, Si and Ge).
(3) Ethane-like structure of A_2H_6 (A=C, Si and Ge).

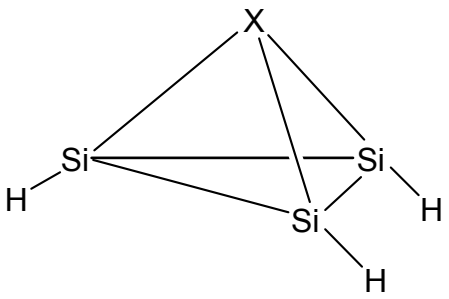

X=N, NH^+ and PO

Figure 4. Structure of Si_3H_3X (X=N, NH^+ and PO).

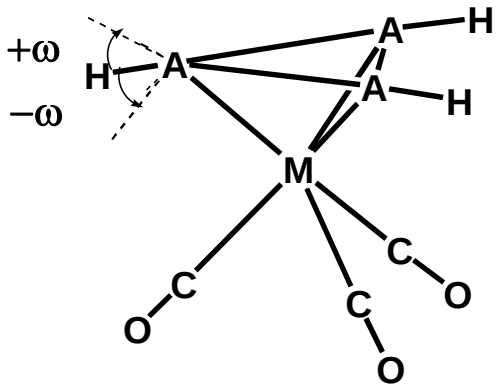

Figure 5. The definition of ω. ω is positive if hydrogens are tilted away from the metal otherwise ω is negative.

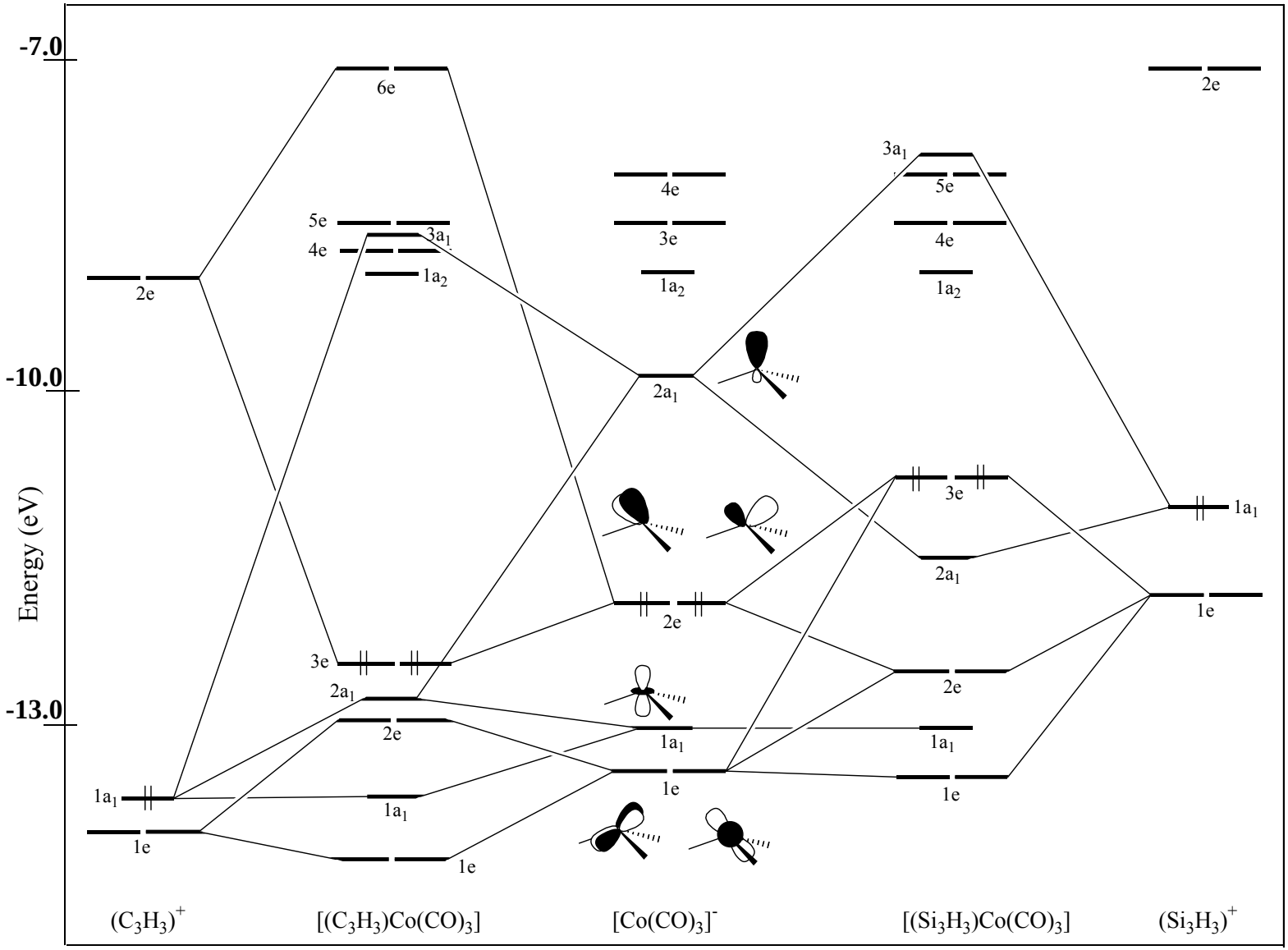

Figure 6. Interaction diagram for $[(C_3H_3)Co(CO)_3]$ and $[(Si_3H_3)Co(CO)_3]$. Only the HOMO electrons are shown.

Table 1. Number of imaginary frequencies (NIM), and NBO charges (in e) of structures **1–6** (Figure 1) at the B3LYP/B1 level.

Structure	NIM	Natural charge
1, C (C_{3v})	0	Co:-0.06, ring-C:-0.28, H:0.26, C:0.49, O:-0.45
Si (C_{3v})	0	Co:-0.40, Si:0.23, H:-0.10, C:0.45, O:-0.45
Ge (C_3) [a]	0	Co:-0.35, Ge:0.19, H:-0.07, C:0.45, O:-0.45
2, C (C_{3v})	0	Rh:0.13, ring-C:-0.29, H:0.26, C:0.44, O:-0.44
Si (C_{3v})	0	Rh:-0.23, Si:0.18, H:-0.10, C:0.44, O:-0.44
Ge (C_3) [a]	0	Rh:-0.20, Ge:0.14, H:-0.07, C:0.44, O:-0.44
3, C (C_{3v})	0	Ir:0.31, ring-C:-0.33, H:0.26, C:0.40, O:-0.44
Si (C_{3v})	0	Ir:-0.06, Si:0.16, H:-0.10, C:0.40, O:-0.44
Ge (C_3) [a]	0	Ir:-0.02, Ge:0.12, H:-0.07, C:0.40, O:-0.44
4, C (C_{3v})	0	Ni:0.35, ring-C:-0.19, H:0.31, C:0.46, O:-0.36
Si (C_{3v})	0	Ni:0.08, Si:0.32, H:-0.06, C:0.42, O:-0.37
Ge (C_{3v})	0	Ni:0.12, Ge:0.28, H:-0.03, C:0.42, O:-0.37
5, C (C_{3v})	0	Co:-0.25, C:-0.32, ring-H:0.24, P:0.18, H:0.00
Si (C_{3v})	0	Co:-0.66, Si:0.16, ring-H:-0.12, P:0.17, H:0.01
Ge (C_{3v})	0	Co:-0.58, Ge:0.10, ring-H:-0.09, P:0.17, H:0.01
6, C (C_{3v})	0	Ni:0.27, C:-0.24, ring-H:0.28, P:0.06, H:0.04
Si (C_{3v})	0	Ni:-0.06, Si:0.25, ring-H:-0.08, P:0.06, H:0.04
Ge (C_{3v})	0	Ni:-0.03, Ge:0.21, ring-H:-0.05, P:0.05, H:0.04

[a] These structures are transition states under C_{3v} symmetry (Refer to text).

Chapter References

1. Abel E.W., Stone G. A., Wilkinson G., *Comprehensive Organometallic Chemistry II: a review of the literature 1982 -1994*, 1st Edition, Oxford ; New York : Pergamon, 1995

2. Elschenbroich Ch., Salzer A., *Organometallics*, 2nd edition.; VCH: New York, 1992

3. Collman J. P., Hegedus L. S., Norton J. R., Finke R. G., *Principles and Applications of Organotransition Metal Chemistry; University Science Books*: Mill Valley, CA, 1987

4. Chiang T., Kerber R. C., Kimball S. D., Lauher J. W., *Inorg. Chem*. 1979, *18*, 1687

5. Hughes R. P., Tucker D. S., Rheingold A. L., *Organometallics* 1993, *12*, 3069

6. Mealli C., Midollini S., Moneti S., Sacconi L., *J. Organomet. Chem.* 1981, *205*, 273

7. (a) Rausch M. D., Tuggle R. M., Weaver D. L., *J. Am. Chem. Soc*. 1970, *92*, 4981. (b) Tuggle R. M., Weaver D. L., *Inorg. Chem*. 1971, *10*, 1504

8. Churchill M. R., Fettinger J. C., McCullough L. G., Schrock P. R., *J. Am. Chem. Soc*. 1984, *106*, 3356

9. Drew M. G., Brisdon B. J., Day A., *J. Chem. Soc., Dalton Trans*. 1981, 1310

10. (a) Jemmis E. D., Hoffmann R., *J. Am. Chem. Soc.* 1980, *102*, 2570. (b) Ansyln E. V., Brusich M. J., Boddard W. A., *Organometallics* 1993, *12*, 1289. (c) Woo T., Folga E., Ziegler T., *Organometallics* 1993, *12*, 1289. (d) Lichtenberger D. L., Hoppe M. L., Subramanian L., Kober E. M., Hughes R. P., Hubbard J. L., Tucke D. S., *Organometallics* 1993, *12*, 2025. (e) Lin Z., Hall M. B., *Organometallics* 1994, *13*, 2878

11. (a) Stewart G. W., Henis J. M. S., Gaspar P. P., *J. Chem. Phys*. 1973, *58*, 890. (b) Mandich M. L., Reents W. D. Jr., *J. Chem. Phys*. 1991, *95*, 7360

12. (a) Korkin A. A., Glukhovtsev M., Schleyer P. v. R., *Int. J. Quantum Chem*. 1993, *46*, 137. (b) Srinivas G. N., Jemmis E. D., Korkin, A. A., Schleyer P. v. R., *J. Phys. Chem.* A 1999, *103*, 11034

13. (a) Jemmis E. D., Srinivas G. N., *J. Am. Chem. Soc*. 1996, *118*, 3738. (b) Srinivas G. N., Jemmis E. D., *J. Am. Chem. Soc*. 1997, *119*, 12968

14. Srinivas G. N., Hamilton T. P., Jemmis E. D., McKee M. L., Lammertsma K., *J. Am. Chem. Soc.* 2000, *122*, 1725

15. (a) Jemmis E. D., Srinivas G. N., Leszdzynski J., Kapp J., Korkin A. A., Schleyer P. v. R., *J. Am. Chem. Soc.* 1995, *117*, 11361. (b) So S. P., *Chem. Phys. Lett.* 1999, *313*, 587

16. Skiguchi A., Tsukamoto M., Ichinohe M., *Science* 1997, *275*, 60

17. (a) Huheey J. E., Keiter E. A., Keiter R. L., *Inorganic Chemistry*, 4th ed.; Harper Collins College: New York, 1993. (b) Haaland A., Marinsen K. G., Schlykov S. A., Volden H. V., Dohmeier C., Schnockel H., *Organometallics* 1995, *14*, 3116

18. (a) Becke A. D., *J. Chem. Phys.* 1993, *98*, 5648. (b) Lee C., Yang W., Parr R. G., *Phys. Rev.* B 1988, *37*, 785. (c) Pople J. A., Raghavachari K., Schlegel H. B., Binkley J. S., *Int. J. Quantum Chem. Symp.* 1979, *13*, 255

19. (a) Becke A. D., *Phys. Rev.* A 1988, *38*, 3098. (b) Perdew J. P., *Phys. Rev*. B 1986, *33*, 8822

20. Basis sets were obtained from the extensible Computational Chemistry Environment Basis Set Database, Version 1.0, as developed and distributed by the Molecular Science Computing Facility, Environmental and Molecular Sciences Laboratory, which is part of the Pacific Northwest Laboratory, P. O. Box 999, Richland, WA 99352, and funded by the U. S. Department of Energy under Contract DE-AC06-76RLO 1830. Contact David Feller, Karen Schuchardt, or Don Jones for additional information.

21. (a) Stevens W. J., Basch H., Krauss M. M., *Chem. Phys*. 1984, *81*, 6026. (b) Stevens W. J., Krauss M., Basch H., Jasien P. G., *Can. J. Chem*. 1982, *70*, 612. (c) Cundari T. R., Stevens W. J., *J. Chem. Phys*. 1993, *98*, 5555

22. (a) Hehre W. J., Radom L.; Schleyer P. v. R., Pople J. A., *Ab Initio Molecular Orbital Theory*; Wiley: New York, 1986. (b) Hehre W. J., Ditchfield R., Pople J. A., *J. Chem. Phys*. 1972, *56*, 2257

23. (a) Wachters A. J. H., *J. Chem. Phys*. 1970, *52*, 1033. (b) Wachters A. J. H., IBM Technol. Rept. RJ584, 1969. (c) Bauschlicher C. W. Jr., Langhoff S. R., Barnes L. A., *J. Chem. Phys.* 1989, *91*, 2399

24. Frisch M. J., Trucks G. W., Schlegel H. B., Scuseria G. E., Robb M. A., Cheeseman J. R., Zakrzewski V. G., Montgomery J. A. Jr., Stratmann R. E., Burant J. C., Dapprich S., Millam J. M., Daniels A. D., Kudin K. N., Strain M. C., Farkas O., Tomasi J., Barone V., Cossi M., Cammi R., Mennucci B., Pomelli C., Adamo C., Clifford S., Ochterski J., Petersson G. A., Ayala P. Y., Cui Q., Morokuma K., Malick D. K., Rabuck A. D., Raghavachari K., Foresman J. B., Cioslowski J., Ortiz J. V., Stefanov B. B., Liu G., Liashenko A., Piskorz P., Komaromi I., Gomperts R., Martin R. L., Fox D. J., Keith T., Al-Laham M. A., Peng C. Y., Nanayakkara A., Gonzalez C., Challacombe M., Gill P. M. W., Johnson B. G., Chen W., Wong M. W. Andres J. L., Head-Gordon M., Replogle E. S., Pople, J. A., Gaussian 98, revision A.9; Gaussian, Inc.: Pittsburgh, PA. 1998

25. We thank the National Computational Science Alliance (NCSA) for allotting the computational time on an SGI/GRAY Origin 2000 supercomputer (Grant No. CHE000018N)

26. Cotton F. A., Wilkinson G., Murillo C. A., Bochmann M., *Advanced Inorganic Chemistry*, 6th ed.; Wiley-Interscience: New York, 1999

27. (a) Wong M. W., Rdom L., *J. Am. Chem. Soc.* 1993, *115*, 1507. (b) Li W. K., Riggs N. V., *J. Mol. Struct. (THEOCHEM)* 1992, *257*, 189

28. (a) Nagase S., Kobayashi K., Nagashima M., *J. Chem. Soc*., *Chem. Commun*. 1992, 1302. (b) Srinivas G. N., Kiran B., Jemmis E. D., *J. Mol. Struct. (THEOCHEM*), 1996, *361*, 205

29. Schleyer P. v. R., Kaupp M., Hampel F., Bermer M., Mislow K., *J. Am. Chem. Soc*. 1992, *114*, 6791

30. (a) Robinson W. T., Libers J. A., *Inorg. Chem*. 1967, *6*, 1208. (b) Robiette A. G., Sheldrick G. M., Simpson R. N. F., Aylett B. J., Campbell J. M., *J. Organomet. Chem*. 1968, *14*, 279

31. (a) Schmedake T. A., Haaf M., Paradise B. J., Powell D., West R., *Organometallics* 2000, *19*, 3263. (b) Denk M., Hayashi R. K., West R., *J. Chem. Soc. Chem. Commun.* 1994, *33*. (c) Shimada S., Rao M. L. N., Hayashi T., Tanaka M., *Angew. Chem., Int. Ed*. 2001, *40*, 213

32. (a) Fujimoto H., Hoffmann R., *J. Phys. Chem*. 1974, *78*, 1167. (b) Hoffmann R., *Angew. Chem., Int. Ed. Engl.* 1982, *21*, 711

CHAPTER 4

H-BRIDGED $A_3H_3^+$ (A=Si AND Ge) AS π LIGANDS IN ORGANOMETALLICS

Properties of H-Bridged $A_3H_3^+$ (A=Si AND Ge) Ligands

The difference of structure and bonding of carbon and its heavier analogs have been of great interest in recent years. However, the well-established bonding rules of carbon chemistry are of little help in deducing the structure of the compounds of silicon (Si) and Germanium (Ge), the heavier group 14 analogs. For example, unlike ethylene and acetylene, Si_2H_4, C_2, is nonplanar and Si_2H_2, C_{2v} has a doubly bridged geometry (Figure 7). A triply H-bridged structure, C_{3v}, is a minimum for trisilacyclopropane. The heavier group 14 X_3H_6 bridged structures are even lower in energy than the classical cyclopropane-like alternatives.

The H-bridged structures are also found to be stable, sometimes even global minima for Si and Ge compared to classical structures known for C. Here are some examples: (i) Acetylene analogs Si_2H_2 and Ge_2H_2 prefer a double bridged structure (**7**, C_{2v}). (ii) A triply H-bridged structure (**8**, C_{3v}) is a minimum for trisilacyclopropane and trigermacyclopropane. (iii) The lowest energy structures of $Si_3H_5^+$ (**9**, C_s) and $Si_2H_3^+$ (**10**, D_{3h}) have two and three bridging H's respectively (Figure 8).

A similar trend is also found in 2π-Hückel aromatic cyclopropenium ions $A_3H_3^+$ (A= C, Si and Ge). The potential energy surface of $Si_3H_3^+$ is rich in possibilities, showing dramatic contrasts with that of the carbon analog. $C_3H_3^+$ has four minima on its potential energy surface. The structure of the cyclopropenyl cation **11** shown in figure 9 is the global minimum and the other minima **12**, **13** and **14** are higher in energy than **11** by 31.5, 76.5 and 189.2 kcal/mol, respectively (Figure 9). The energy value of isomer

14 is out of diagram therefore not shown in Figure 10. In contrast, $Si_3H_3^+$ has twelve minima within a 46-kcal/mol range (Figure 10), though the classical trisilacyclopropenium ion is the global minimum (**15**, D_{3h}, Figure 11). The triply H-bridged structure (**16**, C_{3v}, Figure 11) is also a minimum for $Si_3H_3^+$, but it is 30 kcal/mol higher in energy than **15Si** at the B3LYP/6-31G(d) level (Figure 11). In the case of Ge, **16** is also a minimum and its stability is competitive with **15**. **16Ge** is 9.4 and 3.8 kcal/mol higher in energy than **15Ge** at the B3LYP/6-31G(d) and G2 levels respectively. Pyramidal structures based on **15Si** and **16Si** have shown remarkable differences. The classical structures **17** (C_{3v}) are calculated to be less stable than the H-bridged isomers **18** (C_{3v}, Figure 11). Though η^3–ligand properties of **15Si** and **15Ge** are studied in organometallics, there are no reports available regarding **16** as a ligand in organometallic chemistry.

In view of the findings **7-10** and the relative stabilities of **17** and **18**, we reasoned that organometallic complexes with ligand **16** might also be stable. Though η^3–ligand properties of **15Si** and **15Ge** are studied in organometallics (Section I), there are no reports available regarding **16** as a ligand in organometallic chemistry. The results of the theoretical study of H-bridged η^3 complexes $(A_3H_3)Co(CO)_3$ (**1a**, C_{3v}), $(A_3H_3)Rh(CO)_3$ (**2a**, C_{3v}) and $(A_3H_3)Ir(CO)_3$ (**3a**, C_{3v}) (A= Si and Ge) are also reported here and compared with that of the non-bridged isomers (**1-3**).

Results and Discussion

Computational Methods

The geometries of all the structures were optimized using the hybrid Hartree-

Fock/DFT B3LYP method. Another DFT method, which combines Becke's exchange functional with Perdew's nonlocal correlation functional method (B3P86), was also used for comparison. The standard 6-31G(d) basis set was used for ligands and for metals the SBKJC-21G relativistic effective core potentials and their associated basis sets ([4211/4211/411]) were used. The combination of 6-31G(d) and SBKJC-21G is represented as basis set B1. The geometries were also optimized at the B3LYP level using the small core Stuttgart-RSC relativistic effective core potentials and their associated basis sets (Co: [311111/22111/411/1], Rh and Ir: [311111/22111/411]) on the metals and 6-31G(d) for ligands (represented as basis set B2). The nature of the stationary points was determined from harmonic force constants and vibrational frequencies. All of the computations were carried out with Gaussian-98 program package on an NCSA supercomputer. The natural charges were obtained from natural bond orbital (NBO) analysis. The results at the B3LYP/B1 level are used in the discussion unless specifically noted otherwise. For detailed descriptions of computational methods and basis sets, please refer to chapter 2 (Theoretical background) in the text.

Molecular Geometries

All the complexes are calculated to be minima and the H-bridged structures (**1a-3a**) are lower in energy than the non-bridged complexes **1–3**. In fact, the stability of H-bridged structures increases from Si to Ge (Table 2). On average, the H-bridged Si complexes are 7.2 and 5.7 kcal/mol more stable than the non-bridged isomers at the B3LYP and B3P86 levels, respectively. Similarly, H-bridged Ge complexes are 32.0

and 28.4 kcal/mol more stable than the non-bridged isomers at the B3LYP and B3P86 levels. There is no significant change in relative energies obtained from the two basis set combinations (B1 and B2; Table 2). The energy difference between H-bridged and non-bridged structures is found to be slightly higher in Co and Ir complexes and less in Rh complexes (Table 2).

The bond distances in **1a–3a** are calculated to be slightly shorter at the B3P86 level than at the B3LYP level (Figure 12), which is the same case in non-bridged complexes **1–3** as discussed previously in Section I. There is a variation of ±0.016 Å for bond distances between the B3LYP/B1 and B3LYP/B2 levels. On average, the Si-Si and Ge-Ge distances are 2.683 ± 0.038 Å and 2.843 ± 0.034 Å, respectively, at the B3LYP level. In accordance with the covalent radii of Co (1.16 Å), Rh (1.25 Å) and Ir (1.27 Å), the A-A distance is longest in the Ir complex (**2a**) and shortest in the Co complex (**1a**). Similarly the metal M-A distance is longest in the Ir complex and shortest in the Co complex. The non-bridged complexes (**1–3**) were also reported to show similar trends (Section I) in geometrical parameters.

The A-A distances in **1a-3a** are longer than those in the free ligands (**16Si**: 2.571 Å and **16Ge**: 2.729 Å, Figure 11). Similar results are found when comparing distances to those in **7** (Figure 8, **7Si**: 2.221 Å and **7Ge**: 2.358 Å) and **10** (Figure 8, **10Si**: 2.417 Å and **10Ge**: 2.611 Å). The A-A distances in **1a–3a** are much shorter than in **8** (Figure 8, **8Si**: 3.133 Å and **8Ge**: 3.260 Å). The M-A distances are slightly shorter in complexes **1a–3a** (by ~0.027 Å and 0.025 Å for Si and Ge) than those in **1–3**, which suggests a strong metal-ligand bonding in **1a–3a**.

Electronic Structures

Comparison of the electronic structures of H-bridged and non-bridged isomers may give some insight into the stability of H-bridged isomers. A diagram showing the important interactions between **16Ge** and $[Ir(CO)_3]^-$ leading to **3a**, and **15Ge** and $[Ir(CO)_3]^-$ leading to **3Ge** constructed by the FMO method is shown in Figure 13. The frontier orbitals of $Ir(CO)_3$ (ML_3 type) and **15Ge** (C_3H_3 type) are well known in the literature. The bonding in **3Ge** is explained by considering the following interactions between $Ir(CO)_3$ and **15Ge**. The 2e orbital, HOMO, of $Ir(CO)_3$ interacts with 2e (π^*) and 1e of the ligand leading to a three orbital interaction, resulting in the 3e, HOMO, of **3Ge**. Similarly, a second three orbital interaction between $1a_1$ (π) of the ligand and $1a_1(Z^2)$, $2a_1$ (Z) of the metal leads to $1a_1$, $2a_1$ and $3a_1$ orbitals in **3Ge**. The frontier orbitals in **16Ge** are somewhat different than in **15Ge**. The σ-π mixing due to the non-planar bridging hydrogens stabilizes both the $1a_1$ (π) and 2e (π^*) orbitals of **16Ge**. For example, the eigenvalues of the π MO are –11.92 and –13.36 eV for **5Ge** and **6Ge** ligands respectively, at the B3LYP/6-31G(d) level. Similarly, the eigenvalues of the π^* MOs are –7.20 and –8.27 eV for **15Ge** and **16Ge**. Because of these low-energy valence MOs of **16Ge**, the three orbital interactions between the metal $1a_1$ and $2a_1$, and ligand $1a_1$ is much more effective than that found with **15Ge**. A similar effect is also found for the three orbital interactions between metal 2e and ligand 2e and 1e. These bonding features reveal that the low-energy valence MOs of the H-bridged ligand form better bonding with $Ir(CO)_3$ than those of the non-bridged ligand. Although it is difficult to pinpoint exactly what makes the bridged system **3a–Ge** more stable than the non-bridged system **3Ge**, the relative stabilities discussed above are plausible contributing

factors. Similar results were found for **1a–Ge** and **3a–Ge**. The silicon systems **1a–Si**, **2a–Si** and **3a–Si** have also shown similar results, though to a lesser extent. The above-discussed bonding features also reveal that there is a charge transfer from ligand to metal.

NBO Charges

The NBO charges for **1a–3a** complexes are listed in Table 2. The results support the interpretation that there is charge transfer from ligand to metal. The non-bridged systems **1–3** have been reported previously to shown similar trends. Therefore, both H-bridged and classical ligands **15** and **16** behave as π donor ligands. The systematic decrease in the NBO charges on the metal and Si/Ge ligands down the group shows that the electron transfer from ligand to metal is decreasing from Co to Ir complexes. Since the CO is a σ donor and a π acceptor, whereas the Si/Ge ligands are only π donor ligands, the reduced Mulliken overlap population between M–C (carbonyl) is higher than M-Si/Ge (for example, the overlap populations are Co-C: 0.41e, Co-Si: 0.08e in **1a–Si** and Co-C: 0.41e, Co-Si: 0.03e in **1Si**). The NBO analysis also reveals that the lone pair on the A_3H_3 ring contains mainly s (~84%) character, which leaves maximum p-character (~94%) on A for other bonds.

Conclusions

Calculations at B3LYP and B3P86 levels show the following: organonmetallic complexes (**1a–3a**) based on the H-bridged $A_3H_3^+$ (A=Si and Ge) ligand are minima. Compared to complexes (**1–3**) based on the classical $A_3H_3^+$ ligand, **1a–3a** complexes

are more stable, and their average stability increases from Si (B3LYP: 7.2 and B3P86: 5.7 kcal/mol) to Ge (B3LYP: 32.0 and B3P86: 28.4 kcal/mol). The electronic structure analysis also reveals that there is a charge transfer from the ligand to the metal in Si and Ge complexes (**1a–3a**).

Si_2H_4, C_2 Si_2H_2, C_{2v}

Figure 7. Structures for nonplanar Si_2H_4, C_2, and doubly-bridged Si_2H_2, C_{2v}.

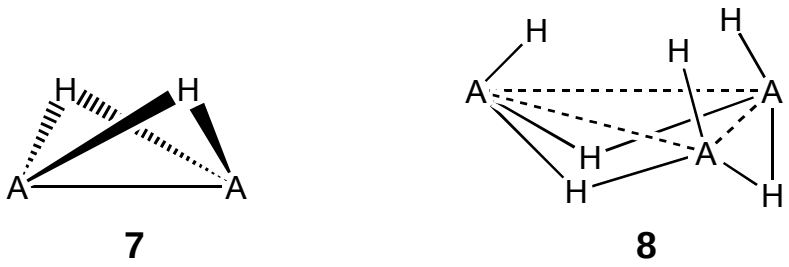

7 **8**

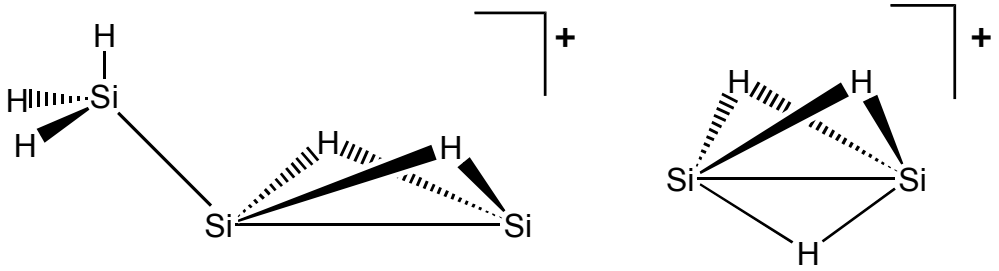

9 **10**

Figure 8. **7** Doubly-bridged structure of A_2H_2 (A=Si and Ge, C_{2v}).
8 Triply H-bridged structure of A_3H_6 (A=Si and Ge, C_{3v}).
9 $Si_3H_5^+$ with two bridging H's (C_s).
10 $Si_2H_3^+$ with three bridging H's (D_{3h}).

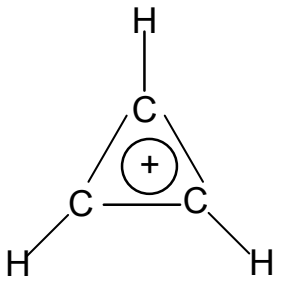

11

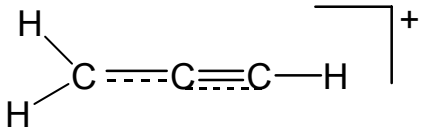

12

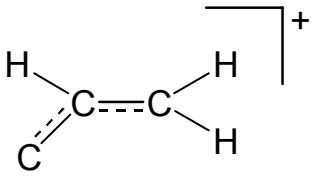

13

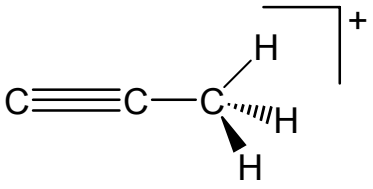

14

Figure 9. Four minima structures of $C_3H_3^+$ on the potential energy surface.

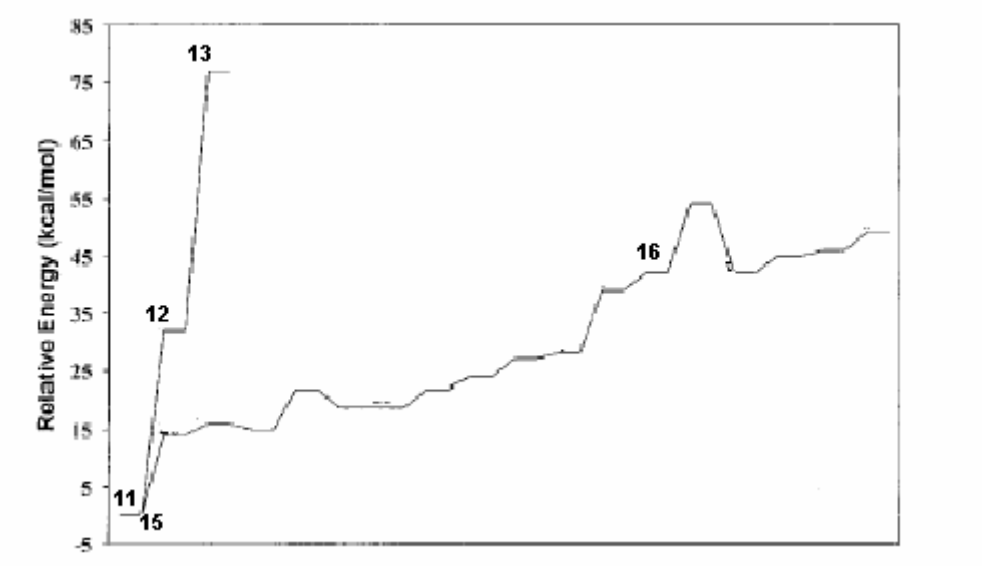

Figure 10. Schematic diagram representing the contrasting relative energies of the isomers of $Si_3H_3^+$ and $C_3H_3^+$. Isomer **14** is not shown in the diagram.

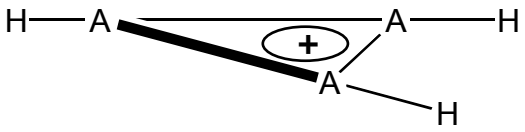

15

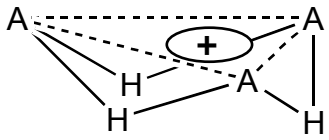

16

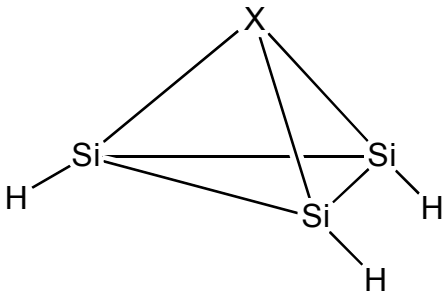

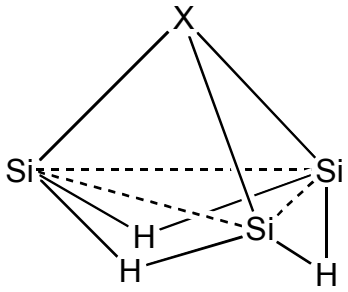

X=BH^-, CH, N, NH^+, NO, SiH, P, PH^+ and PO

17 **18**

Figure 11. **15** The classical structure for $A_3H_3^+$ (D_{3h}).
16 H-bridged structure for $A_3H_3^+$ (C_{3v}).
17 Pyramidal structure based on (**15**) (C_{3v}).
18 Pyramidal structure based on (**16**) (C_{3V}).

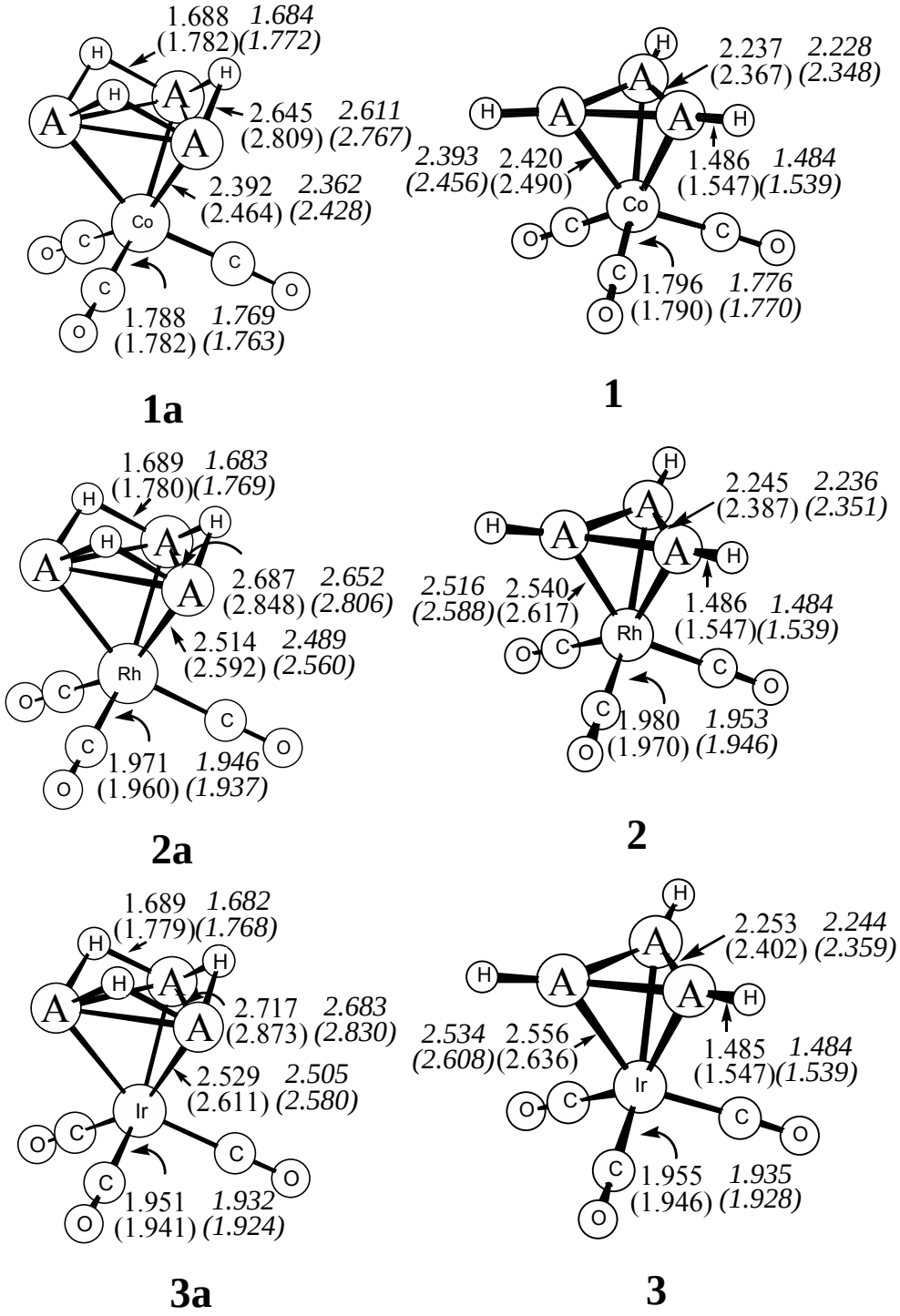

Figure 12. Optimized geometries and important bond distances for Si and Ge (in parentheses) at the B3LYP/B1 level. The values in italics are at the B3P86/B1 level. Structures **1-3** are given for comparison.

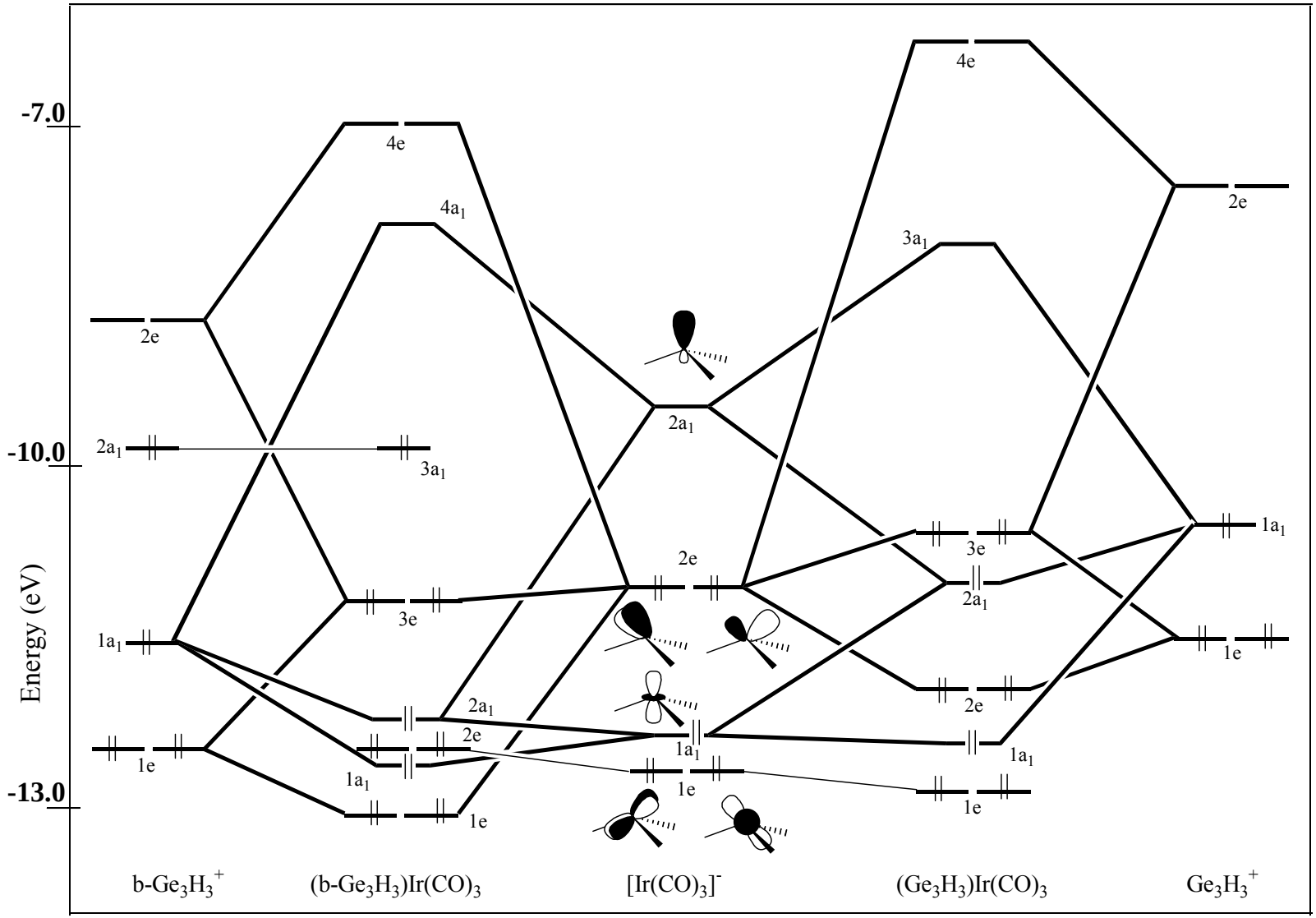

Figure 13. Interaction diagram between **16Ge** and $[Ir(CO)_3]^-$ leading to **1a–Ge** (on left) and between **15Ge** and $[Ir(CO)_3]^-$ leading to **1Ge** (on right). Only the HOMO electrons are shown.

Table 2. Relative energies (kcal/mol) [a] and NBO charges (in e) of the isomers shown in Figure 9 [b].

Structure	B3LYP/ B1	B3LYP/ B2	B3P86/ B1	NBO charges
1a-Si	0.0	0.0	0.0	Co:-0.47, Si:0.35, H:-0.24, C:0.48, O:-0.43
1-Si	7.2	6.7	6.1	
2a-Si	0.0	0.0	0.0	Rh:-0.30, Si:0.30, H:-0.24, C:0.47, O:-0.43
2-Si	5.5	5.7	4.0	
3a-Si	0.0	0.0	0.0	Ir:-0.13, Si:0.28, H:-0.24, C:0.43, O:-0.42
3-Si	8.9	8.9	7.1	
1a-Ge	0.0	0.0	0.0	Co:-0.42, Ge:0.33, H:-0.22, C:0.47, O:-0.43
1-Ge	31.4	31.0	28.0	
2a-Ge	0.0	0.0	0.0	Rh:-0.25, Ge:0.28, H:-0.23, C:0.46, O:-0.43
2-Ge	30.6	30.8	27.0	
3a-Ge	0.0	0.0	0.0	Ir:-0.07, Ge:0.26, H:-0.23, C:0.42, O:-0.43
3-Ge	34.0	34.2	30.2	

[a] Relative energies are calculated after scaling the zero-point energy by 0.9806.[34]

[b] All the compounds in Figure 9 are minima.

Chapter References

1. Apeloig Y., Karni M. in *Theoretical Aspects and Quantum Chemical Calculation of Silaaromatic Compounds. The Chemistry of Silicon Compounds, ed*. Z. Pappoport and Y. Apeloig, Wiley, New York, 1998, vol.2

2. (a) Bogey M., Bolvin H., Cordonnier M., Demuynck C., Destombes J. L., Csaszar A. G., *J. Chem. Phys*. 1994, *100*, 8614, (b) Grev R. S., Schaefer III H. F., *J. Chem. Phys*. 1992, *97,* 7990, (c) Codonnier M., Bogey M., Demuynck C., Destombes J. L., *J. Chem. Phys*. 1992, *97*, 6894, (d) Brenda T. C., Schaefer III H. F., *J. Phys. Chem*. 1990, *94*, 5593, (e) Koseki S., Gordon M. S., *J. Phys. Chem.* 1989, *93*, 118, (f) Kalcher J., Sax A., Olbrich G., *Int. J. Quantum Chem*., 1984, *25*, 543, (g) Binkley S., *J. Am. Chem. Soc*. 1984, *106*, 603, (h) Köhler H. J., Lischka H., *Chem. Phys. Lett*. 1984*, 112*, 33

3. (a) Palagyi Z., Schaefer III H. F., Kapuy E., *J. Am. Chem. Soc*. 1993, *115*, 6901, (b) Grev R. S., Deleeuw B. J., Schaefer III H. F., *Chem. Phys. Lett*. 1990, *165*, 257

4. Srinivas G. N., Kiran B., Jemmis E. D., *J. Mol. Struct. (THEOCHEM)* 1996, *361*, 205

5. Korkin A. A., Murashov V. V., Leszczynski J., Schleyer P. v. R., *J. Mol. Struct. (THEOCHEM)* 1996, *388*, 43

6. (a) Raghavachari K., *J. Chem. Phys*. 1992, *96*, 4440, (b) Curtiss I. A., Raghavachari K., Deutsch P. W., Pople J. A., *J. Chem. Phys*. 1991, *95*, 2433, (c) Al-Laham M. A., Raghavachari M., *J. Chem. Phys.* 1991, *95*, 2560, (d) Raghavachari K., *J. Chem. Phys.* 1991, *95*, 7373, (e) Colegrove B. T., Schaefer III H. F., *J. Chem. Phys*. 1990, *93*, 7230, (f) Köhler H. J., Lischka H., *Chem. Phys. Lett*. 1984, *112*, 33

7. (a) Srinivas G. N., Jemmis E. D., Korkin A. A., Schleyer P. v. R., *J. Phys. Chem. A*, 1999, *103*, 11034, (b) Korkin A. A., Glukovtsev M., Schleyer P. v. R., *Int. J. Quantum Chem*. 1993, *46*, 137

8. (a) Jemmis E. D., Srinivas G. N., Leszczynski J., Kapp J., Korkin A. A., Schleyer P. v. R., *J. Am. Chem. Soc*. 1995, *117*, 11361, (b) So S. P., *Chem. Phys. Lett.* 1999, *313*, 587

9. (a) Jemmis E. D., Srinivas G. N., *J. Am. Chem. Soc.* 1996, 1*18*, 3738, (b) Srinivas G. N., Jemmis E. D., *J. Am. Chem. Soc.* 1997, *119*, 12968

10. Srinivas G. N., Hamilton T. P., Jemmis E. D., McKee M. I., Lammertsma K., *J. Am. Chem. Soc*. 2000, *122*, 1725

11. (a) Jacobsen H., Ziegler H., *J. Am. Chem. Soc*. 1994, *116*, 3667, (b) Windus T., Gordon M. S., *J. Am. Chem. Soc*. 1992, *114*, 9559, (c) Triniquier G., *J. Am. Chem. Soc.* 1991, *113*, 144, (d) Trinquier G., Malrieu K., *J. Am. Chem. Soc.* 1991, *113*, 8634, (e) Curtiss L. A., Raghavachari K., Deutsch P. W., Pople J. A., *J. Chem. Phys*. 1991, *95*, 2433, (f) Karni M., Apeloig Y., *J. Am. Chem. Soc.* 1990, *112*, 8589, (g) Grev R. S., Schaefer III H. F., Baines K. M., *J. Am. Chem. Soc.* 1990, *112*, 9458, (h) Schleyer P. v. R., Kost D., *J. Am. Chem. Soc.* 1988, *110,* 2105, (i) Teramae H., *J. Am. Chem. Soc.* 1987, *109*, 4140, (j) Olbrich G., *Chem. Phys. Lett*. 1986, *130*, 115, (k) Krogh-Jespersen K., *J. Am. Chem. Soc*. 1985, *107*, 537, (l) Krogh-Jespersen K., *J. Phys. Chem*. 1982, *86*, 1492

12. (a) Bogey M., Bolvin H., Cordonnier M., Demuynck C., Destombes J. L., Császár A. G., *J. Chem. Phys.* 1994, *100*, 8614, (b) Grev R. S., Schaefer III H. F., *J. Chem, Phys.* 1992, *97*, 7990, (c) Cordonnier M., Bogey M., Demuynck C., Destombes J. L., *J. Chem. Phys*. 1992, *97*, 7984, (d) Bogey B., Bolvin H., Demuynck C., Destombes J. L., *Phys. Rev. Lett.* 1991, *66*, 413, (e) Brenda T. C., Schaefer III H. F., *J. Phys. Chem.* 1990, *94*, 5593, (f) Koseki S., Gordon M. S., *J.*

Phys. Chem. 1989, *93*, 118, (g) Kalcher J., Sax A., Olbrich G., *Int. J. Quantum Chem.* 1984, *25*, 543, (h) Binkley S., *J. Am. Chem. Soc.* 1984, *106*, 603, (i) Köhler H. J., Lischka H., *Chem. Phys. Lett.* 1984, *112*, 33, (j) Lischka H., Kohler H., *J. Am. Chem. Soc.* 1983, *105*, 6646

13. Srinivas G. N., Kiran B., Jemmis E. D., *J. Mol. Struct.: THEOCHEM* 1996, *361*, 205

14. (a) Wong M. W. and Radom L., *J. Am. Chem. Soc.* 1993, *115*, 1507, (b) López L., Sordo, J. A., Sordo T. L., *J. Chem. Soc. Chem. Commun*. 1993, 1751, (c) Maluendes S. A., Mclean A. D., Yamashita K, Herbst E., *J. Chem. Phys.* 1993, *99*, 2812, (d) Li W-K., Riggs N. V., *J. Mol. Struct. (THEOCHEM),* 1992, *257*, 189, (e) Raghavachari K., Whiteside R. A., Pople J. A. Schleyer P. v. R., *J. Am. Chem. Soc*. 1981, *103*, 5649

15. Srinivas G. N., Yu. L, Schwartz, M., *Organometallics* 2001, 20, 5200

16. (a) Becke A. D., *J. Chem. Phys*. 1993, *98*, 5648, (b) Lee C., Yang W, Parr R. G., *Phys. Rev. B* 1988, *37*, 785, (c) Vosko S. H., Wilk L., Nusair M., *Can. J. Phys.* 1980, *58*, 1200

17. (a) Becke A. D., *Phys. Rev. A* 1988, *38*, 3098, (b) Perdew J. P., *Phys. Rev. B* 1986, *33*, 8822

18. (a) Hehre W. J., Radom L., Schleyer P. v. R., Pople J. A., *Ab initio Molecular Orbital Theory*; Wiley, New York, 1986, (b) Hehre W. J., Ditchfield R., Pople J. A., *J. Chem. Phys*. 1972, *56*, 2257

19. Basis sets were obtained from the extensible Computational Chemistry Environment Basis Set Database, Version 1.0, as developed and distributed by the Molecular Science Computing Facility, Environmental and Molecular Sciences Laboratory, 99352, USA, and funded by the U. S. Department of Energy under contract DE-AC06-76RLO 1830. Contact David Feller, Karen Schuchardt, or Don Jones for additional information.

20. (a) Stevens W. J., Basch H., krauss M., *J. Chem. Phys*. 1984, *81*, 6026, (b) 612, (c) Cundari T. R., Stevens W. J., *J. Chem. Phys*. 1993, *98*, 5555

21. (a) Dolg M., Wedig U., Stoll H., Preuss H., *J. Chem. Phys*. 1987, *86*, 866, (b) Andrae D., Haeussermann U., Dolg M., Stoll H., Preuss H., *Theor. Chim. Acta,* 1990, *77*, 123

22. Pople J. A., Raghavachari K., Schlegel H. B., Binkley J. S., *Int. J. Quantum Chem. Symp.* 1979, *13*, 255

23. Gaussian 98, Revision A.9, Frisch M. J., Trucks G.W., Schlegel H. B., Scuseria, G. E., Robb M. A., Cheeseman J. R., Zakrzewski V. G., Montgomery J. A., Stratmann Jr.,R. E., Burant J. C., Dapprich S., Millam, J. M., Daniels A. D., Kudin

K. N., Strain M. C., Farkas O., Tomasi J., Barone V., Cossi M., Cammi R., Bennucci B., Pomelli C., Adamo C., Clifford S., Ochterski J., Petersson G. A., Ayala P. Y., Cui Q., Morokuma K., Malick, D. K., Rubuck A. D., Raghavachari K., Foresman J. B., Cioslowski J. J., Ortiz V. A., Baboul G., Stefanov B. B., Liu G., Liashenko A., Piskorz P., Komaromi I., Gomperts R., Martin R. L., Fox D. J., Keith T., Al-Laham M. A., Peng C. Y., Nanayakkara A., Challacombe M, P., Gill M. W., Johnson B., Chen W., Wong M. W., Andres J. L., Gonzalez C., Head-Gordon M., Replogle E. S. and Pople J. A. Gaussian, Inc., Pittsburgh PA, 1998.

24. We thank the National Computational Science Alliance (NCSA) for allotting the computational time on an SGI/CRAY Origin 2000 supercomputer (Grant CHE 000018N)

25. Reed A. E., Curtiss L. A., Weinhold F., *Chem. Rev*. 1988, *88*, 899

26. Cotton F. A., Wilkinson G., Murillo C. A., Bochmann M., *Advanced Inorganic Chemistry*, Wiley-Interscience, New York, 6th ed., 1999

27. (a) Fujimoto H., Hoffmann R., *J. Phys. Chem*. 1974, *78*, 1167, (b) Hoffman R., *Angew. Chem., int. Ed. Engl*. 1982, *21*, 711

28. Jemmis E. D., Hoffmann R., *J. Am. Chem. Soc.* 1980, *102*, 2570

29. For a detailed analysis on how σ-π mixing stabilizes both π^* and π (which contains six orbital delocalization) orbitals in H-bridged three membered systems, please see: Srinivas G. N. Ph. D. Thesis. University of Hyderabad, India, 1996; Jemmis E. D., Subramanian G., Srinivas G. N., *J. Am. Chem. Soc*. 1992, *114*, 7939

CHAPTER 5

SCALE FACTORS FOR C≡O VIBRATIONAL FREQUENCIES IN ORGANOMETALLIC COMPLEXES

Theoretical Determination of Vibration Frequencies

Introduction

The experimental vibrational spectrum is an important property of chemical compounds, which is of significant utility in their identification and in determination of the structure of newly synthesized materials [1]. The determination of vibrational frequencies by ab initio computational methods is becoming increasingly important. For example, the identification of experimentally observed reactive intermediates for which the theoretically predicted frequencies can serve as fingerprints. Quantum mechanical calculation of the vibrational frequencies has proven to be very helpful in analysis of the vibrational spectra and assignment of the various modes. However, it is found that, almost invariably, computed frequencies are greater than experiment due to the assumption of harmonic potential, basis set deficiencies and the lack of (or incomplete) treatment of electron correlation effects [2-18]. The overestimation of ab initio harmonic vibrational frequencies is found to be relatively uniform. For example, the theoretical HF harmonic frequencies were generally found to be 10-15% too high, partly because of the neglect of anharmonic effects and partly because of the inherent limitations of HF theory.

To compensate for these deficiencies, multiplicative scale factors have been developed for a number of methods and basis sets, and have led to fairly satisfactory agreement with observed fundamentals [18]. For example, a scale factor 0.89 was

proposed in 1981 for HF/3-21G after extensive comparison with a large experimental dataset [4]. Other calculations at the HF/6-31G (d) level gave similar results and a standard scale factor of 0.8929 is now widely used for the prediction of fundamental frequencies at this level [5]. At MP2/6-31G (d) level, Hout, Levi and Hegre were the first to use a set of 36 molecules with atoms up to fluorine and determined a scale factor of 0.921 best fit the observed fundamental frequencies in 1982 [7]. In a later study by DeFrees and McLean, somewhat larger scale factors (0.96 for first-row molecules and 0.94 for second-row molecules) were determined by an average of the experimental/theoretical frequency ratios for individual modes, a procedure that is likely leading to some distortions if there are significant errors for low-frequency vibrations [8]. Other more sophisticated correlated methods were also reported in literature to determine the scale factors on harmonic vibrational frequencies. Procedures such as QCISD, CCSD, and CCSD (T) have been shown by several researchers to provide excellent agreement with experimental harmonic frequencies when used with a variety of basis sets (double zeta plus polarization and larger). However, these studies have been generally limited to small polyatomic molecules because the computational cost of these methods is very expensive. Currently available scale factors have been derived based upon experimental data for organic and main group inorganic compounds. There has been no scale factors available derived for use in transition metal complexes.

C≡O Stretching Frequencies in Organometallics

In organometallic complexes, ligands have a very different electronic environment from organic groups because of synergistic ligand-metal and ligand-ligand

interactions. The C≡O stretching frequencies in transition metal carbonyls have proven particularly useful in the study of these complexes because they exhibit very intense IR bands in an isolated region of the spectrum (~1900-2100 cm^{-1}) and the frequencies (and patterns) are very sensitive to the complex's structure and the C≡O's interactions with other ligands [19].

To better interpret and analyze transition metal carbonyl spectra, a series of theoretical calculations were carried out in this study to investigate systematic errors and derive scale factors for C≡O stretching vibrations in these complexes. The large majority of metal carbonyls have linearly bonded CO's (M-C≡O). Therefore, our investigation was restricted to this type of bonding, and was excluded those complexes with bridging or π-complexed CO's.

Because they are comparatively large molecules, it is difficult to perform higher level ab initio computations on organometallic complexes. Hence, the majority of studies of these species have utilized the basic Hartree-Fock method [20-22], typically with modest sized basis set (most commonly 6-31G (d)). However, one expects electron correlation effects to be significant in these systems, and a correlated treatment should be utilized in order to obtain accurate results [23-29]. Fortunately, the advent of density functional theory (DFT) [30-32] has provided an alternative means of including electron correlation in the study of the vibrational frequencies of organometallic complexes with comparable computer time to HF while the accuracy of the results are comparable to much more expensive ab initio treatments, such as MP2, CCSD, etc. Pople *et al* have shown that B-LYP/6-31G (d) harmonic vibrational frequencies reproduce observed fundamentals with surprising accuracy. They found an average

error of only 13 cm^{-1} for a small set of molecules with up to three heavy atoms. In another study, Rauht and Pulay developed scaling factors for the B-LYP/6-31G (d) method based on a set of 20 small molecules with a wide range of functional groups. Their overall frequency scale factor for the B-LYP/6-31G (d) method was determined to be 0.990 with an RMS (root mean square) deviation of 26 cm^{-1}. Rauhut and Pulay also developed a scaling factor, 0.963, for the B3LYP/6-31G (d) method that resulted in a slightly lower overall RMS deviation of 19 cm^{-1}. It has been well documented that one such hybrid DFT method, B3LYP, yields reasonably accurate results on organometallic complexes [33-36].

In this study, a total of 31 organometallic complexes with accurately measured C≡O frequencies were investigated. They span the range of transition metals from Cr-Ni in the third row, Mo-Pd in the fourth row and W-Pt in the fifth row and contain a variety of ancillary ligands. The most commonly used methods in computational organometallic chemistry, HF and B3LYP, were used, because compounds of interest are organometallics involving transitional metals beyond third row in the periodic table. It is computationally expensive to use higher level correlated methods, such as MP2, QCISD and CCSD, etc on such complexes. Whereas, HF and B3LYP methods have been proven to give comparable accurate results using much less computational time.

Results and Discussion

Computational Methods

All the calculations in this part of work were carried out with the GAUSSIAN-98 program package [37]. The geometries of all the structures were optimized using the

HF and B3LYP methods. The two most commonly used relativistic effective core potentials (ECP), SBKJC-21G [38-40] and Lanl2DZ [41-43], and their associated basis sets were used for the metals. The standard 6-31G (d) together with SBKJC-21G ECP is represented as basis set B1, and B2 represents the combination of Lanl2DZ and 6-31G (d). The data set consisted of 31 complexes with a total of 46 carbonyl frequencies are listed in Table 3.

Scale Factor Determination

It is well known that there are three sources of error in quantum mechanically computed vibrational frequencies: (1) the assumption of a harmonic force field; (2) the neglect or inadequate treatment of electron correlation effects; and (3) basis set deficiencies [18]. Therefore, it is common to multiply computed vibrational frequencies by a scale factor developed to minimize the RMS error from experiment for a test set of accurately measured frequencies.

Scott and Radom [18] have developed an extensive set of vibrational scale factors for a number of levels of calculation and basis sets, based upon fits to a very large experimental data set (composed of 122 organic and inorganic molecules and 1066 experimental frequencies, including stretches, bends and torsions). The optimum scaling factors λ was determined through a least-squares procedure by minimizing the residuals

$$\Delta = \sum_{i}^{all} (\lambda \omega_i^{cal} - \tilde{\nu}_i^{expt})^2 \qquad (9.1)$$

leading to

$$\lambda = \sum_{i}^{all} \omega_i^{cal} \tilde{\nu}_i^{expt} / \sum_{i}^{all} (\omega_i^{cal})^2 \qquad (9.2)$$

where ω_i^{cal} and $\tilde{\nu}_i^{expt}$ are the *i*th theoretical harmonic and *i*th experimental fundamental frequencies (in cm^{-1}), respectively. After the optimum scaling factor λ is obtained, a minimized residual, Δ_{min}, was calculated for each mode

$$\Delta_{min} = (\lambda \omega_i^{cal} - \tilde{\nu}_i^{expt})^2 \qquad (9.3)$$

Then the molecular root mean square error (rms_{mol}) was defined as

$$rms_{mol} = (\sum_{i}^{n_{mol}} \Delta_{min} / n_{mol})^{1/2} \qquad (9.4)$$

where the sum is over all the modes of a particular molecule (n_{mol}). The overall root mean square error (rms_{ov}) is defined as

$$rms_{ov} = (\sum_{i}^{n_{all}} \Delta_{min} / n_{all})^{1/2} \qquad (9.5)$$

where the sum is over all of the modes for all of the molecules considered (n_{all}). The scale factors, 0.8953 and 0.9614, were obtained at HF/B1 and B3LYP/B1 levels, respectively.

Improvement on Generic Scale Factors

In this study, the generic scale factors obtained by Scott and Radom [18] were first tested on the complexes. As shown in Table 4, utilization of the scale factor 0.8963 for HF/B1 and HF/B2 frequencies yielded extremely large RMS and average errors on the order ~100 cm^{-1}. Hence, calculations were carried out to find the appropriate scale factors at the HF/B1 and HF/B2 levels to compare with the generic scale factors. Following the standard procedures, the total squared error of equation (9.1) was

computed, where ω_i^{cal} is the computed harmonic frequency, $\tilde{\nu}_i^{expt}$ is the measured (anharmonic) value and λ is the scale factor. The sum is over all 46 experimental frequencies (Table 3). The scale factor for each method is determined by the value of λ which minimizes Δ^2. The residual deviations of the scaled frequencies from experiment are given in Table 3. The complexes and experimental C≡O frequencies are contained in the first two columns of Table 3. The literature references for the experimental data are displayed in the third column of the table. Comparison of different scale factors with RMS and average errors are given in Table 4.

The present scale factors for HF/B1 and HF/B2 (~0.85) are significantly smaller compared to the generic value (0.8953) for HF/6-31G (d). It is not surprising that the scale factor for these vibrations will be less than the value developed primarily for the vibrations of singly bonded atoms, because the correlation effects is much greater than the norm in triply bonded C≡O due to the close proximately of a large number of bonding electrons.

It's already noted that the generic scale factor, 0.8953, for the HF/B1 and HF/B2 frequencies generated large RMS and average errors; it is interesting to note that the general scale factor, 0.9614, available in literature at B3LYP/6-31G(d) level worked fine for the metal carbonyls. The agreement of the scaled frequencies is quite acceptable, with the RMS error 32 cm^{-1} and 36 cm^{-1} at B3YLP/B1 and B3LYP/B2 levels, respectively. Such errors represent an approximately 1.6% from the average experimental frequency (~2000 cm^{-1}). Our attempt to improve the scale factors at B3LYP level has resulted in values ~0.95 (Table 4) for both B1 and B basis sets, which is quite similar to the generic scale factor. Hence, only errors from experimental

frequencies using the generic scale factor are shown in Table 3. The scaled frequencies with 0.9550 (Table 4) gave an RMS error of 30 cm^{-1} corresponding to 1.5% error from the average experimental frequencies. Thus the newly developed scale factors for B3LYP level yields only 0.1% improvements relative to the generic one.

As noted from Table 4, the two basis sets, B1 and B2, yield very similar errors for a given level of calculation (HF or B3LYP). This is not really surprising, as both B1 and B2 utilize the 6-31G (d) basis to characterize ancillary ligands, and differ only in the ECP used to describe the central metal. Therefore, any differences in computed C≡O frequencies arise only indirectly from differences in characterization of the M-C bonds.

Error Analyses

The relative RMS errors of the B3LYP frequencies ~32 cm^{-1} imply that the calculations give comparably accurate results. However, this is a result of several outlier frequencies, notably in $CoH(CO)_4$, $Rh(Co)H(PH_3)_3$, $Ir(CO)Cl(PH)_3)_2H_2$ and $ReCl(CO)(PPh_3)_4$ (Table 3), which inflate that net errors.

A better comparison of the scaled HF and B3LYP frequencies is afforded by the distribution of errors, which is summarized in the last three columns of Table 4. It is observed from the table that only 35-40% of the computed HF frequencies lie within 1% of experiment (when new scale factors are used). However, there are over 60% of the B3LYP frequencies are within 1% of accuracy. In addition, only 15-20% of the B3LYP frequencies are more than 2% from experiment (corresponding to the four outliers named above and $Ni(CO)(PH_3)_3$), compared to 25-30% of the HF frequencies. Thus, it

may be concluded that scaled vibrational frequencies computed using the B3LYP functional are significantly more reliable than those obtained at the Hartree-Fock level.

The greater reliability of the B3LYP frequencies is actually not surprising. As noted above, one expects markedly greater electron correlation effects in the triply bonded carbonyls than in most vibrations. Therefore, the B3LYP method is better able to predict variations in electron correlation resulting from changes in the C≡O's bonding environment than is the Hartree-Fock method, in which correlation effects are assumed to be a constant in all systems, incorporated into the scale factor.

Conclusions

In this study, scale factors have been developed to correct computed harmonic vibrational frequencies of the C≡O stretching modes in metal carbonyls using two of the most common levels of calculation (HF and B3LYP) and two widely used metal effective core potentials (ECP) (SBKJC-21G and Lanl2DZ). It is observed that B3LYP scale factor available in the literature (0.9614) works very wells for the transition metal C≡O vibrational frequencies. However, the Hartree-Fock scale factors found here are markedly lower than those proposed for general systems, and can be attributed to the greater amount of electron correlation present in the triply bonded carbonyls than found in most bonds. Scaled B3LYP frequencies are significantly more reliable than those obtained from HF calculations because the former method can explicitly account for variations in electron correlation with changing bonding environments.

Table 3. Experimental data and errors in scaled frequencies.[a]

Structure	Expt	Ref[b]	With generic scale factor[c]		With New scale factor[d]		With generic scale factor[c]	
			HF/B1	HF/B2	HF/B1	HF/B2	B3LYP/B1	B3LYP/B2
$Ni(CO)_4$	2057.00	60,61	57.7	71.13	-45.43	-39.56	-14.02	-4.41
$Ni(CO)(PH_3)_3$	1923.00	47	120.97	140.67	21.29	33.33	61.33	72.87
$Pd(CO)_4$	2066.00	62,63	86.3	90.78	-18.66	-21.40	-10.53	-8.60
$Pd(CO)(PH_3)_3$	1955.00	48	159.7	161.49	56.57	51.40	52.40	57.21
$Pt(CO)_4$	2049.00	62,63	77.34	80.92	-26.36	-29.87	-7.95	-9.87
$Pt(CO)Cl_2PH_3$	2135.00	49,50	105.04	110.41	-4.20	-6.38	-17.04	-11.27
$RhF(CO)(PH_3)_2$	1971.00	53	141.01	68.53	38.02	-45.09	-64.37	-53.80
$CoH(CO)_4$	2116.00	51,52	-50.77	111.84	-50.77	-0.77	-20.60	-8.10
	2053.00		-10.77	134.84	-10.77	22.23	1.44	13.94
	2030.00		12.23	158.92	12.23	48.13	19.10	27.75
$RhCl(CO)(PH_3)_2$	1980.00	53	142.76	160.66	39.24	49.32	18.75	27.40
$Rh(CN)(CO)(PH_3)_2$	2003.00	53	134.98	147.51	30.72	35.65	12.09	19.79
$Rh(CO)H(PH_3)_3$	1923.00	54	184.54	197.97	81.76	87.65	83.44	90.17
$IrF(CO)(PH_3)_2$	1957.00	53	80.7	83.39	-18.67	-22.74	22.52	24.45
$IrCl(CO)(PH_3)_2$	1965.00	53	88.82	93.29	-11.34	-13.77	23.18	28.94
$Ir(CN)(CO)(PH_3)_2$	1990.00	53	87.99	90.68	-13.34	-17.55	12.60	16.44
$Ir(CO)Cl(PH_3)_2H_2$	1982.00	54	181.94	187.31	76.41	74.48	87.89	85.01
$Fe(CO)_5$	2022.00	64,65	141.04	152.68	35.56	39.57	11.36	15.21
	2000.00		-14.22	18.90	-111.06	-86.11	4.52	15.09
$CpFe(CO)_2Cl$	2061.00	55,56	173.67	182.62	64.69	65.92	0.24	9.86
	2019.00		212.09	221.94	103.29	105.38	13.40	25.90
$Ru(CO)_5$	2035.00	66	106.56	106.56	2.12	-4.83	6.05	5.09
	1999.00		89.73	86.15	-12.12	-22.30	11.29	8.40
$Os(CO)_5$	2034.00	66	78.01	82.49	-24.98	-27.60	-2.56	0.32
	1991.00		63.71	64.61	-36.49	-42.31	5.83	7.75
$OsCl(CO)(PH_3)_3H$	1912.00	54	118.54	124.81	19.52	18.87	43.49	54.06

(table continues)

Table 3 (*continued*).

$[Mn(CO)_6]^+$	2094.00	67	135.3	142.46	26.58	26.13	16.27	19.16
$[Mn(CO)_5]^-$	1898.00	68	62.71	68.97	-32.91	-33.34	16.15	19.99
	1863.00		50.26	57.42	-43.05	-42.47	19.42	27.11
$[Re(CO)_6]^+$	2085.00	69	95.06	97.74	-11.26	-15.79	5.08	7.97
$ReCl(CO)_5$	2056.00	57	73.92	78.40	-29.95	-32.62	-16.87	-13.99
	1987.00		64.13	73.09	-35.89	-34.07	4.06	10.79
Tr-$ReCl(CO)_3(PPh_3)_2$	2049.00	58	85.4	91.66	-18.69	-19.68	4.55	12.24
	1954.00		117.72	123.99	16.69	15.91	20.72	28.41
	1904.00		90.73	102.37	-6.55	-1.99	38.03	48.60
Tr-$ReBr(CO)_3(PPh_3)_2$	2060.00	58	73.5	78.87	-30.54	-32.38	-6.45	0.28
	1960.00		110.83	117.99	9.84	9.91	15.68	22.41
	1910.00		87.41	98.16	-9.99	-6.29	32.99	43.56
$ReCl(CO)(PPh_3)_4$	1790.00	58	148.32	164.44	53.80	62.78	103.00	119.34
$ReBr(CO)_4PPh_3$	2104.00	59	63.52	68.00	-42.18	-44.98	-10.07	-6.23
	2019.00		85.85	91.22	-16.79	-18.54	1.86	6.67
	2001.00		103.85	108.33	1.21	-1.39	10.25	15.06
	1939.00		88.85	98.70	-10.04	-7.29	29.95	37.64
$W(CO)_6$	1998.00	70	53.13	61.19	-46.89	-45.92	-7.90	-2.13
$Mo(CO)_6$	2003.00	70	74.1	75.89	-27.20	-32.24	-1.37	-2.33
$Cr(CO)_6$	2000.00	70	84.26	89.63	-17.38	-19.06	3.56	6.44

[a] in cm^{-1}
[b] refers to experimental reference numbers in text.
[c] the generic scale factors 0.8953 (HF) and 0.9614 (B3LYP) are from ref. 18.
[d] for new scale factors refer Table 4.

Table 4. Scale factors and errors.[a]

Method	Scale Factor	RMS Err. (AVG. Err)	0-1% Error	1-2% Error	>2% Error
HF/B1	0.8953[b]	106.6 (93.9)	6%	0%	94%
HF/B2	0.8953[b]	116.9 (109.1)	2%	0%	98%
HF/B1	0.8516	40.0 (-1.6)	41%	35%	24%
HF/B2	0.8487	40.4 (-0.5)	35%	35%	30%
B3LYP/B1	0.9614[b]	32.0 (13.8)	70%	15%	15%
B3LYP/B2	0.9614[b]	35.8 (19.8)	59%	21%	20%
B3LYP/B1	0.9550	29.1 (0.3)	63%	26%	11%
B3LYP/B2	0.9521	30.1 (0.4)	61%	28%	11%

[a] RMS and Average Errors in cm^{-1}
[b] The scale factors are from ref. 18.

Chapter References

1. Norman B.C., Lawrence H. D., Stephen E. W., *Introduction to INFRAREd and Raman Spectroscopy, 3ed*., 1990, San Diego, CA

2. Pulay P., *Mol. Phys.* 1969, *17*, 197

3. Pople J. A., Krishnan R., Schlegel H. B., Bimkley J. S., *Int. J. Quantum Chem. Symp.* 1979, *13*, 225

4. Pople J. A., Schlegel H. B., Krishnan R., Defrees D. J., Binkley J. S., Frisch M. J, Whiteside R. A., Hout R. F., Hehre W. J., *Int. J. Quantum Chem. Symp.* 1981, *15*, 269

5. Pople J. A., Head-Gordon M, Fox D. J., Raghavachari K., Curtiss L. A., *J. Chem. Phys.* 1989, *90*, 5622

6. Curtiss L. A., Raghavachari K., Trucks G. W., Pople J. A., *J. Chem. Phys.* 1991, *94*, 7221

7. Hout R. F., Levi B. A., Hehre W. J., *J. Comput. Chem.* 1982, *3*, 234

8. DeFrees D. J., McLean A. D., *J. Chem. Phys.* 1985, *82*, 333

9. Handy N. C., Amos R. D., Gaw J. F., Rice J. E., Simandiras E. D., *Chem. Phys. Lett.* 1985, *120*, 151

10. Hendre W. J., Radom L., Schleyer P. V. R., Pople J. A., *Ab Initio Molecular Orbital Theory,* Wiley, New York, 1986

11. Healy E. F., Holder A., *J. Mol. Struct.* 1993, *281*, 141

12. Pople J. A., Scott A. P., Wong M. W., Radom L., *Isr. J. Chem.* 1993, *33*, 345

13. Harris N. J., *J. Phys. Chem*. 1995, *99*, 14689

14. Rauhut G., Pulay R., *J. Phys. Chem*. 1995, *99*, 3093

15. Bauschlicher C. W., Patriadge H., *J. Chem. Phys.* 1995, *103*, 1788

16. Finley J. W., Stephens P. J., *J. Mol. Struct. (Theochem)* 1995, *357*, 225

17. Peterson P. E., Abu-Omar M., Johnson T. W., Parham R., Goldin D., Henry C., Cook A., Dunn K. M., *J. Phys. Chem.* 1995, *99*, 5927

18. Scott A. P., Radom L., *J. Phys. Chem*. 1996, *100*, 16502

19. Braterman P. S., *Metal Carbonyl Spectra, Academic press,* New York, 1975

20. Frenking G., Antes I., Böhme M., Dapprich S., Ehlers A., W., Jonas V., Neuhaus A., Otto M., Stegmann R., Veldkamp A., Vyboishchikov S. F., in: Lipkowitz K. B., Boyd D. B., et al. (Eds.), *Reviews in Computational Chemistry,* vol 8, VCH, New York, 1996, p. 63

21. Cundari T. R., Benson M. T., Lutz M. L., Sommerer S. O., in: Lipkowitz K. B., Boyd D. B. (Eds.), *Reviews in Computational Chemistry,* vol 8, VCH, New York, 1996, p. 145

22. Please see the special issue on Computational Transition Metal Chemistry, *Chem. Rev*. 2000, *100*, issue 2

23. Thomas J. R., Deleeuw B. J., Vacek G., Schaefer H. F., *J. Chem. Phys.* 1993, *98*, 1336

24. Thomas J. R., Deleeuw B. J., Veck G., Crawford T. D., Yamaguchi Y., Schaefer H. F., *J. Chem. Phys*. 1993, *99*, 403

25. Martin J. M. L., *J. Chem. Phys.* 1994, *100*, 8186

26. Martin J. M. L., Taylor P. R., *Chem. Phys. Lett.* 1994, *225*, 473

27. Martin J. M. L., *Chem. Phys. Lett.* 1995, *242*, 343

28. Csazar A. G., Allen W. D., *J. Chem. Phys.* 1994, *100*, 2746

29. Oliphant N. Bartlett R. J., *J. Chem. Phys*. 1994, *100*, 6550

30. Hutter J. Luthi H. P., Diederich F., *J. Am. Chem. Soc.* 1994, *116*, 750

31. Barone V., Adamo C., Lelj F., *J. Chem. Phys.* 1995, *102*, 364

32. Rauhut G., Pulay P., *J. Am. Chem. Soc*. 1995, *117*, 4167

33. Becke A. D., *J. Chem. Phys.* 1993, *98*, 5648

34. Lee C., Yang W., Parr R. G., *Phys. Rev. B* 1998, *37*, 785

35. Vosko S. H., Wilk L., Nusair M., *Can. J. Phys*. 1980, *58*, 1200

36. Niu S., Hall M. B., *Chem. Rev.* 2000, *100*, 353

37. Frisch M. J., Trucks G. W., Schlegel H. B., Scuseria G. E., Robb M. A., Cheeseman J. R., Zakrzewski V. G., Montgomery Jr. J. A., Stratmann R. E., Burant J. C., Dapprich S., Millam J. M., Daniels A. D., Kudin K. N., Strain M. C., Farkas O., Tomasi J., Barone V., Cossi M., Cammi R., Mennucci B., Pomelli C., Adamo C., Clifford S., Ochterski J., Petersson G. A., Ayala P. Y., Cui Q., Morokkuma K., Malick D. K., Rabuck A. D., Raghavachari K., Foresman J. B., Cioslowski J., Ortiz J. V., Baboul A. G., Stefanov B. B., Liu G., Liashenko A.,

Piskorz P., Komaromi I., Gomperts R., Martin R. L., Fox D. J., Keith T., Al-Laham M. A., Peng C. Y., Nanayakkara A., Challacombe M., Gill P. M. W., Johnson B., Chen W., Wong M. W., Andres J. L., Gonzalez C., Head-Gordon M., Replogle E. S., Pople J. A., GAUSSIAN 98, Revision A. 9, Gaussian, Inc., Pittsburgh PA, 1998

38. Stevens W. J., Basch H., Krauss M., *J. Chem. Phys.* 1984, *81*, 6026

39. Stevens W. J., Krauss M., Basch H., Jasien P. G., *Can. J. Chem.* 1982, *70*, 612

40. Cundari T. R., Stevens W. J., *J. Chem. Phys.* 1993, *98*, 5555

41. Hay P. J., Wadt W. R., *J. Chem. Phys*. 1985, *82*, 270

42. Wadt W. R., Hay P. J., *J. Chem. Phys.* 1985, *82*, 284

43. Hay P. J., Wadt W. R., *J. Chem. Phys.* 1985, *82*, 299

CHAPTER 6

A COMPUTATIONAL STUDY ON C/Si/Ge BIOISOSTERISM

Background Information

Hormones, in particular the sex hormones, were the first growth factors discovered to be involuntary helpers of cancers. Female breast cancer and male prostate cancer are hormone-dependent. Shutting down the main production sites of sex hormone either by removing the ovaries or by castration is a well-known and most effective therapy; however these procedures are irreversible operations and can cause psychological stress. Modern hormone therapy attempts to spare the patient such procedures by using hormone antagonists. The releasing hormone LHRH (luteinizing hormone-releasing hormone, which is also known as gonadorelin (GnRH)), together with its specific receptor plays an important role in neuroendocrinology [1-3]. The decapeptide LHRH is synthesized in hypothalamic neurons and is secreted into the blood stream. Ultimately it stimulates secretion of the sex-specific hormones in testes and ovaries. The LHRH antagonists can be employed to hinder deployment of the hormone itself and its promoting activity [4]. Cetrorelix (Ac-D-Nal^{1}-4-Cl-D-Phe^{2}-D-Pal^{3}-Ser^{4}-Tyr^{5}-D-Cit^{6}-Leu^{7}-Arg^{8}-Pro^{9}-D-Ala^{10}-NH_2, Figure 14) is a highly active LHRH antagonist, which is used in the hormone-dependent tumor treatment [5-6]. It was used in various laboratories as lead structure for the discovery of stable derivatives with good aqueous solubility and long-lasting *in vivo* activity [7]. One looks for modifications particularly at positions 5, 6 and 7 [8-12]. One of these modifications is to add unnatural side chains to the pure amino acids.

Synthetic unnatural amino acids have been proven useful for probing the structural requirements for the biological activity of numerous peptides and proteins, and have also been used as building blocks for the synthesis of novel biologically active peptides [13-16]. In addition, unnatural amino acids have been of interest as precursors of drugs and plant-protective agents. Group 14 elements have generated much interest in the past decade [17-20]. The heavier elements Si and Ge share many of the same properties with carbon. However, unlike their carbon analogs, which have been extensively studied, the Si and Ge-containing compounds' chemical and pharmacological properties are less understood. A series of Si and Ge-containing amino acids in the form of $H_2NCH(CH_2SiR_3)COOH$ and $H_2NCH(CH_2GeR_3)COOH$ (R=Me, Me_2Ph) were synthesized and reported (**4Si, 4Ge, 5Si and 5Ge**) [21]. They are listed in Figure 15 together with their C analogs (**4C** and **5C**). Another Si-containing compound, $H_2NCH(CH_2SiMe_2CH{=}CH_2)COOH$ (**6**), was also synthesized and its structure is included in Figure 15. The biological activities of these synthetic unnatural amino acids were tested by introducing in the decapeptides and were compared with their C analogs [21].

The decapeptides **1–3** (Figure 16) with the unnatural Si- and Ge-containing amino acids were synthesized and studied by Tacke *et al* in their systematic studies on bioorganosilicon and bioorganogermanium chemistry [17-20]. The decapeptides are derivatives of Cetrorelix. They only differ from Cetrorelix on the residue at position 5. The Cetrorelix bears an (S)-tyrosine residue at position 5 while the synthesized decapeptides **1–3** have synthetic unnatural amino acids, Me_3El-Ala (El=C, Si and Ge), instead. The decapeptides **1–3** were characterized by *in vitro* and *in vivo* studies. The

results show that they all behave as potent LHRH antagonists. The *in vitro* study used the recombinant cell lines as the human LHRH. The results show that the binding affinities (Ka values) of **1–3** for the human LHRH receptor are quite similar, but slightly lower compared with the reference compound Cetrorelix. These findings are in accordance with the results of the antagonistic potencies (IC_{50} values). Thus, incorporation of the Me_3El-Ala (El=C, Si and Ge) at position 5 of Cetrorelix causes a marginal reduction in both binding affinity and antagonistic potency, whereas these properties are quite similar in C/Si/Ge analogs **1–3**.

The decapeptides **1–3** were also studied for their *in vivo* activity in the male rat. All three compounds produced an immediate and strong decrease of hormone levels. However, Si and Ge-containing decapeptides, **2** and **3**, showed much longer lasting effect than C-containing decapeptide **1**. In a short conclusion, the Si and Ge-containing decapeptides **2** and **3** showed an advantage over their carbon analog **1** *in vivo*, but no significant differences between the Si/Ge analogs **2** and **3** could be detected *in vivo* settings.

The results reported clearly demonstrate that Si and Ge-substituted amino acids may be a useful tool to improve the biological properties of peptides, however, the improved *in vivo* activities of **2** and **3** cannot yet be explained in terms of differences in the chemical and physicochemical properties. In this study, we have performed a computational investigation of decapeptides **1–3**. We focused our studies on residues at position 5 of decapeptides. The residues studied include Si and Ge-containing compounds and their C analogs (**4C**, **4Si**, **4Ge**, **5C**, **5Si** and **5Ge**). We have studied

their chemical and electronic properties with a goal to explain the improvement of Si and Ge-containing compounds over their C analogs.

Results and Discussion

Computational Methods

All the calculations were carried out with the Gaussian-98 program package. The geometries of all the structures were optimized using the HF, MP2 and DFT method at B3YLP level. Some molecules were optimized with CCSD for comparison. The standard 6-31G(d) basis set was used; later the 6-311G(d, p) basis set was also used on some molecules for comparison purposes. The combinations of the B3LYP method with 6-31G(d) and 6-311G(d, p) basis sets are denoted as D1 and D2, respectively.

Justification of the Theoretical Methods

Before the theoretical study of decapeptides, two studies were carried out to justify the theoretical methods chosen in this study and to examine the effectiveness and efficiency of the combination of basis sets and theoretical levels. First, three natural amino acids, which are structurally similar to **4–5**, such as leucine (Leu), Isoleucine (Ile) and valine (Val) (Figure 17), were chosen as standards. The theoretical results would be compared with the experimental data from literature to see if the chosen combination of theoretical levels and basis sets are appropriate for this research. Then, calculations were carried out on Methyl/Silyl/Germyl Alanine **7** (Figure 18, **7C** is Methyl alanine, **7Si** is Silyl alanine and **7Ge** is Germyl alanine), which is a

simple version of **4–5**; only the R groups were replaced with three hydrogen atoms around the C, Si and Ge to simplify the calculation process. It is believed that the simplified molecules will provide an adequate test of the combination of theoretical methods and basis sets, but at lower computational cost.

Results and Discussion

First, theoretical calculations were carried out on the natural amino acids, leucine, isoleucine and valine. The calculated bond distances, bond angles and dihedral angles were compared with experimental data for the degree of agreement, in order to justify the chosen theoretical methods.

The structures of amino acids in our theoretical studies were based on the crystal structures available in the literature. The crystal structures of isoleucine and valine are cations with terminals NH_3^+ and COOH; and the structure of leucine is neutral with terminal NH_3^+ and COO^- groups. The range of the experimental data was obtained for all major bond distances, bond angles and dihedral angles involving C, N and O elements. Since all the bond angles were found to be very close to experimental data, they are not listed in the following tables. Only bond distances and dihedral angles are discussed. All the bond distances calculated at the B3LYP level are longer than those calculated at the HF and MP2 levels (Tables 5-7).

Table 5 lists the results of theoretical calculations for leucine compared with the experimental data of nineteen crystal structures from literature. The last two columns list the range, MIN and MAX, of the experimental data. All the calculated bond distances involving only C atoms are within the experimental data range. The

calculated C and O double bond (C1=O20) in the –COOH group and the single bond between C and N (C2–N19) were a little bit shorter than the MIN of experimental data (0.0051Å and 0.015 Å shorter, respectively) at HF level, while the C and O (C1–O21) single bond lengths in the –COOH group is a little bit over the MAX range (0.001 Å). The possible reasons for the difference will be discussed below. Dihedral angles involving only C atoms (C1-C2-C3-C4, C2-C3-C4-C5 and C2-C3-C4-C6) are within a 4-degree range from the experimental data. For dihedral angles involving N and O atoms, the differences are larger. Although we don't know the exact reasons for such differences, the probable reasons are counter ion/molecule effects and crystal packing effects in the molecule. In crystal structures of leucine, some have dimer structures and some have counter ion/molecule, such as H_2O, sulfonic acid and NO_3^-, which may offset negative and positive charges of NH_3^+ and COO^- or may incur hydrogen bond between NH_3^+ and COO^- of leucine. In contrast, the leucine molecule studied theoretically is a single isolated molecule without counter ions. Therefore, it lacks the unknown crystal packing effects that the experimental crystal molecules have, which may result in the differences in the bond distances and dihedral angles involving N and O atoms.

Similar results were also obtained for amino acids isoleucine and valine. The theoretical and experimental data for isoleucine and valine are listed in Table 6 and Table 7, respectively. Eighteen crystal structures from the literature were used for comparison for isoleucine and nine crystal structures were used in the case of valine. All the calculated bond distances are within the experimental data range for isoleucine except the double bond between C and O (C1=O21) in the –COOH group. It is

calculated to be 0.0177 Å shorter than the experimental value at HF level. The single bond between C1 and O20 is a little big longer at D1, D2 and MP2. Again, most calculated bond distances are within the range of experimental values for valine except those involving terminal O and N atoms. For example, the double bond between C1 and O19 is 0.0054 Å shorter than the MIN range at HF level. The C1–O20 is 0.0032 Å longer than the MAX using MP2. And the calculated C2–N18 bond is all a little bit over the MAX range of experimental data. Dihedral angles involving only C atoms (C1-C2-C3-C4, C1-C2-C3-C6, C2-C3-C4-C5 and C6-C3-C4-C5 for isoleucine; C1-C2-C3-C4 and C1-C2-C3-C5 for valine) are within the range of the experimental data or within 2-degree difference range. For other dihedral angles involving N and O atoms, the differences again are large. However, the experimental data from different literature sources also differ greatly in some dihedral angles. For example, the dihedral angle of N19-C2-C3-C4 in some crystal structures of isoleucine ranges from -152.95 to -155.53 while others are ~ -82 degree. There are three different groups of experimental data -70s (-72.35 – -79.22), 70s (72.26 – 78.84), and -80s (-80.0 – -80.46) for the dihedral angle of O20-C1-C2-C3. The crystal structures from literature have different counter ions, such as Cl^-, Br^-, NO_3^- ions and some of them are dimers. They may affect the three dimensional structures of amino acids, resulting in different dihedral angles in literature. As has been mentioned in the case of leucine, the possible reason that could be responsible for the large differences between the theoretical results and experimental data is the presence of counter ions that may offset the positive charge from NH_3^+, or form hydrogen bond in the crystal structures between two amino acids. The other possible reason may be the unknown crystal packing effect.

To verify the counter ions effect on the structures of amino acids, we added a chloride ion (Cl^-) to valine and did calculations at B3LYP level with 6-31G(d) basis set. The major bond distances and dihedral angles were listed in Table 7. The bond distances involving C atoms are pretty close to those without Cl^- ion. The C1–O20 single bond in –COOH is found to be 0.0268 Å longer with Cl^- ion at the same theoretical level and it is 0.023 Å longer than the MAX range of experimental value. The C2–N8 bond is 0.053 Å shorter than that without Cl^- ion at the same level and is a little bit shorter (0.002 Å) than the MIN range of the experimental value. The calculated dihedral angles are very different from both those without the counter and the experimental data. Therefore, the addition of the counter ion affects the geometrical parameters greatly.

Since the experimental dihedral angles from crystal structures of amino acids are not consistent, we picked two extreme cases of the crystal structures for each amino acid which contain very short and log bond distances and did an overlay to help us visualize the differences in their structures. The overlay of two extreme crystal structures of leucine after omitting all H atoms is shown in Figure 19 with RMS value of 0.0582. The crystal structures are pretty close to each other from the overlay view. The largest cone angles found is O20–C–O20, O21–C–O21 and N–C–N with a difference of 14.6, 22.8 and 4.2 degree, respectively. The cone angles of all other crystal structures fall between those ranges. It means that the 19 crystal structures of leucine from literature have similar structures despite the diverse dihedral angles. The overlay of two extreme cases of experimental structures of isoleucine is shown in Figure 20. As can be seen, there are some differences in them. The biggest differences are at terminal N

and O atoms. The differences in cone angles of N–C–N and C1–C–C1 are 96.4 and 104.5 degree, respectively. For valine, the largest cone angle is N–C–N with 107.0 degree. There are also some differences in O19–C–O19 (25.3 degree), O20–C–O20 (25.7 degree), C4–C–C4 (29.1 degree) and C5–C–C5 (32.5 degree). Again, the cone angles of all other crystal structures fall between those ranges. The overlay views of two extreme cases have shown that crystal structures from literature differ in their molecular structures, especially at terminal N and O atoms.

Based on the above comparison of theoretical results and experimental data for leucine, isoleucine and valine, considering the counter ion effect and differences in crystal structures from literature, our calculated results are in agreement with the experimental data in general, except at certain bond distances and dihedral angles where terminal N and O atoms are involved. Therefore, our chosen theoretical methods are appropriate to reproduce the experimental data and suitable for this study.

Then, different computational methods and basis sets were used on Methyl/Silyl/Germyl Alanine **7** (**7C**, **7Si** and **7Ge** Figure 18), which is a simplified derivative of **4–5**, to find the most effective and efficient combination of theoretical levels and basis sets in this study. The computational methods HF, MP2 and B3LYP level were combined with 6-31G(d) and 6-311G(d, p) basis sets, which are denoted as HF (HF/6-31G(d)), D1 (B3LYP/6-31G(d)), D2 (B3LYP/6-311G(d, p)) and MP2 (MP2/6-31G(d)) in Tables 8–10 for **7C**, **7Si** and **7Ge**, respectively. The differences in bond distances, bond angles and dihedral angles were compared for different combinations. Since all the bond angles and dihedral angles agree very well with each other, all within

a 10-degree difference range, they are not listed in the tables. Only bond distances are listed and discussed.

The first three columns of Tables 8–10 compare the results of three different methods (HF, DFT and MP2) with the same basis set (6-31G(d)). The last column compares the results of the B3LYP method, but with two different basis sets. It shows that all bond distances are calculated to be longer at D1 (B3LYP/6-31G(d)) than at HF (HF/6-31G(d)) level except in **7Si**, in which the C3-Si bond is calculated to be a little bit shorter than with D1; however the difference is only 0.0003Å, which is negligible. The overall difference between these two combinations is not large; the biggest difference is ~0.026Å, which all occur between C and O single and double bonds at C1–O7 and C1=O6. The second biggest difference occurs between C and N bond (C2–N5), which has an approximate of 0.015 Å difference. All other bond distances agree well with each other at these two theoretical levels. Similar results were found using MP2 (MP2/6-31G(d)) and HF. The biggest difference also occurs at C1–O7 single bond and C1=O6 double bond with an approximate ~0.033Å difference. The second largest difference occurs at C2–N5 with a maximum difference of 0.0122 Å in **7C**. All other bond distances agree quite well with each other. Results of MP2 and D1 were also compared. They are found to be close to each other with a maximum difference of 0.0124 Å at C2–C3 in **7Si**. Therefore, using the B3LYP method could achieve comparable results with those using a computationally more expensive method such as MP2 in this study.

The last column of Tables 8–10 compares the results from the same DFT method B3LYP but using two different size basis sets: the standard 6-31G(d) (D1) and

polarized 6-311G(d, p) (D2). All the bond distances are found close to each other within a range of 0.007 Å, except a 0.0227 Å difference at C3–Ge4 in **7Ge**. We conclude that using a larger size basis set doesn't significantly improve the results in our study.

The simplified molecules **7C/7Si/7Ge** were also optimized with CCSD combined with 6-31G(d). The results serve as a reference point for HF, DFT and MP2 with the same basis set. The differences of major bond distances were compared and listed in Table 11–13. For **7C** (Table 11), the biggest difference occurs at C1=O6 and C1–O7 between CCSD and HF with a difference of 0.0246 Å and 0.0265 Å, respectively. The second biggest difference is at C2–N5 with a 0.0149 Å. The results obtained from DFT and MP2 are pretty close to those from CCSD, all within 0.007 Å range difference. For **7Si/7Ge** (Table 12 and 13), the bond distances of C1=O6 are all calculated to be much shorter at CCSD and the bond distances of C1–O7 are much longer at CCSD compared with those obtained from HF, DFT and MP2. The differences are all over 0.1 Å. The C2–N5 bond is calculated to be longer at CCSD compared with HF, 0.0127 Å for **7Si** and 0.0133 Å for **7Ge**. But the differences between DFT, MP2 and CCSD are within 0.003 Å. This shows that there is no consistency between the HF, DFT, MP2 and CCSD geometrical parameters. Since as discussed previously in comparison with natural amino acids, most of DFT results seem to be within the range of the experimental data. And also based on the comparison of simplified molecule 7 at different theoretical levels, the HF and DFT (B3LYP) methods in combination with 6-31G(d) basis set can achieve similar results with those using expensive MP2 method. The large size basis set also doesn't affect results greatly. Therefore, the less

computationally expensive HF and DFT methods and the 6-31G(d) basis set were used in the following studies, unless otherwise indicated.

The following study focused on the relationship between the dihedral angle (1, 2, 3, 4) and torsional potentials of residues at position 5 in the decapeptides, which largely determines the ligand-peptide interactions, which is a key factor to explain the biological and pharmacological properties of molecules of interest in our study.

A scan of the dihedral angle D (1, 2, 3, 4) from 0 to 360 degree with 10-degree interval was carried out on **7C**, **7Si** and **7Ge** at HF and B3LYP levels. Figures were plotted with D (1, 2, 3, 4) (X-axis) against relative energy in KJ/mol (Y-axis) for **7C**, **7Si** and **7Ge**, respectively, in Figures 22–24. HF results were shown as squares and B3LYP results as circles. Energy maxima and minima along the potential energy surface (PES) were observed as expected. An energy minimum and maximum occur every 60 degree as the conformation changes from staggered to eclipsed. There are three maxima points and three minima points within the 360-degree range in each molecule, which form a three-fold potential in each case. All the maxima and minima points occur at an approximate certain value of D (1, 2, 3, 4) along the PES graphs. Three maxima occur around 0, 120 and 240 degree and three minima occur around 60, 180 and 300 degree of D (1, 2, 3, 4). Therefore, we then simplified our calculations by focusing on those maxima and minima points. Since the HF and B3LYP results exhibit the same trends, the results at the B3LYP level are used in the following discussion unless specifically noted otherwise.

Optimizations with the 6-31G(d) basis set were carried out at every maximum and minimum point. The optimized D (1, 2, 3, 4) values and relative energies for **7C**,

7Si and **7Ge** are listed in Tables 14–16 and are plotted in Figures 25–27 together with their corresponding Newman projection structures at every maximum and minimum point. The Newman structures were drawn along C2–C3 bond in each case. Every staggered position corresponds to a maximum point and every eclipsed position corresponds to a minimum point in Figures 25–27. There are three maxima and three minima points in each case. The three maxima points all occur around 0, 120 and 240 degree, which correspond to an eclipsed position (denoted as max1, max2 and max3 in tables 11-13). Similarly, all the optimized minima points occur around 60, 180, 300 degree, each corresponding to a staggered position (denoted as min1, min2 and min3 in the tables 11-13). Take **7C** for example, three maxima points occur at 1.79, 118.46 and 236.79 degree and three minima points occur at 70.39, 185.39 and 293.70 degree (Table 11). The global minimum is at min3, where the three heavy groups (–COOH, $–CH_3$ and $–NH_2$) are 60-degree away from each other in the Newman structure (Figure 22). However, the energy values of three minima are all very close to each other; the difference is less than 1 KJ/mol. In the case of **7Si** and **7Ge**, the global minima both occur at min1, but min2 is very close to the global minimum (0.45 KJ/mol and 1.45KJ/mol higher in energy for **7Si** and **7Ge**, respectively), in which the –COOH and $–SiH_3$/GeH_3 are in staggered position from each other. The global maximum for all three analogs of **7** is at max1, where the –COOH is in eclipsed position with $–CH_3$/SiH_3/GeH_3 in the Newman structure.

After working on the simplified molecule **7** and deriving a general trend along PES vs. dihedral angle, similar calculations were carried out on C, Si and Ge-containing analogs of **4-5** (Tables 17–22 and Figure 28–33). Again, we focused on the energy

change around dihedral angles D (1, 2, 3, 4). Optimizations were carried out on the maxima (0, 120 and 240 degree) and the minima points (60, 180 and 300 degree) on those molecules. All global maxima occur at max1, where the –COOH overlaps with –CMe_3/$SiMe_3$/$GeMe_3$ or –CMe_2Ph/$SiMe_2Ph$/$GeMe_2Ph$ in **4** and **5**, respectively. The global minima for **4C** and **4Si** both occur at min2 (172.71 degree for **4C** and 180.15 for **4Si**), where the –COOH is farthest (180-degree) to the group of –CMe_3/$SiMe_3$ in the Newman structure. However, the global minimum for **4Ge** occurs at min3 (289.13 degree), where the three large groups (–COOH, –$GeMe_3$ and –NH_2) are 60-degree away from each other. And the min2 (167.83 degree) has the highest energy value among the three minima, which is 11.97 KJ/mol higher than the global minimum.

The global minima for **5C** and **5Si** analogs occur at min2 (185.34 degree for **5C** and 181.28 degree for **5Si**) and the global minimum for **5Ge** happens at min1 (55.77 degree), where the –$GeMe_2Ph$ group is closest to –COOH and opposite to –NH_2. However, the energy difference between min1 and min2 is only 0.01 KJ/mol, which is negligible.

Conclusion

The results have shown that there are some similarities and differences in C, Si and Ge-containing analogs as residues at position 5 in the decapeptides. All studied molecules **4–5**, including methyl/silyl/germyl alanine **7**, the simplified derivatives of **4–5**, have a three-fold PES scanning along the dihedral angle D (1, 2, 3, 4). All three maxima and three minima occur at approximately same angles. Further optimization at those points revealed some similarities and differences of global maximum and global

minimum in C, Si and Ge-containing analogs, which result in different energy depth on the PES in the figures.

For methyl/silyl/germyl alanine **7**, the global maxima all occur at max1 where –COOH is in eclipsed position with CH_3/SiH_3/GeH_3 in the Newman Structure. The global minimum for methyl alanine **7C** occurs at min3 while min1 is the global minimum for silyl/germyl alanine **7Si** and **7Ge**. Max1 is also the global maximum for C, Si and Ge-containing analogs of molecules **4-5**. The C and Si–containing analogs, **4C**, **4Si**, **5C** and **5Si**, showed the same global minimum at min2. However, min2 is the highest in energy among 3 minima for **4Ge**. The global minimum is min3 for **4Ge**. The global minimum for **5Ge** is min1, but it is only 0.01 KJ/mol higher in energy than min2.

The figures have also shown that the different relative energy levels among three maxima points. For all C analogs (**7C**, **4C** and **5C**), the max2 is lowest in energy, which results in a small hill between min1 and min2. It was not observed in Si and Ge–containing analogs.

Future Work

Although the results have shown that there are some differences in C, Si and Ge-containing analogs as residues in our interested decapeptides, no definitive conclusions can be drawn at this point. Many questions have not yet been answered, including the differences between the electronic structures of Si and Ge-containing analogs and those of their C analogs. Future work will include:

1. Further investigate the differences in potential energy surface (PES) of Si/Ge substituted amino acids to their C analog, including the differences of NBO charges of

different elements at maxima and minima points to examine the electronic structures differences.

2. Molecular Mechanical (MM) studies will be employed later after Quantum Mechanical (QM) study. Molecular mechanics version 2 (MM2) will be considered because it contains the parameters for Si and Ge–containing bonds. A set of parameters from the QM study will also be needed to derive improved force field constants. The parameters will be used on the atoms at position 5 of decapeptides **1–3** to determine the energy minima along the PES.

3. The optimized geometries of decapeptides **1–3** of energy minima from above will then be used for Molecular dynamic (MD) study. This study will help to examine the tertiary structures of decapeptides **1–3** compared with Cetrorelix.

4. Compare Cetrorelix binding with GnRH receptors with those of C/Si/Ge analogs. The difference of the binding structures between C/Si/Ge analogs will help to elucidate the differences in the biological properties of Si/Ge substituted decapeptides.

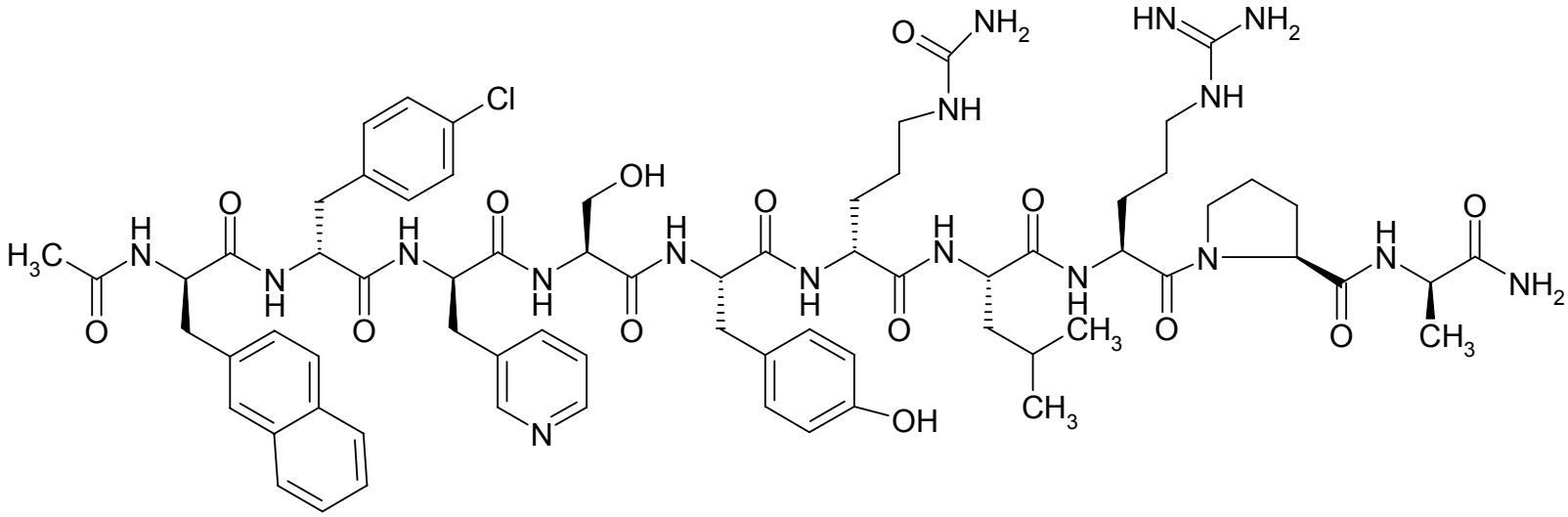

Ac-D-Nal[1]-4-Cl-D-Phe[2]-D-Pal[3]-Ser[4]-Tyr[5]-D-Cit[6]-Leu[7]-Arg[8]-Pro[9]-D-Ala[10]-NH_2

Figure 14. The peptide sequence and chemical structure of cetrorelix.

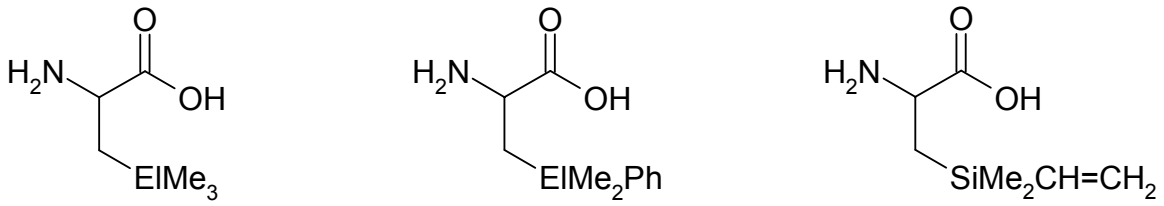

4C: El = C
4Si: El = Si
4Ge: El = Ge

5C: El = C
5Si: El = Si
5Ge: El = Ge

6

Figure 15. A series of Si- and Ge-containing derivatives of residue at position 5 of cetrorelix and their C analogs.

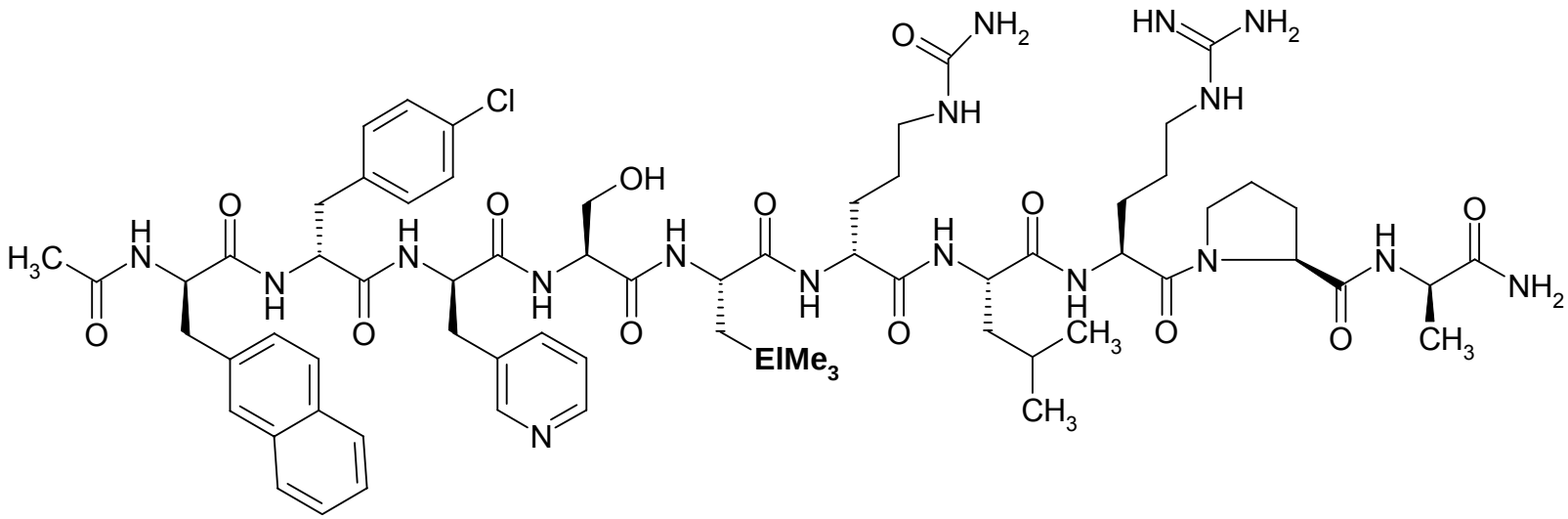

1: El = C, Ac-D-Nal[1]-4-Cl-D-Phe[2]-D-Pal[3]-Ser[4]- **Me_3C-Ala[5]** -D-Cit[6]-Leu[7]-Arg[8]-Pro[9]-D-Ala[10]-NH_2

2: El = Si, Ac-D-Nal[1]-4-Cl-D-Phe[2]-D-Pal[3]-Ser[4]- **Me_3Si-Ala[5]** -D-Cit[6]-Leu[7]-Arg[8]-Pro[9]-D-Ala[10]-NH_2

3: El = Ge, Ac-D-Nal[1]-4-Cl-D-Phe[2]-D-Pal[3]-Ser[4]- **Me_3Ge-Ala[5]** -D-Cit[6]-Leu[7]-Arg[8]-Pro[9]-D-Ala[10]-NH_2

Figure 16. Synthesized decapeptides **1–3** bearing Me_3El-Ala (El = C, Si and Ge) at position 5.

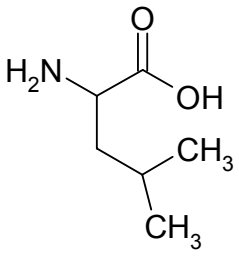

Leucine (Leu)

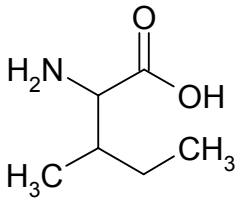

Isoleucine (Ile)

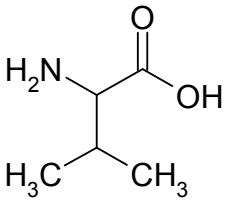

Valine (Val)

Figure 17. Chemical structures of leucine, isoleucine and valine.

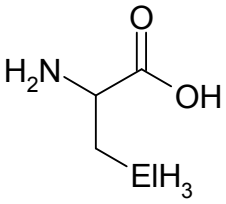

7C: El = C
7Si: El = Si
7Ge: El = Ge

Figure 18. C, Si and Ge-containing molecule **7**, a simplified derivatives of **4** and **5**.

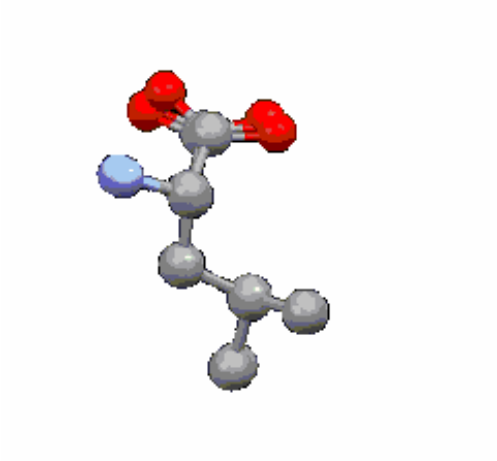

Figure 19. Overlay view of representative experimental crystal structure of leucine.

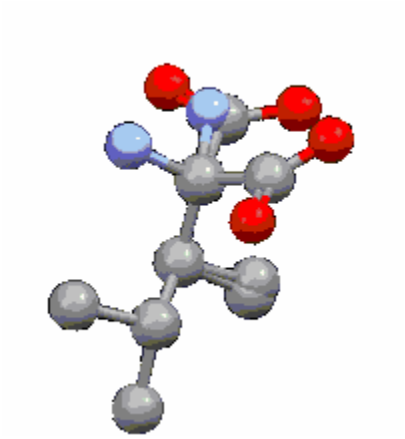

Figure 20. Overlay view of representative experimental crystal structures of isoleucine.

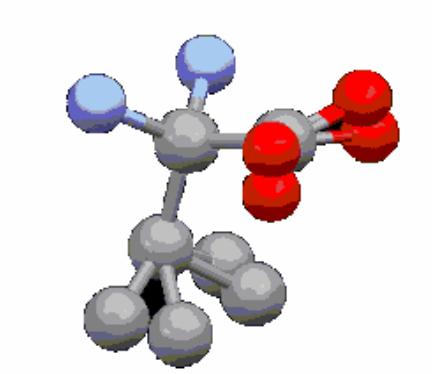

Figure 21. Overlay view of representative experimental crystal structures of valine.

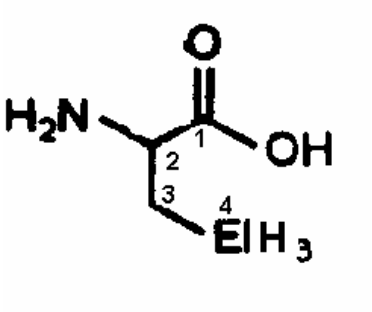

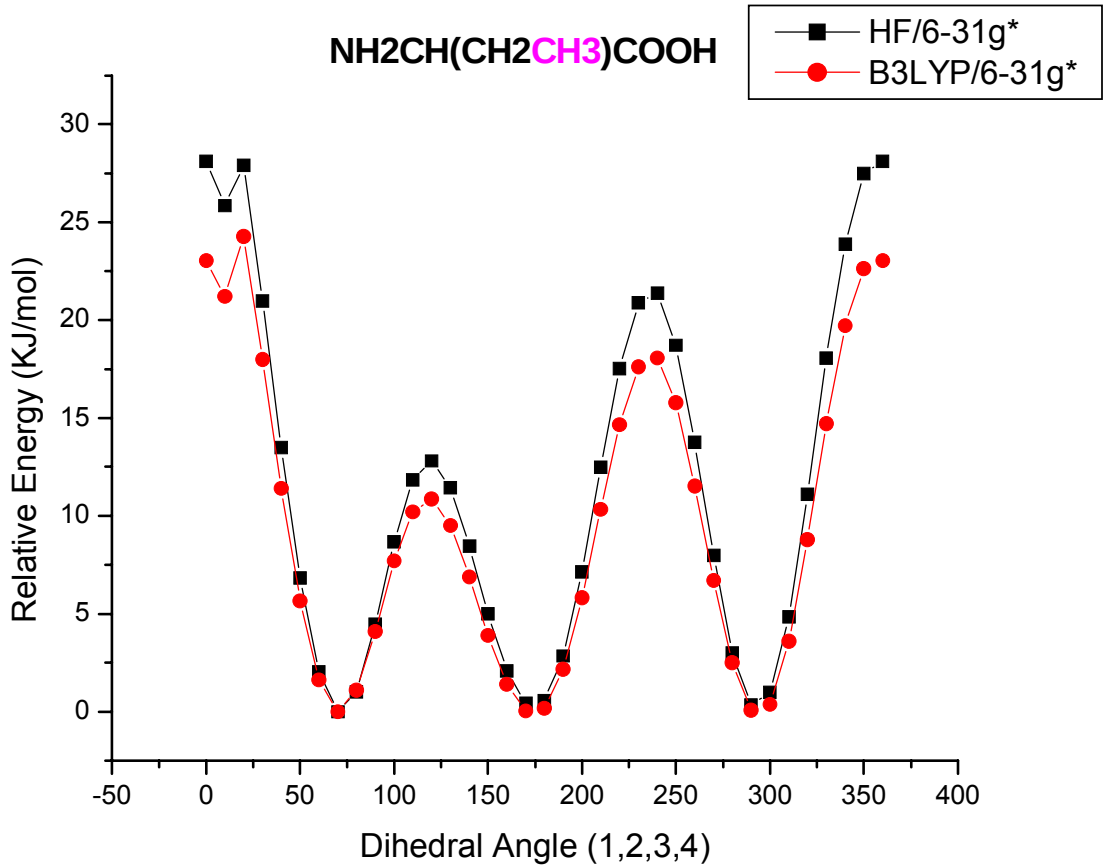

Figure 22. Potential energy surface (PES) vs. Dihedral angle (C1-C2-C3-C4) for **7C**

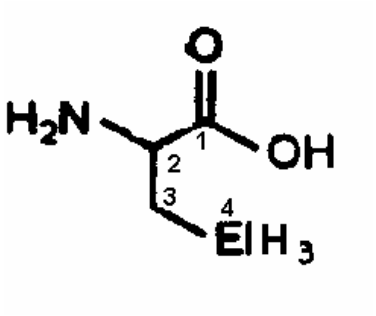

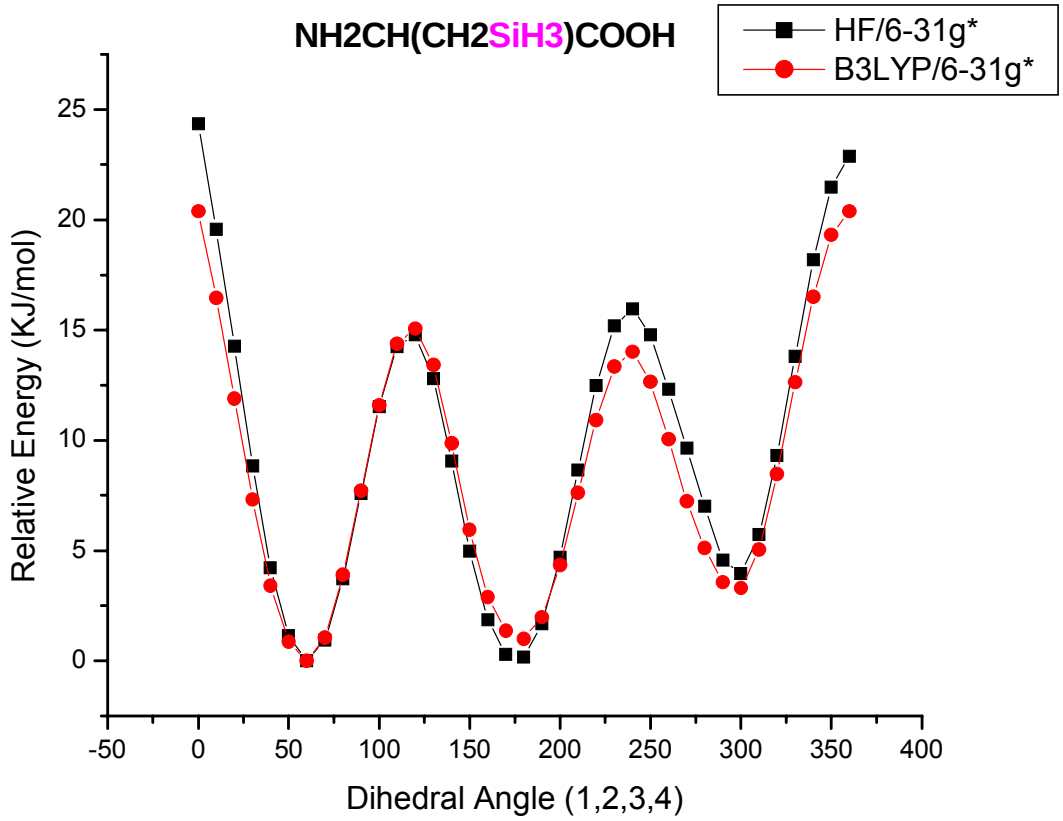

Figure 23. Potential energy surface (PES) vs. dihedral angle (C1-C2-C3-Si4) for **7Si**.

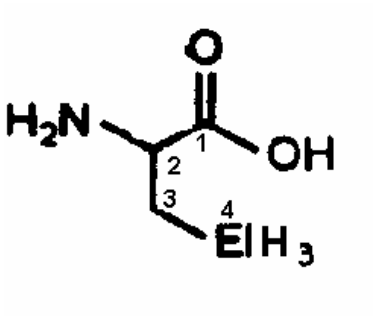

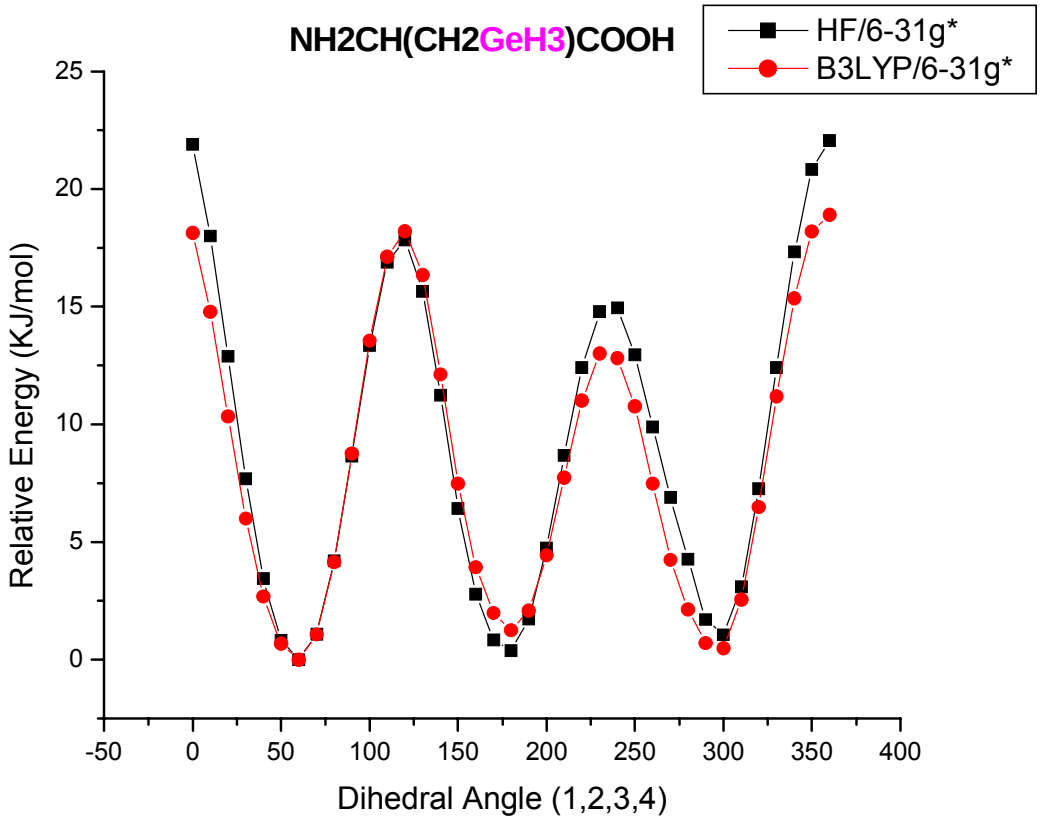

Figure 24. Potential energy surface (PES) vs. dihedral angle (C1-C2-C3-Ge4) for **7Ge**.

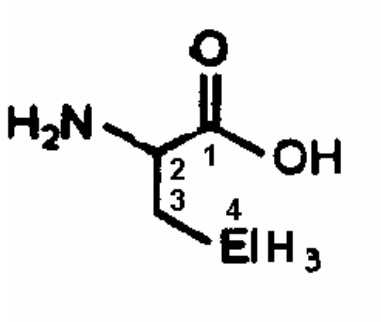

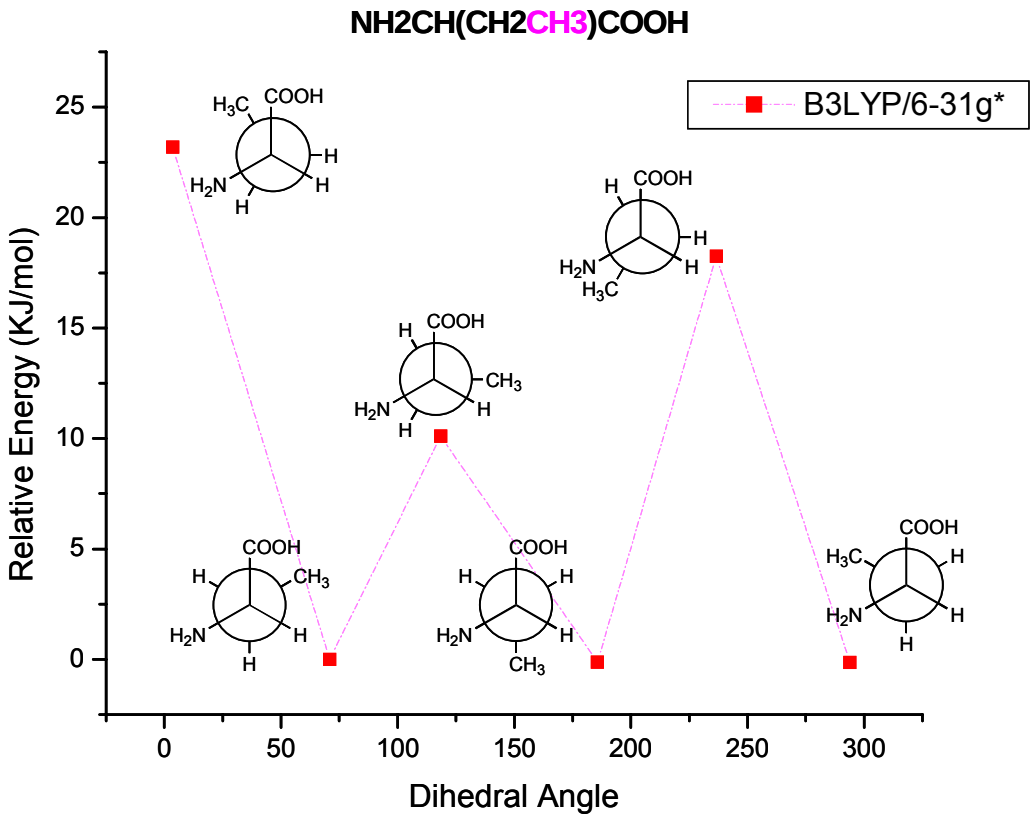

Figure 25. Optimized maxima and minima points of **7C**.

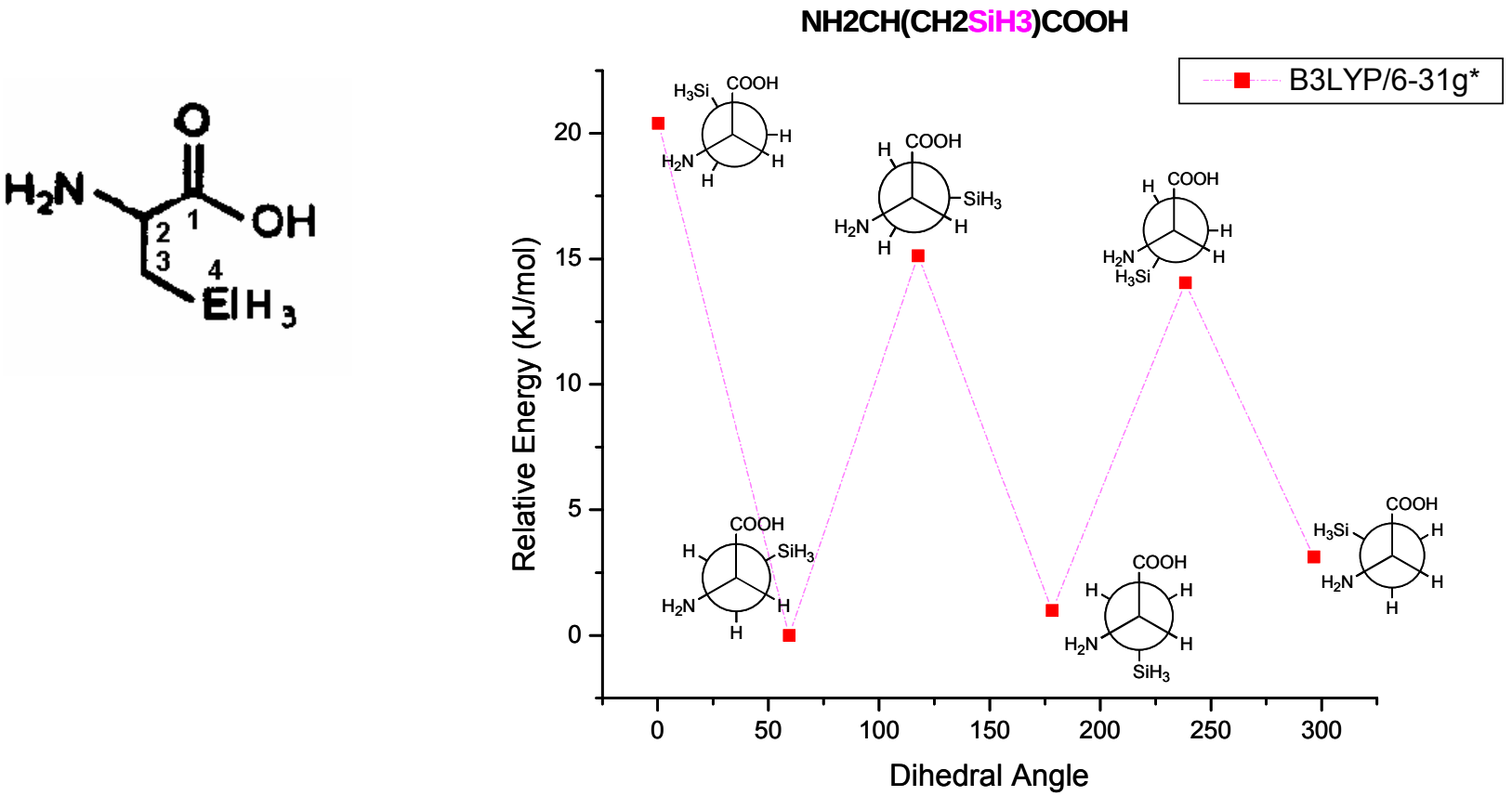

Figure 26. Optimized maxima and minima points of **7Si**.

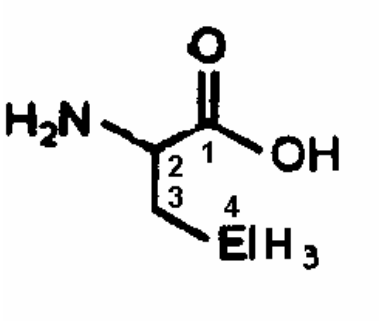

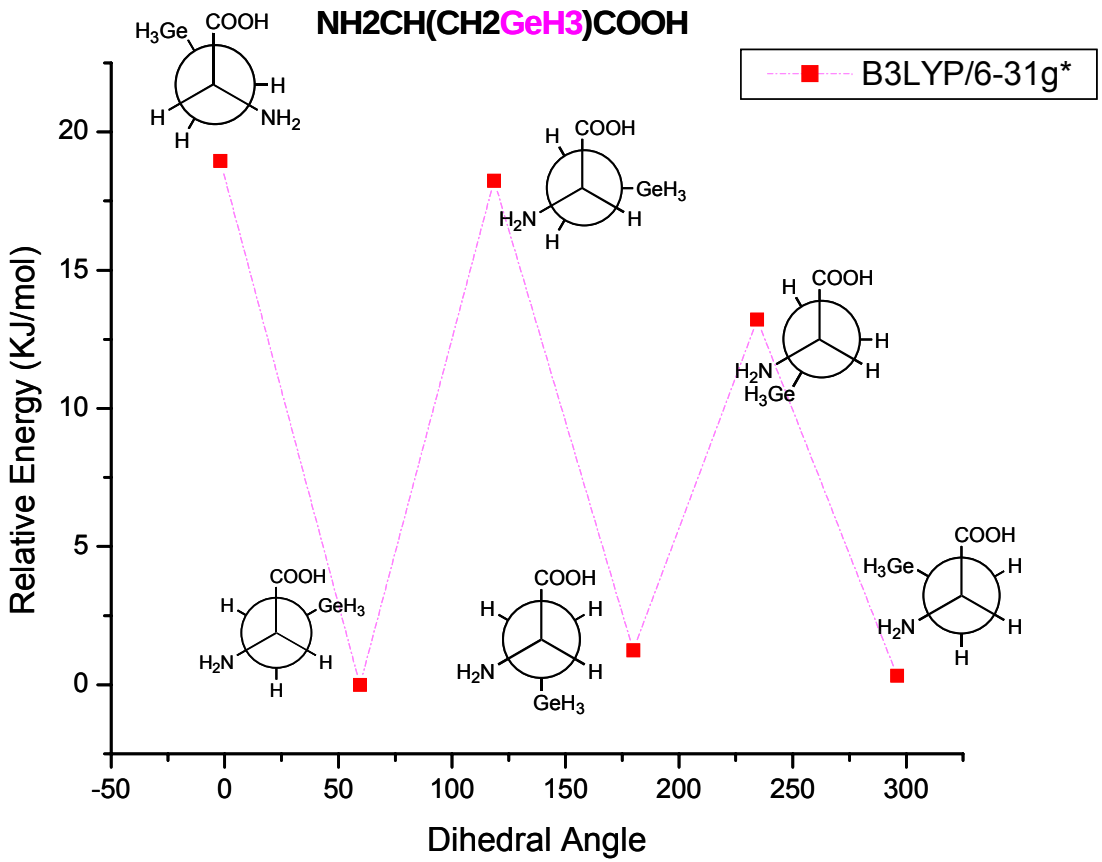

Figure 27. Optimized maxima and minima points of **7Ge**.

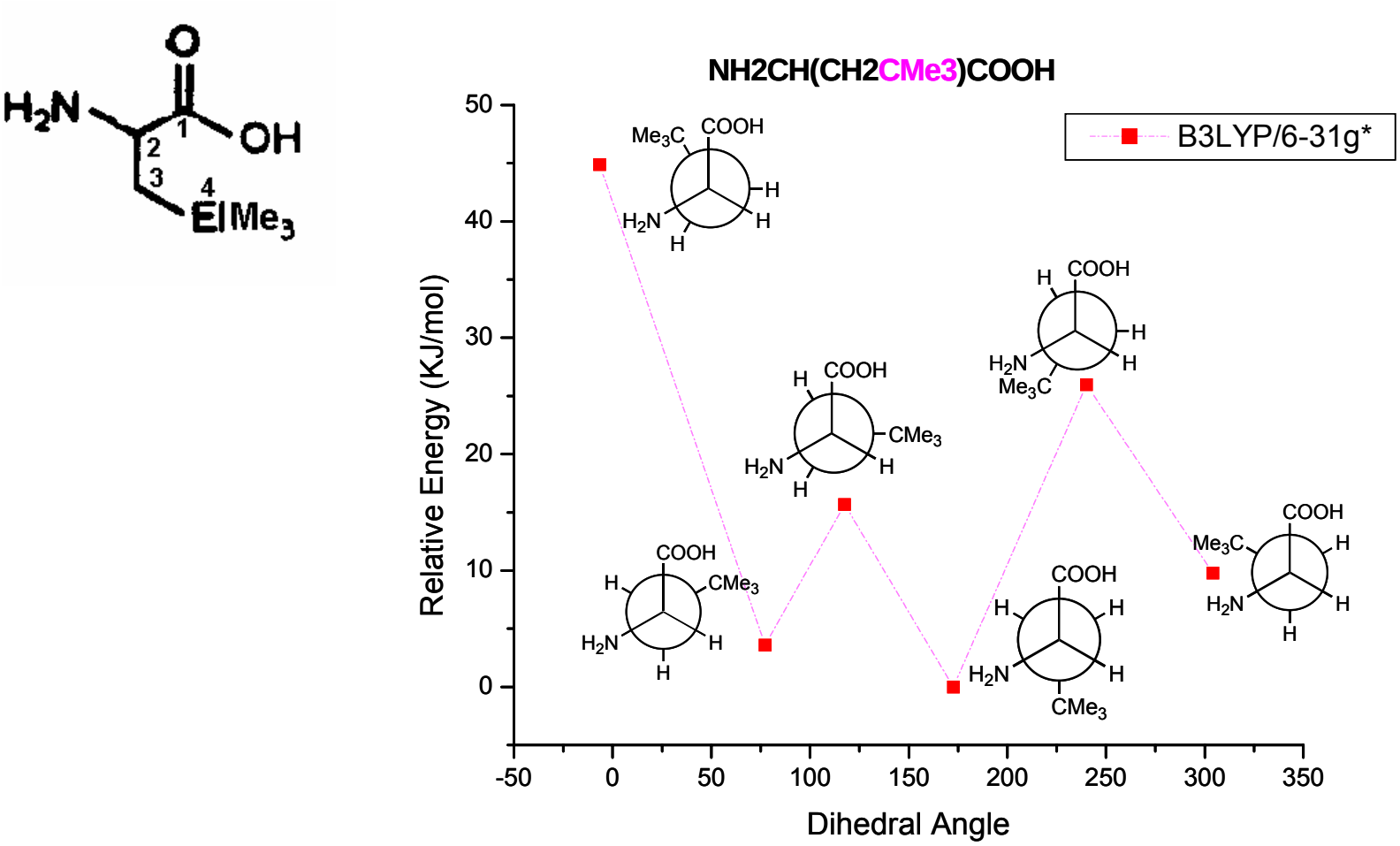

Figure 28. Optimized maxima and minima points **4C**.

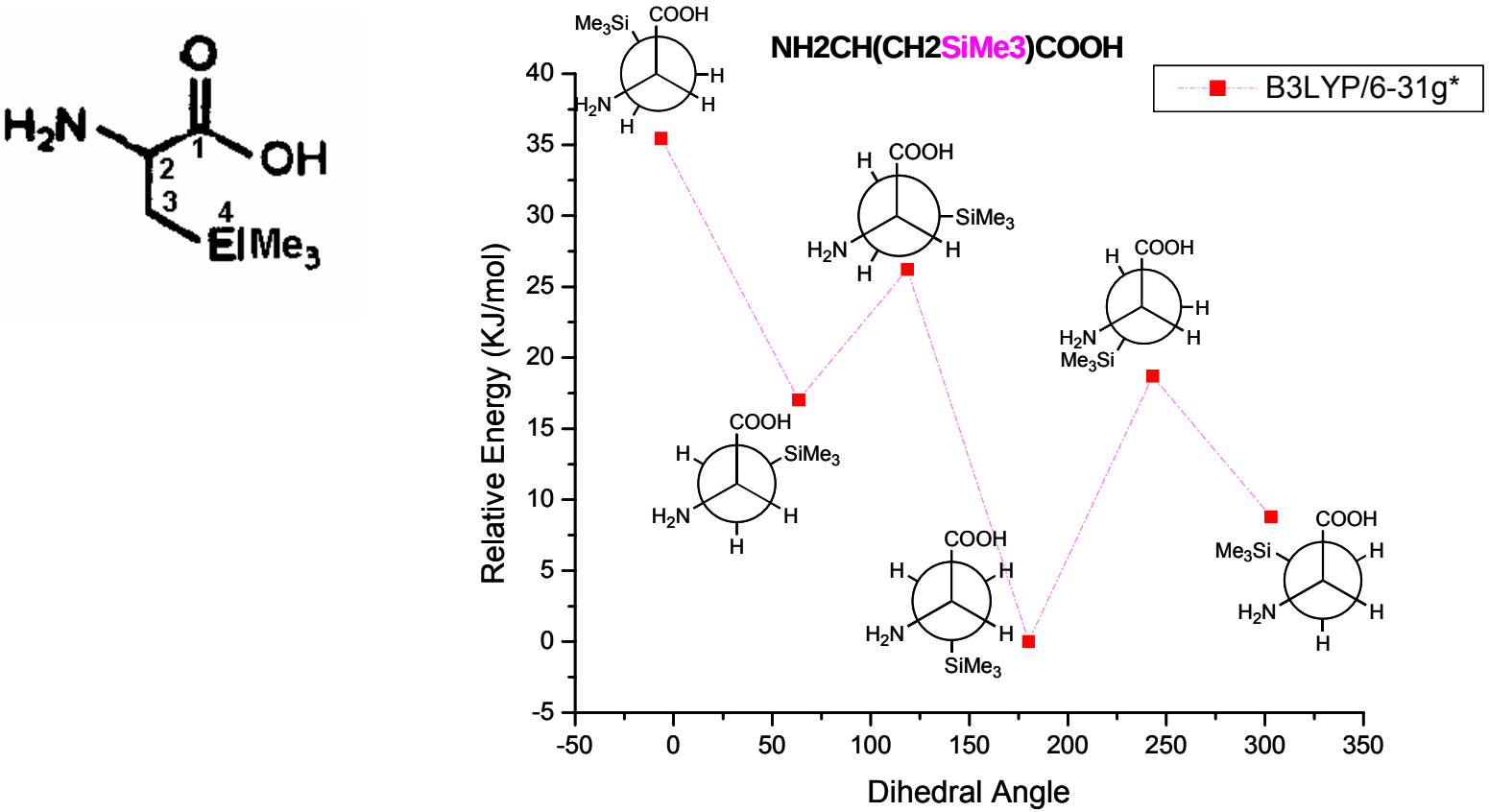

Figure 29. Optimized maxima and minima points of **4Si**.

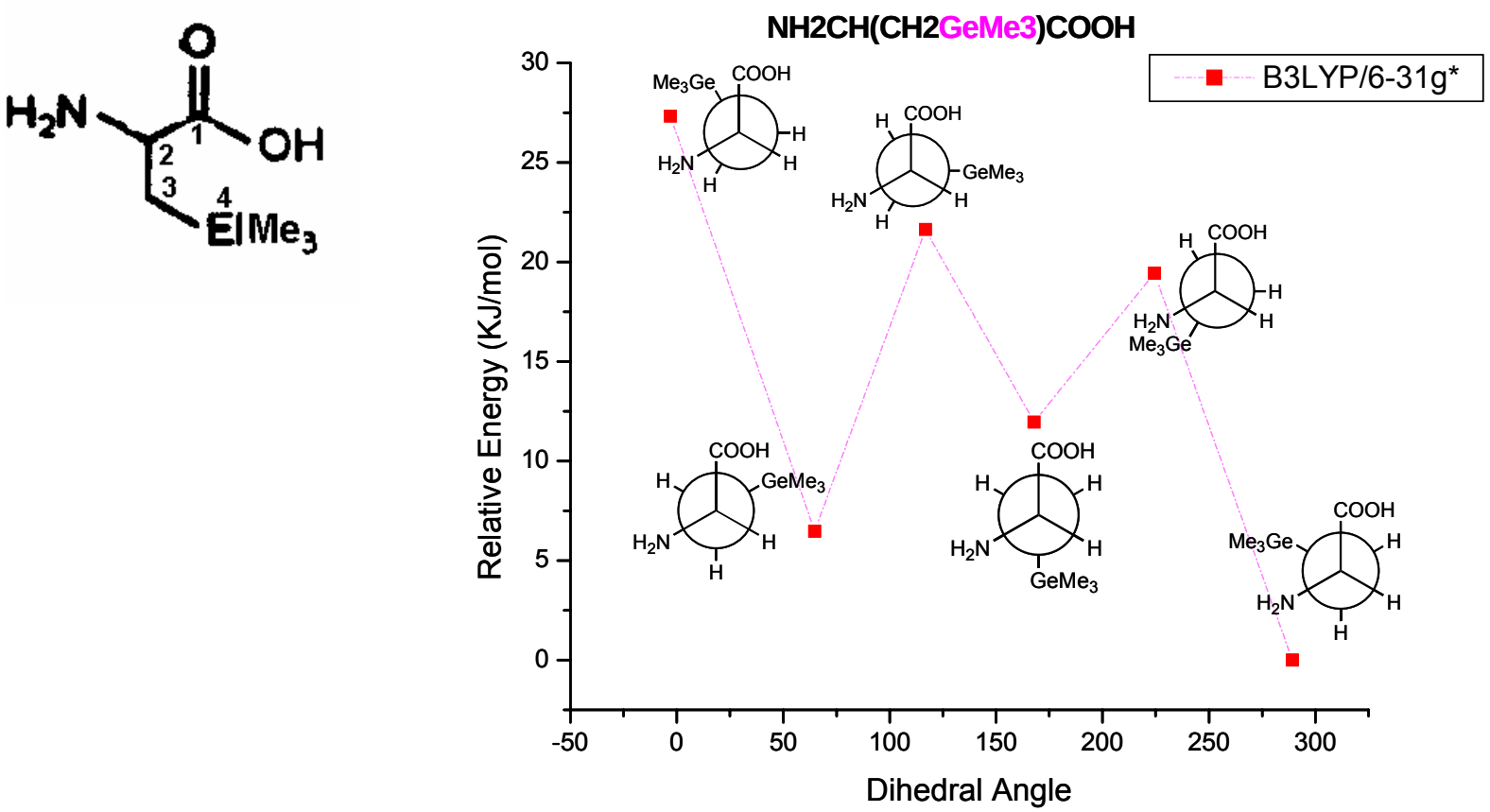

Figure 30. Optimized maxima and minima points of **4Ge**.

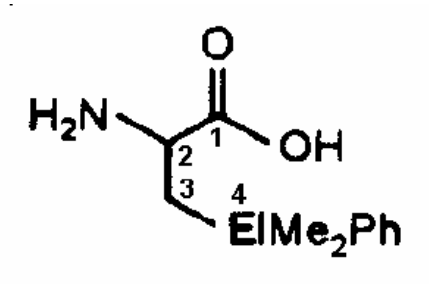

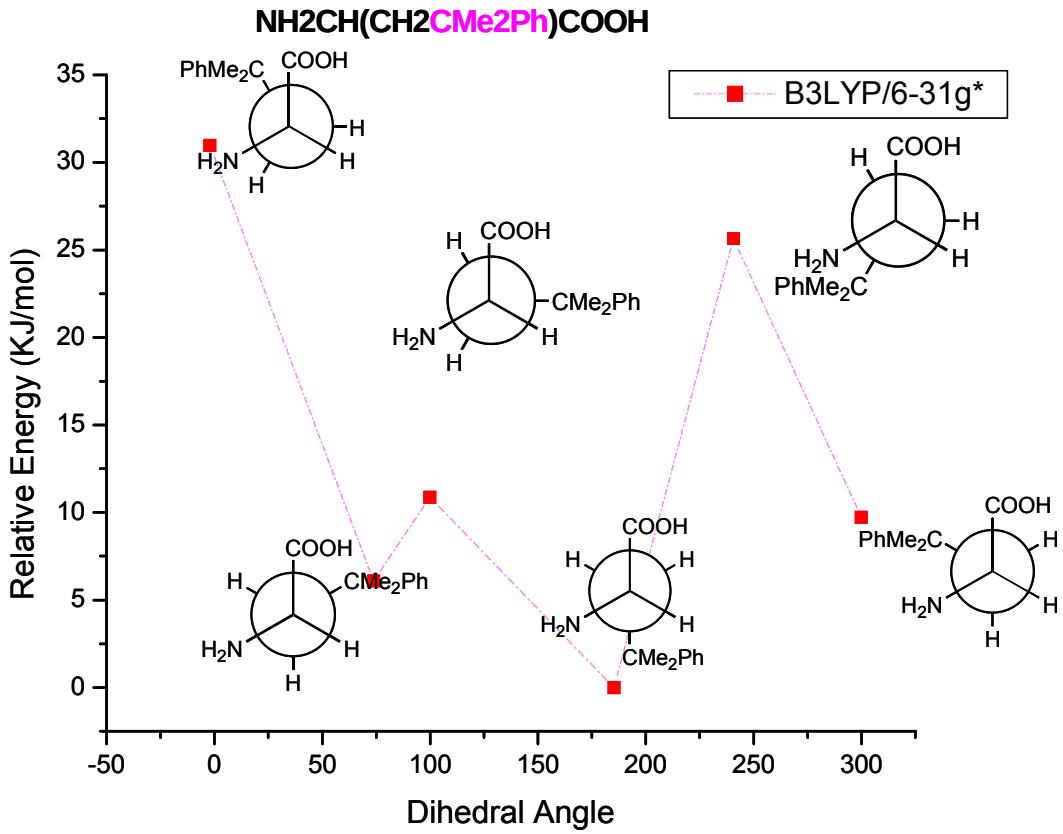

Figure 31. Optimized maxima and minima points of **5C**.

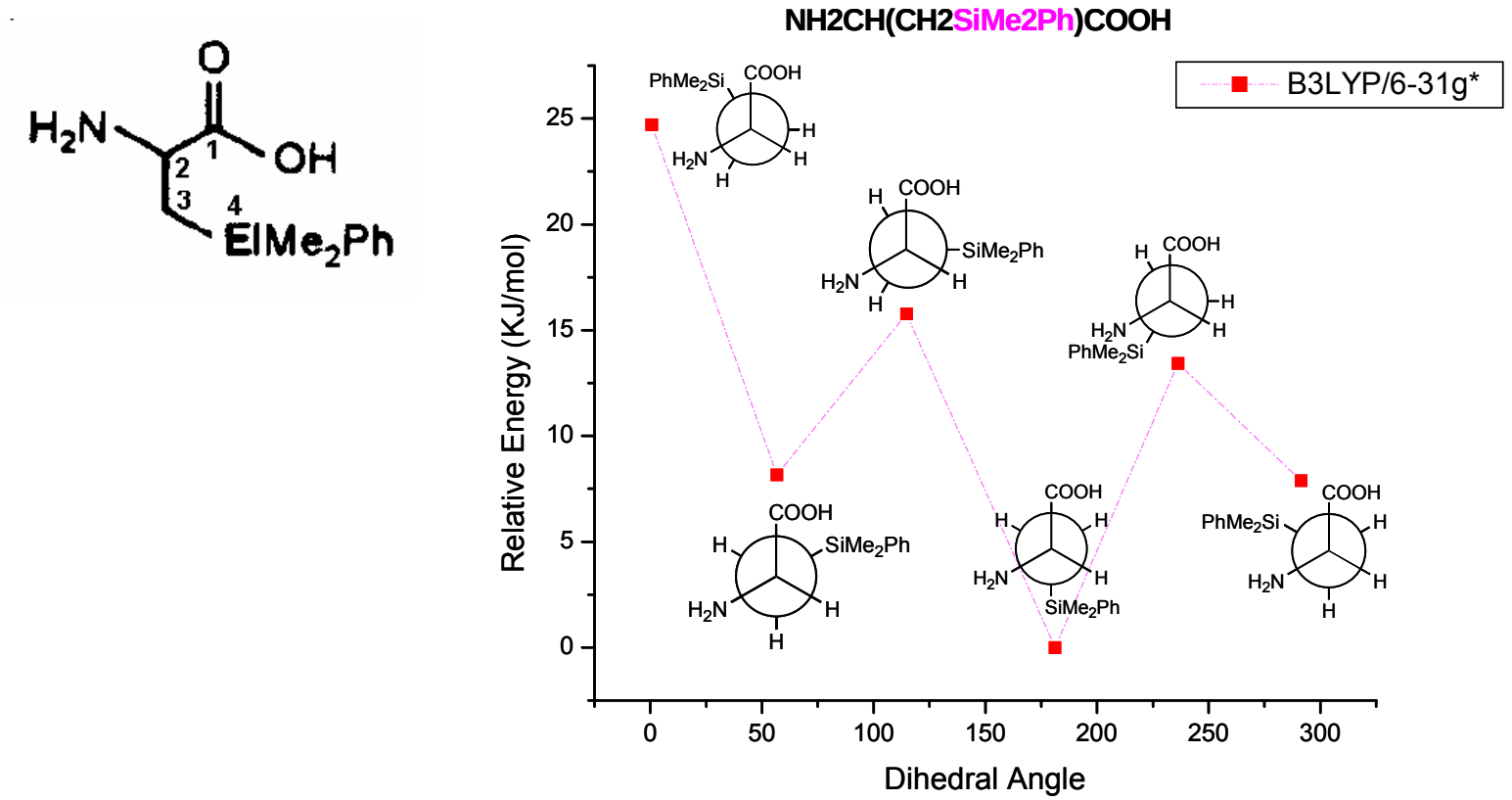

Figure 32. Optimized maxima and minima points of **5Si**.

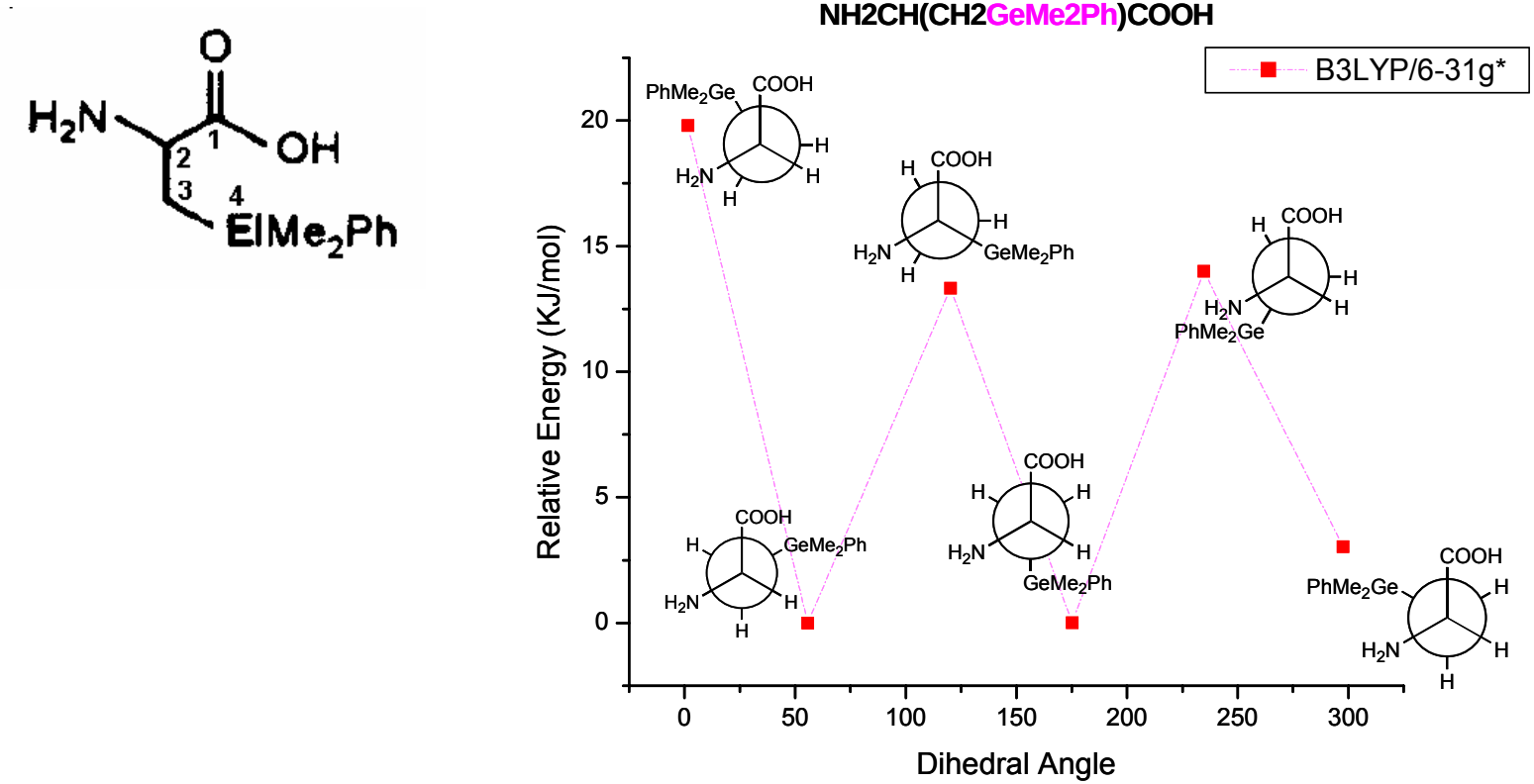

Figure 33. Optimized maxima and minima points of **5Ge**.

Table 5. Theoretical and experimental data of bond distances and dihedral angles for leucine.

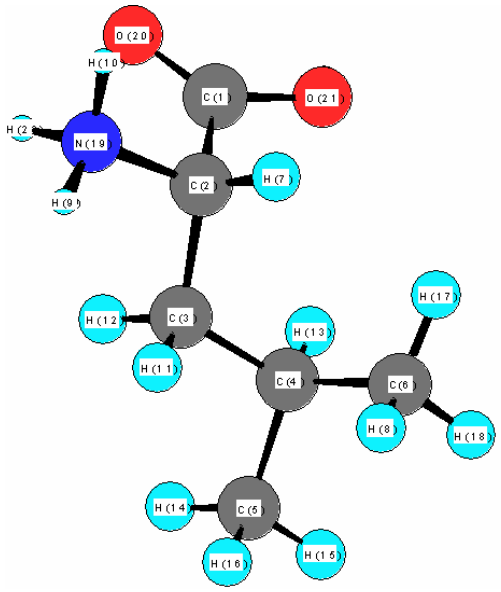

Bond distances Dihedral angles	HF	D1	D2	MP2	MIN	MAX
C1–C2	1.528	1.5418	1.5416	1.5293	1.506(5)	1.616
C2–C3	1.54	1.5448	1.5423	1.5346	1.434	1.57(1)
C3–C4	1.5374	1.5416	1.5397	1.5315	1.504	1.5337(14)
C4–C5	1.5324	1.5364	1.5347	1.5286	1.496	1.67
C4–C6	1.5318	1.5357	1.5338	1.5275	1.429	1.571
C1=O20	1.1859	1.2102	1.2027	1.2182	1.191	1.263(1)
C1–O21	1.322	1.3422	1.3406	1.3484	1.222	1.321
C2–N19	1.461	1.4776	1.4764	1.4729	1.47(6)	1.529
C1-C2-C3-C4	58.93	57.59	59.30	56.56	62.14	77.2(6)
C2-C3-C4-C5	-177.67	-178.47	-177.04	-179.75	-178.54	-164.04(10)
C2-C3-C4-C6	58.98	57.57	59.15	56.91	56.55	73.8
N18-C2-C3-C4	178.22	176.55	178.50	174.68	-175.9	-164.3(4)
O20-C1-C2-C4	-86.94	-79.49	-79.05	-84.37	81.96	115.29
O19-C1-C2-C3	91.22	98.77	99.27	92.93	-94.07	-64.9(6)
O20-C1-C2-N19	153.86	161.08	161.37	157.33	-36.29	-4.02
O20-C1-C2-N19	-27.98	-20.66	-20.31	-25.37	147.29	173.73

Table 6. Theoretical and experimental data of bond distances and dihedral angles for isoleucine.

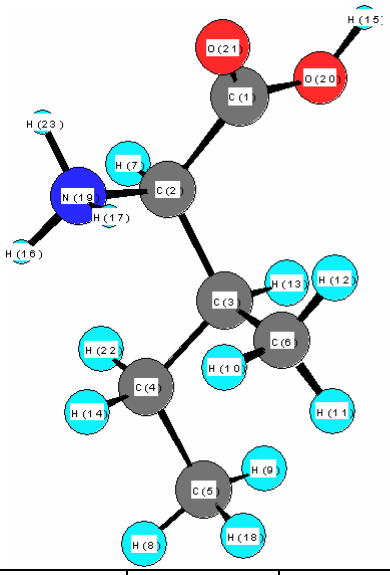

Bond distances Dihedral angles	HF	D1	D2	MP2	MIN	MAX
C1–C2	1.5359	1.55	1.5494	1.5398	1.492	1.546(14)
C2–C3	1.547	1.5521	1.5504	1.5405	1.530(9)	1.580(14)
C3–C4	1.539	1.5439	1.5421	1.5342	1.522(18)	1.568(13)
C4–C5	1.5301	1.5329	1.5311	1.5274	1.52	1.568(23)
C3–C6	1.5345	1.5374	1.5355	1.53	1.505(19)	1.549(12)
C1=O21	1.1862	1.2104	1.2028	1.2184	1.203(9)	1.2619(12)
C1–O20	1.3202	1.3413	1.3397	1.3462	1.243(13)	1.333
C2–N19	1.4629	1.4792	1.4778	1.4756	1.445	1.510(12)
C1-C2-C3-C4	73.30	73.06	73.05	73.89	40.38	84.14
C1-C2-C3-C6	-54.86	-54.47	-54.59	-53.00	-85.27	-40.46
C2-C3-C4-C5	167.01	169.24	169.42	169.80	169.1	178.32
C6-C3-C4-C5	-64.90	-63.52	-63.15	-63.66	-66.41	-56.74
N19-C2-C3-C4	-159.73	-161.19	-160.60	-161.15	-150s and -80s	
N19-C2-C3-C6	72.11	71.28	71.75	71.97	150s and 80s	
O21-C1-C2-C3	-32.13	-35.67	-34.65	-36.10	84.26	122.14
O20-C1-C2-C3	150.61	146.40	147.33	146.02	-70s, 80s and 70s	
O21-C1-C2-N19	-162.06	-165.12	-164.56	-164.71	-36.71	22.43
O20-C1-C2-N19	20.69	16.95	17.43	17.41	145.52	164.08

Table 7. Theoretical and experimental data of bond distances and dihedral angles for valine.

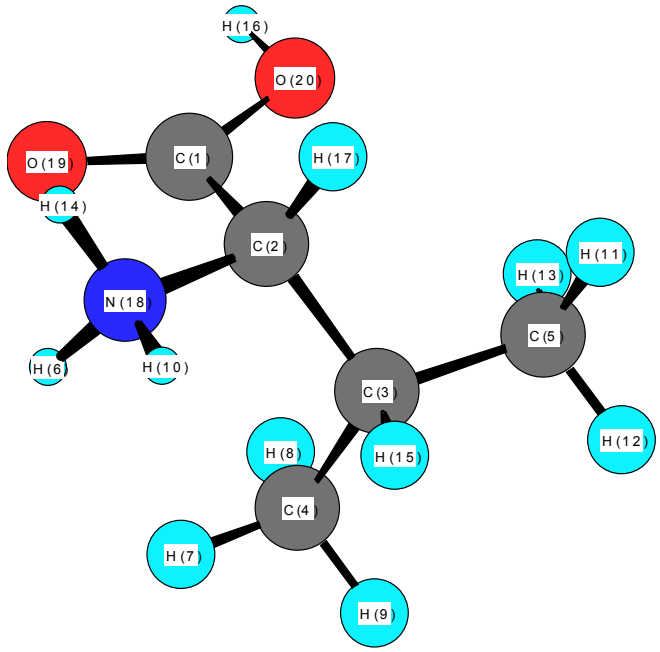

Bond distances Dihedral angles	HF	D1	D2	MP2	Counter Ion Cl^-	MIN	MAX
C1–C2	1.5221	1.5364	1.5338	1.5246	1.528	1.502	1.528(10)
C2–C3	1.549	1.5543	1.5521	1.5406	1.559	1.504	1.558
C3–C4	1.5334	1.5371	1.5351	1.5296	1.535	1.39(2)	1.524(2)
C3–C5	1.5337	1.5367	1.5345	1.5296	1.536	1.485	1.55(3)
C1=O19	1.1869	1.2155	1.2073	1.2224	1.213	1.192	1.215(2)
C1–O20	1.3044	1.3232	1.321	1.3298	1.350	1.299(5)	1.327(6)
C2–N18	1.511	1.528	1.5257	1.5135	1.475	1.477	1.501
C1-C2-C3-C4	-47.73	-50.53	-51.89	-52.56	-67.50	-56.93	-48.08
C1-C2-C3-C5	78.65	76.08	74.86	73.02	59.37	57.56	77.1
N18-C2-C3-C4	70.17	65.79	64.62	63.10	169.50	63.5	73.38
N18-C2-C3-C5	-163.45	-167.60	-168.63	-171.32	-63.62	-161.54	-170.89
O19-C1-C2-C3	111.70	108.06	104.45	99.89	-96.15	91.74	110.20
O20-C1-C2-C3	-68.77	-71.70	-75.09	-79.19	83.40	-87.57	-68.4
O19-C1-C2-N17	-122.76	-126.88	-130.44	-134.79	27.21	-32.49	25.24
O20-C1-C2-N17	56.77	53.37	50.02	46.14	-153.24	147.99	170.3

Table 8. Comparison of bond distances at different theoretical levels of **7C**.

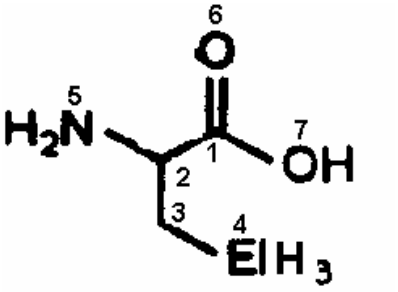

Bond distances	D1-HF	MP2-HF	MP2-D1	D2-D1
C1–C2	0.0081	-0.0024	-0.0105	-0.002
C2–N5	0.0144	0.0122	-0.0022	-0.0006
C2–C4	0.0052	-0.0048	-0.01	-0.0022
C1=O6	0.023	0.0312	0.0082	-0.0069
C1–O7	0.0263	0.0307	0.0044	-0.002
C3–C4	0.0035	-0.0022	-0.0057	-0.0017

Table 9. Comparison of bond distances at different theoretical levels of **7Si**.

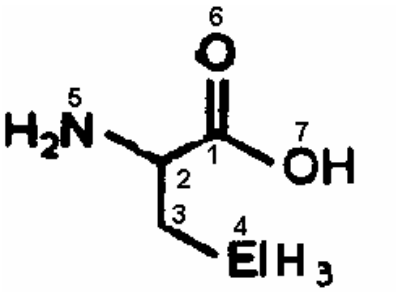

Bond distances	D1-HF	MP2-HF	MP2-D1	D2-D1
C1–C2	0.0078	-0.0029	-0.0107	-0.0021
C2–N5	0.0105	0.0097	-0.0008	-0.0009
C2–C3	0.0116	-0.0008	-0.0124	-0.0008
C1=O6	0.0257	0.032	0.0063	-0.0019
C1–O7	0.023	0.0308	0.0078	-0.0069
C3–Si4	-0.0003	-0.0048	-0.0045	-0.0039

Table 10. Comparison of bond distances at different theoretical levels of **7Ge**.

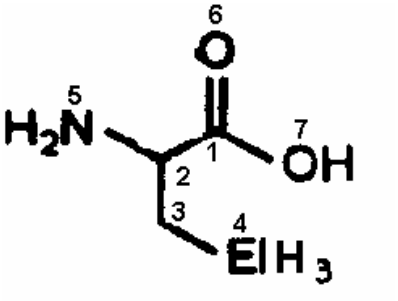

Bond distances	D1-HF	MP2-HF	MP2-D1	D2-D1
C1–C2	0.008	-0.0029	-0.0109	-0.0025
C2–N5	0.0115	0.0102	-0.0013	-0.0009
C2–C3	0.0095	-0.0006	-0.0101	-0.0011
C1=O6	0.026	0.0328	0.0068	-0.0017
C1–O7	0.0229	0.0304	0.0075	-0.0069
C3–Ge4	0.0018	-0.0002	-0.002	0.0227

Table 11. Comparison of bond distances at different theoretical levels with CCSD of **7C**.

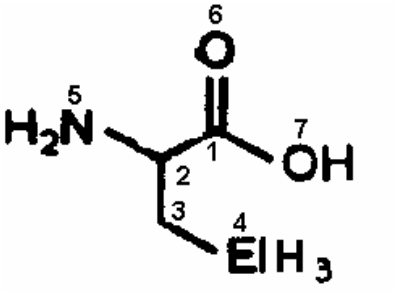

Bond distances	CCSD – HF	CCSD – D1	CCSD – MP2
C1–C2	0.0018	-0.0063	0.0042
C2–N5	0.0149	0.0005	0.0027
C2–C3	-0.0013	-0.0065	0.0035
C1=O6	0.0246	0.0016	-0.0066
C1–O7	0.0265	0.0002	-0.0042
C3–C4	0.0007	-0.0028	0.0029

Table 12. Comparison of bond distances at different theoretical levels with CCSD of **7Si**.

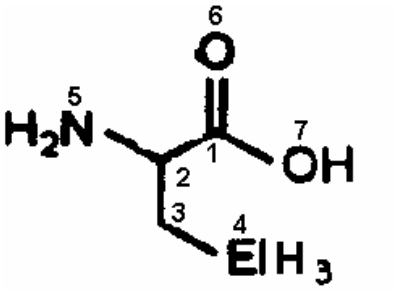

Bond distances	CCSD – HF	CCSD – D1	CCSD – MP2
C1–C2	0.0012	-0.0066	0.0041
C2–N5	0.0127	0.0022	0.003
C2–C3	0.0012	-0.0104	0.002
C1=O6	-0.1212	-0.1469	-0.1532
C1–O7	0.1738	0.1508	0.143
C3–Si4	0.0001	0.0004	0.0049

Table 13. Comparison of bond distances at different theoretical levels with CCSD of **7Ge**.

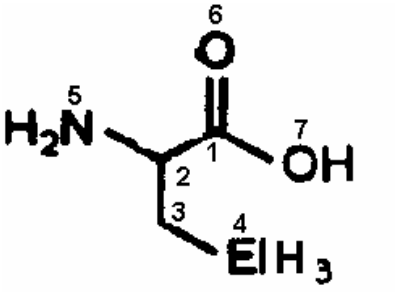

Bond distances	CCSD – HF	CCSD – D1	CCSD – MP2
C1–C2	0.0016	-0.0064	0.0045
C2–N5	0.0133	0.0018	0.0031
C2–C3	0.0013	-0.0082	0.0019
C1=O6	-0.1209	-0.1469	-0.1537
C1–O7	0.1737	0.1508	0.1433
C3–Ge4	0.0058	0.004	0.006

Table 14. Optimized dihedral angle and relative energy at maxima and minima points for **7C**.

Points	D(1,2,3,4)	RE (KJ/mol)
max1	1.79	24.09
min1	70.39	0.55
max2	118.46	11.03
min2	185.39	0.18
max3	236.79	18.26
min3	293.70	0.00

Table 15. Optimized dihedral angle and relative energy at maxima and minima points for **7Si**.

Points	D(1,2,3,4)	RE (KJ/mol)
max1	0.45	19.57
min1	59.25	0.00
max2	117.05	13.59
min2	177.06	0.45
max3	239.02	14.06
min3	297.26	3.42

Table 16. Optimized dihedral angle and relative energy at maxima and minima points for **7Ge**.

Points	D(1,2,3,4)	RE (KJ/mol)
max1	-1.88	20.03
min1	59.67	0.00
max2	117.45	15.22
min2	176.93	1.45
max3	238.09	16.01
min3	296.37	3.73

Table 17. Optimized dihedral angle and relative energy at maxima and minima points for **4C**.

Points	D(1,2,3,4)	RE (KJ/mol)
max1	-6.56	44.9
min1	77.16	3.59
max2	117.51	15.67
min2	172.71	0.00
max3	240.08	25.97
min3	304.09	9.77

Table 18. Optimized dihedral angle and relative energy at maxima and minima points for **4Si**.

Points	D(1,2,3,4)	RE (KJ/mol)
max1	-6.42	35.46
min1	63.48	17.02
max2	118.6	26.23
min2	180.15	0.00
max3	242.97	18.71
min3	303.03	8.81

Table 19. Optimized dihedral angle and relative energy at maxima and minima points for **4Ge**.

Points	D(1,2,3,4)	RE (KJ/mol)
max1	-3.09	27.34
min1	64.75	6.48
max2	116.74	21.64
min2	167.83	11.97
max3	224.48	19.45
min3	289.13	0.00

Table 20. Optimized dihedral angle and relative energy at maxima and minima points for **5C**.

Points	D(1,2 3,4)	RE (KJ/mol)
max1	-2.12	30.97
min1	73.86	6.08
max2	99.83	10.87
min2	185.34	0.00
max3	240.72	25.66
min3	299.76	9.73

Table 21. Optimized dihedral angle and relative energy at maxima and minima points for **5Si**.

Points	D(1,2,3,4)	RE (KJ/mol)
max1	0.53	24.72
min1	56.64	8.16
max2	114.65	15.76
min2	181.28	0.00
max3	236.28	13.43
min3	291.40	7.89

Table 22. Optimized dihedral angle and relative energy at maxima and minima points for **5Ge**.

Points	D(1,2,3,4)	RE (KJ/mol)
max1	1.57	19.80
min1	55.77	0.00
max2	120.19	13.33
min2	175.18	0.01
max3	234.65	14.01
min3	297.55	3.04

Chapter References

1. Schally A. V., McCann S. M., *Fertil. Steril.* 1995, *64*, 452 – 453

2. (a) Schally A. V., Arimura A., Kastin A. J., *Science* 1971, *173*, 1036 – 1038, (b) Matsuo H., Baba Y., Nair R. M., Arimura A., Schally A. V., *Biochem. Biophys. Res. Commun.* 1971, *43*, 1334 – 1339, (c) Amoss K., Burgus R., Blackwell R., Vale W., Fellows R., Buillemin R., *ibid.* 1971, *44*, 205 – 210, (d) Baba Y., Matsuo H., Schally A. V., *ibid.* 1971, *44*, 459 – 463

3. Emons G., Schally A. V., *Hum. Reprod.* 1994, *9*, 1364 – 1370

4. Weinbauer G. F., Nieschlag E., *Peptides in Oncology I* (Ed.: K. Höffgen), Springer, Heidelberg, 1992, 113 – 136

5. Kutscher B., Bernd M., Beckers T., Polymeropoulos E. E., Engel J., *Angew. Chem.* 1997, *109*, 2240 – 2254

6. Kutscher B., Bernd M., Beckers T., Polymeropoulos E. E., Engel J., *Angew. Chem. Int. Ed. Engl*. 1997, *36*, 2148 – 2161

7. Reissmann T., Engel J., Kutscher B., Bernd M., Hilgard P., Peukert M., Szelenyi I., RFeichert S., Gonzalez-Barcena D., Nieschlag E., Comaru-Schally A. M., Schally A. V., *Drugs of the Future* 1994, *19*, 228 – 237

8. Ljungqvist A., Feng D. M., Hook W., Shen Z. X., Bowers C., Folkers K., *Proc. Natl. Acad. Sci*. USA 1988, *85*, 8236 – 8240

9. Leal J., Gordon K., Danforth D. R., Williams R. F., Hodgen G. D., *Drugs of the Future* 1991, *16*, 529 -537

10. Janecka A., Janecki T., Shan S. M., Bowers C., Folkers K., *J. Med. Chem.* 1994, *37*, 2238 – 2241

11. Janecka A., Ljungqvist A., Suzuki M., Xu J. C., Bowers C., Folkers K., *Med. Chem. Res.* 1991, *1*, 306 – 311

12. Janecka A., Janecki T., Bowers C., Folkers K., *Int. J. Pept. Protein Res.* 1994, *44*, 19 – 23

13. Giannis A., Kolter T., *Angew. Chem.* 1993, *32*, 1244 – 1267

14. Gante J., *Angew. Chem*. 1994, *106*, 1780 – 1802

15. Kleemann A., Leuchtenberger W., Hoppe B., Tanner H., *In Ullmann's Encyclopedia of Industrial Chemistry;* Gerhartz W., Ed.; VCH: Weinheim, Germany, 1985, 57 – 97

16. Ishida H., Inoue Y., *Rev. Heteroat. Chem*. 1998, *19*, 79 – 142

17. Tacke R., Linoh H., *In the Chemistry of Organic Silicon Compounds*, Part 2, Patai S. Rappoport Z., Eds.; Wiley: chichester, U. K., 1989, 1143 – 1206

18. Lukevics E., Ignatovich L., *Appl. Organomet. Chem.* 1992, *6*, 113 – 126

19. Tacke R., Wagner S. A., *In the Chemistry of Organic Silicon Compounds*, Vol 2, Part 3; Rappoport Z., Apeloig Y., Eds.: Wiley: chichester, U.K., 1998, 2363 – 2400

20. Tacke R., Heinrich T., Kornek T., Merget M., Wagner S. A., GrossJ., Keim C., Lambrecht G., Mutschler E., Beckers T., Bernd M., Reissmann T., *Phosphorus, Sulfur, Silicon*, 1999, *150*, 69 – 87

21. Tacke R., Merget M., Bertermann R., Bernd M., Beckers T., Reissmann T., *Organometallics* 2000, *19*, 3486 – 3497

BIBLIOGRAPHY

Abel E.W., Stone G. A., Wilkinson G., *Comprehensive Organometallic Chemistry II: A review of the literature 1982 -1994*, 1st ed., Oxford ; New York : Pergamon, 1995.

Al-Laham M. A., Raghavachari M., *J. Chem. Phys.* 1991, *95*, 2560.

Amoss K., Burgus R., Blackwell R., Vale W., Fellows R., Buillemin R., 1971, *44*, 205-210.

Andrae D., Haeussermann U., Dolg M., Stoll H., Preuss H., *Theor. Chim. Acta,* 1990, *77*, 123.

Andrae D., Haeussermann U., Dolg M., Stolll H., Preuss H., *Theor. Chim. Acta,* 1990, *77*, 123.

Ansyln E. V., Brusich M. J., Boddard W. A., *Organometallics* 1993, *12*, 1289.

Apeloig Y., Karni M. in *Theoretical Aspects and Quantum Chemical Calculation of Silaaromatic Compounds. The Chemistry of Silicon Compounds, ed*. Z. Pappoport and Y. Apeloig, Wiley, New York, 1998, vol.2.

Baba Y., Matsuo H., Schally A. V., 1971, *44*, 459-463.

Barone V., Adamo C., Lelj F., *J. Chem. Phys.* 1995, *102*, 364.

Barone V., Bencini A., Totti F., Uytterhoeven M. G., *Int. J. Quantum. Chem.* 1997. *61*. 361.

Basis sets were obtained from the extensible Computational Chemistry Environment Basis Set Database, Version 1.0, as developed and distributed by the Molecular Sciences Laboratory, which is part of the Pacific Northwest Laboratory, P.O.Box 999, Richland WA 99352, USA, and funded by the U.S. Department of Energy under contract DE-AC06-76RLO 1830. Contact David Feller, Karen Schuchardt, or Don Jones for additional information.

Bauschlicher C. W. Jr., Langhoff S. R., Barnes L. A., *J. Chem. Phys.* 1989, *91*, 2399.

Bauschlicher C. W., Patriadge H., *J. Chem. Phys.* 1995, *103*, 1788.

Becke A. D., *J. Chem. Phys*. 1993, *98*, 5648.

Becke A. D., *J. Chem. Phys.* 1993, *98*, 5648.

Becke A. D., *J. Chem. Phys.* 1993, *98*, 5648. (b) Lee C., Yang W., Parr R. G., *Phys. Rev.* B 1988, *37*, 785.

Becke A. D., *J. Chem. Phys*. 1993, *98,* 5648.

Becke A. D., *Phys. Rev. A* 1988, *38*, 3098.

Binkley S., *J. Am. Chem. Soc.* 1984, *106*, 603.

Bogey B., Bolvin H., Demuynck C., Destombes J. L., *Phys. Rev. Lett.* 1991, *66*, 413.

Brenda T. C., Schaefer III H. F., *J. Phys. Chem.* 1990, *94*, 5593.

Bogey M., Bolvin H., Cordonnier M., Demuynck C., Destombes J. L., Csaszar A. G., *J. Chem. Phys*. 1994, *100*, 8614.

Boys S. F., *Proc. Roy. Soc. (London)*, 1950, *A200*, 542.

Braterman P. S., *Metal Carbonyl Spectra, Academic Press,* New York, 1975.

Brenda T. C., Schaefer III H. F., *J. Phys. Chem*. 1990, *94*, 5593.

Chiang T., Kerber R. C., Kimball S. D., Lauher J. W., *Inorg. Chem*. 1979, *18*, 1687.

Churchill M. R., Fettinger J. C., McCullough L. G., Schrock P. R., *J. Am. Chem. Soc*. 1984, *106*, 3356.

Codonnier M., Bogey M., Demuynck C., Destombes J. L., *J. Chem. Phys*. 1992, *97*, 6894.

Colegrove B. T., Schaefer III H. F., *J. Chem. Phys*. 1990, *93*, 7230.

Collman J. P., Hegedus L. S., Norton J. R., Finke R. G., *Principles and Applications of Organotransition Metal Chemistry; University Science Books*: Mill Valley, CA, 1987.

Cordonnier M., Bogey M., Demuynck C., Destombes J. L., *J. Chem. Phys*. 1992, *97*, 7984.

Cotton F. A., Wilkinson G., Murillo C. A., Bochmann M., *Advanced Inorganic Chemistry*, 6th ed.; Wiley-Interscience: New York, 1999.

Csazar A. G., Allen W. D., *J. Chem. Phys.* 1994, *100*, 2746.

Cundari T. R., Benson M. T., Lutz M. L. and Sommerer S. O., *Rev. Comput. Chem*. 1996, *8*, 145.

Cundari T. R., Benson M. T., Lutz M. L., Sommerer S. O., in: Lipkowitz K. B., Boyd D. B. (Eds.), *Reviews in Computational Chemistry,* vol 8, VCH, New York, 1996, 145.

Cundari T. R., Stevens W. J., *J. Chem. Phys*. 1993, *98*, 5555.

Curtiss I. A., Raghavachari K., Deutsch P. W., Pople J. A., *J. Chem. Phys*. 1991, *95*, 2433.

Curtiss L. A., Raghavachari K., Trucks G. W., Pople J. A., *J. Chem. Phys.* 1991, *94*, 7221.

Davidson e.R., *Int. J. quantum Chem*. 1998, *69*, 241.

DeFrees D. J., McLean A. D., *J. Chem. Phys.* 1985, *82*, 333.

Denk M., Hayashi R. K., West R., *J. Chem. Soc. Chem. Commun.* 1994, *33.*

Dolg M., Wedi U., Stoll H., Preuss H., *J. Chem. Phys*., 1987, *86*, 866.

Dreizler R.M., Gross E. K. V., Density Functional Theory, Springer, Berlin, 1990.

Drew M. G., Brisdon B. J., Day A., *J. Chem. Soc., Dalton Trans*. 1981, 1310.

Dyall K., *J. Chem. Phys*. 1991, *96*, 1210.

Elschenbroich Ch., Salzer A., *Organometallics*, 2nd ed.,VCH: New York, 1992,

Emons G., Schally A. V., *Hum. Reprod.* 1994, *9*, 1364-1370,

Finley J. W., Stephens P. J., *J. Mol. Struct. (Theochem)* 1995, *357*, 225,

For a detailed analysis on how σ-π mixing stabilizes both π^* and π (which contains six orbital delocalization) orbitals in H-bridged three membered systems, please see: Srinivas G. N. Ph. D. Thesis. University of Hyderabad, India, 1996; Jemmis E. D., Subramanian G., Srinivas G. N., *J. Am. Chem. Soc*. 1992, *114*, 7939

Foresman J. B., *Exploring chemistry with electronic structure methods*, 2nd ed., Gaussian, Inc, 1996.

Foster J. P., Weinhold F., *J. Am. Chem. Soc*. 1980, *102,* 7211-7218.

Frenking G., Antes I., Böhme M., Dapprich S., Ehlers A., W., Jonas V., Neuhaus A., Otto M., Stegmann R., Veldkamp A., Vyboishchikov S. F., in: Lipkowitz K. B., Boyd D. B., et al. (Eds.), *Reviews in Computational Chemistry,* vol 8, VCH, New York, 1996, p. 63.

Frenking G., Antes I., Böhme M., Dapprioh S., Ehlers A. W., Jonas V., Nauhaus A., Otto M., Stegmann R., Veldkamp A., Vyboishchikov S. F., *Rev. Comput. Chem.* 1996*, 8*, 63.

Frisch M. J., Trucks G. W., Schlegel H. B., Scuseria G. E., Robb M. A., Cheeseman J. R., Zakrzewski V. G., Montgomery J. A. Jr., Stratmann R. E., Burant J. C., Dapprich S., Millam J. M., Daniels A. D., Kudin K. N., Strain M. C., Farkas O., Tomasi J., Barone V., Cossi M., Cammi R., Mennucci B., Pomelli C., Adamo C., Clifford S., Ochterski J., Petersson G. A., Ayala P. Y., Cui Q., Morokuma K., Malick D. K., Rabuck A. D., Raghavachari K., Foresman J. B., Cioslowski J.,

Ortiz J. V., Stefanov B. B., Liu G., Liashenko A., Piskorz P., Komaromi I., Gomperts R., Martin R. L., Fox D. J., Keith T., Al-Laham M. A., Peng C. Y., Nanayakkara A., Gonzalez C., Challacombe M., Gill P. M. W., Johnson B. G., Chen W., Wong M. W. Andres J. L., Head-Gordon M., Replogle E. S., Pople, J. A., Gaussian 98, revision A.9; Gaussian, Inc.: Pittsburgh, PA. 1998.

Fujimoto H., Hoffmann R., *J. Phys. Chem*. 1974, *78*, 1167.

Gante J., *Angew. Chem*. 1994, *106*, 1780-1802.

Giannis A., Kolter T., *Angew. Chem.* 1993, *32*, 1244-1267.

Grev R. S., Deleeuw B. J., Schaefer III H. F., *Chem. Phys. Lett*. 1990, *165*, 257.

Grev R. S., Schaefer III H. F., Baines K. M., *J. Am. Chem. Soc.* 1990, *112*, 9458.

Grev R. S., Schaefer III H. F., *J. Chem. Phys*. 1992, *97,* 7990.

Gunnarsson O., Lundquist I., *Phys. Rev*. 1976, *B13,* 4274.

Haaland A., Marinsen K. G., Schlykov S. A., Volden H. V., Dohmeier C., Schnockel H., *Organometallics* 1995, *14*, 3116.

Handy N. C., Amos R. D., Gaw J. F., Rice J. E., Simandiras E. D., *Chem. Phys. Lett.* 1985, *120*, 151.

Harris N. J., *J. Phys. Chem*. 1995, *99*, 14689.

Hay P. J., Wadt W. R., *J. Chem. Phys*. 1985, *82*, 270.

Hay P. J., Wadt W. R., *J. Chem. Phys.* 1985, *82*, 299.

Hay P.J., Wadt W. R., *J. Chem. Phys*. 1982, *77*, 3654.

Healy E. F., Holder A., *J. Mol. Struct.* 1993, *281*, 141.

Hehre W. J., Ditchfield R., Pople J. A., *J. Chem. Phys*. 1972, *56*, 2257.

Hehre W. J., Radom L., Schleyer P. v. R., Pople J. A., *Ab initio Molecular Orbital Theory*; Wiley, New York, 1986, (b) Hehre W. J., Ditchfield R., Pople J. A., *J. Chem. Phys*. 1972, *56*, 2257.

Hehre W. J., Radom L.; Schleyer P. v. R., Pople J. A., *Ab Initio Molecular Orbital Theory*; Wiley: New York, 1986.

Hoffmann R., *Angew. Chem., Int. Ed. Engl.* 1982, *21*, 711.

Hohenberg P., Kohn W., *Phys. Rev*. 1964, *136*, B864.

Hout R. F., Levi B. A., Hehre W. J., *J. Comput. Chem.* 1982, *3*, 234.

Hughes R. P., Tucker D. S., Rheingold A. L., *Organometallics* 1993, *12*, 3069.

Huheey J. E., Keiter E. A., Keiter R. L., *Inorganic Chemistry*, 4th ed.; Harper Collins College: New York, 1993.

Hutter J. Luthi H. P., Diederich F., *J. Am. Chem. Soc.* 1994, *116*, 750.

Ishida H., Inoue Y., *Rev. Heteroat. Chem*. 1998, *19*, 79-142.

Jacobsen H., Ziegler H., *J. Am. Chem. Soc*. 1994, *116*, 3667.

Janecka A., Janecki T., Bowers C., Folkers K., *Int. J. Pept. Protein Res.* 1994, *44*, 19-23.

Janecka A., Janecki T., Shan S. M., Bowers C., Folkers K., *J. Med. Chem.* 1994, *37*, 2238-2241.

Janecka A., Ljungqvist A., Suzuki M., Xu J. C., Bowers C., Folkers K., *Med. Chem. Res.* 1991, *1*, 306-311.

Jemmis E. D., Hoffmann R., *J. Am. Chem. Soc.* 1980, *102*, 2570.

Jemmis E. D., Srinivas G. N., *J. Am. Chem. Soc*. 1996, *118*, 3738.

Jemmis E. D., Srinivas G. N., Leszczynski J., Kapp J., Korkin A. A., Schleyer P. v. R., *J. Am. Chem. Soc*. 1995, *117*, 11361.

Jensen F., *Introduction to Computational Chemistry*, Wiley, 1999.

Jursic B.S., *Theochem*. 1998, *417*, 89.

Kalcher J., Sax A., Olbrich G., *Int. J. Quantum Chem*., 1984, *25*, 543.

Karni M., Apeloig Y., *J. Am. Chem. Soc.* 1990, *112*, 8589.

Kaupp M., Malkina O. L., Malkin V.G., *J. Chem. Phys*. 1997, *106*, 9201.

Kleemann A., Leuchtenberger W., Hoppe B., Tanner H., *In Ullmann's Encyclopedia of Industrial Chemistry;* Gerhartz W., Ed.; VCH: Weinheim, Germany, 1985, 57-97.

Köhler H. J., Lischka H., *Chem. Phys. Lett*. 1984*, 112*, 33.

Kompaneyets A.S., Basic Concepts in Quantum Mechanics, New York, Reinhold Pub. Corp.: 1966.

Korkin A. A., Glukovtsev M., Schleyer P. v. R., *Int. J. Quantum Chem*. 1993, *46*, 137.

Korkin A. A., Murashov V. V., Leszczynski J., Schleyer P. v. R., *J. Mol. Struct. (THEOCHEM)* 1996, *388*, 43.

Koseki S., Gordon M. S., *J. Phys. Chem.* 1989, *93*, 118.

Krogh-Jespersen K., *J. Am. Chem. Soc*. 1985, *107*, 537.

Krogh-Jespersen K., *J. Phys. Chem*. 1982, *86*, 1492.

Kutscher B., Bernd M., Beckers T., Polymeropoulos E. E., Engel J., *Angew. Chem.* 1997, *109*, 2240-2254.

Kutscher B., Bernd M., Beckers T., Polymeropoulos E. E., Engel J., *Angew. Chem. Int. Ed. Engl*. 1997, *36*, 2148-2161.

Leal J., Gordon K., Danforth D. R., Williams R. F., Hodgen G. D., *Drugs of the Future* 1991, *16*, 529 -537.

Lee C., Yang W, Parr R. G., *Phys. Rev. B* 1988, *37*, 785.

Li W-K., Riggs N. V., *J. Mol. Struct. (THEOCHEM),* 1992, *257*, 189.

Lichtenberger D. L., Hoppe M. L., Subramanian L., Kober E. M., Hughes R. P., Hubbard J. L., Tucke D. S., *Organometallics* 1993, *12*, 2025.

Lin Z., Hall M. B., *Organometallics* 1994, *13*, 2878.

Lischka H., Kohler H., *J. Am. Chem. Soc.* 1983, *105*, 6646.

Ljungqvist A., Feng D. M., Hook W., Shen Z. X., Bowers C., Folkers K., *Proc. Natl. Acad. Sci*. USA 1988, *85*, 8236-8240.

López L., Sordo, J. A., Sordo T. L., *J. Chem. Soc. Chem. Commun*. 1993, 1751.

Lukevics E., Ignatovich L., *Appl. Organomet. Chem.* 1992, *6*, 113-126.

Maluendes S. A., Mclean A. D., Yamashita K, Herbst E., *J. Chem. Phys.* 1993, *99*, 2812.

Mandich M. L., Reents W. D. Jr., *J. Chem. Phys*. 1991, *95*, 7360.

Martin J. M. L., *Chem. Phys. Lett.* 1995, *242*, 343.

Martin J. M. L., *J. Chem. Phys.* 1994, *100*, 8186.

Martin J. M. L., Taylor P. R., *Chem. Phys. Lett.* 1994, *225*, 473.

Matsuo H., Baba Y., Nair R. M., Arimura A., Schally A. V., *Biochem. Biophys. Res. Commun.* 1971, *43*, 1334-1339.

Mealli C., Midollini S., Moneti S., Sacconi L., *J. Organomet. Chem.* 1981, *205*, 273.

Mehra J.R., The discovery of Quantum Mechanics. New York: Springer-Verlag, 1982.

Møller C., Plesset M. S., *Phys. Rev*. 1934, *46*, 618.

Nagase S., Kobayashi K., Nagashima M., *J. Chem. Soc*., *Chem. Commun*. 1992, 1302.

Niu S., Hall M. B., *Chem. Rev.* 2000, *100*, 353.

Norman B.C., Lawrence H. D., Stephen E. W., *Introduction to INFRAREd and Raman Spectroscopy, 3ed*., 1990, San Diego, CA.

Nwobi O., Higgins J., Zhou X., Liu R., *Chem. Phys. Lett.* 1997, *272*, 155.

Olbrich G., *Chem. Phys. Lett*. 1986, *130*, 115.

Oliphant N. Bartlett R. J., *J. Chem. Phys*. 1994, *100*, 6550.

Palagyi Z., Schaefer III H. F., Kapuy E., *J. Am. Chem. Soc*. 1993, *115*, 6901.

Parr R. G., Yang W., *Density Functional Theory*, Oxford University Press, 1989.

Perdew J. P., *Phys. Rev. B* 1986, *33*, 8822.

Peterson P. E., Abu-Omar M., Johnson T. W., Parham R., Goldin D., Henry C., Cook A., Dunn K. M., *J. Phys. Chem.* 1995, *99*, 5927.

Please see the special issue on Computational Transition Metal Chemistry, *Chem. Rev*. 2000, *100*, issue 2.

Pople J. A., Head-Gordon M, Fox D. J., Raghavachari K., Curtiss L. A., *J. Chem. Phys.* 1989, *90*, 5622.

Pople J. A., Krishnan R., Schlegel H. B., Bimkley J. S., *Int. J. Quantum Chem. Symp.* 1979, *13*, 225.

Pople J. A., Nesbet R. K., *J. Chem. Phys*. 1959, *22*, 571.

Pople J. A., Raghavachari K., Schlegel H. B., Binkley J. S., *Int. J. Quantum Chem. Symp.* 1979, *13*, 255.

Pople J. A., Schlegel H. B., Krishnan R., Defrees D. J., Binkley J. S., Frisch M. J, Whiteside R. A., Hout R. F., Hehre W. J., *Int. J. Quantum Chem. Symp.* 1981, *15*, 269.

Pople J. A., Scott A. P., Wong M. W., Radom L., *Isr. J. Chem.* 1993, *33*, 345.

Pulay P., *Mol. Phys.* 1969, *17*, 197.

Raghavachari K., *J. Chem. Phys.* 1991, *95*, 7373.

Raghavachari K., *J. Chem. Phys*. 1992, *96*, 4440.

Raghavachari K., Whiteside R. A., Pople J. A. Schleyer P. v. R., *J. Am. Chem. Soc*. 1981, *103*, 5649.

Rauhut G., Pulay P., *J. Am. Chem. Soc*. 1995, *117*, 4167.

Rauhut G., Pulay R., *J. Phys. Chem*. 1995, *99*, 3093.

Rausch M. D., Tuggle R. M., Weaver D. L., *J. Am. Chem. Soc*. 1970, *92*, 4981.

Reed A. E., Curtiss L. A., Weinhold F., *Chem. Rev*. 1988, *88*, 899.

Reed A. E., Curtiss, L. A., Weinhold F., *Chem. Rev*. 1988, 899-926.

Reed A. E., Weinhold F., *F. QCPE Bull*., 1985, *5*, 141.

Reissmann T., Engel J., Kutscher B., Bernd M., Hilgard P., Peukert M., Szelenyi I., R Feichert S., Gonzalez-Barcena D., Nieschlag E., Comaru-Schally A. M., Schally A. V., *Drugs of the Future* 1994, *19*, 228-237.

Ricchards W.G., Ab initio Molecular Orbitall Calculations for Chemists, Oxford: Clarendon Press, 1983.

Robiette A. G., Sheldrick G. M., Simpson R. N. F., Aylett B. J., Campbell J. M., *J. Organomet. Chem*. 1968, *14*, 279.

Robinson W. T., Libers J. A., *Inorg. Chem*. 1967, *6*, 1208.

Roothan C. C. J., *Rev. Mod. Phys*. 1951, *23*, 69.

Schally A. V., Arimura A., Kastin A. J., *Science* 1971, *173*, 1036-1038.

Schally A. V., McCann S. M., *Fertil. Steril.* 1995, *64*, 452-453.

Schleyer P. v. R., Kaupp M., Hampel F., Bermer M., Mislow K., *J. Am. Chem. Soc*. 1992, *114*, 6791.

Schleyer P. v. R., Kost D., *J. Am. Chem. Soc.* 1988, *110,* 2105.

Schmedake T. A., Haaf M., Paradise B. J., Powell D., West R., *Organometallics* 2000, *19*, 3263.

Schrödinger E., *Ann. Physik*, 1926, *79*, 361.

Scott A. P., Radom L., *J. Phys. Chem*. 1996, *100*, 16502.

Shimada S., Rao M. L. N., Hayashi T., Tanaka M., *Angew. Chem., Int. Ed*. 2001, *40*, 213.

Skiguchi A., Tsukamoto M., Ichinohe M., *Science* 1997, *275*, 60.

Slater J.C., *Phys. Rev*. 1930, *36*, 57.

So S. P., *Chem. Phys. Lett.* 1999, *313*, 587.

Srinivas G. N., Hamilton T. P., Jemmis E. D., McKee M. I., Lammertsma K., *J. Am. Chem. Soc*. 2000, *122*, 1725.

Srinivas G. N., Hamilton T. P., Jemmis E. D., McKee M. L., Lammertsma K., *J. Am. Chem. Soc.* 2000, *122*, 1725.

Srinivas G. N., Jemmis E. D., *J. Am. Chem. Soc.* 1997, *119*, 12968.

Srinivas G. N., Jemmis E. D., Korkin A. A., Schleyer P. v. R., *J. Phys. Chem. A*, 1999, *103*, 11034.

Srinivas G. N., Kiran B., Jemmis E. D., *J. Mol. Struct.: THEOCHEM* 1996, *361*, 205.

Srinivas G. N., Yu. L, Schwartz, M., *Organometallics* 2001, 20, 5200.

Stevens W. J., Basch H., Krauss M. M., *Chem. Phys*. 1984, *81*, 6026.

Stevens W. J., Basch H., Krauss M., *J. Chem. Phys*. 1984, *81*, 6026, 612.

Stevens W., Krauss J. M., Basch H., Jasien P.G., *Can. J. Chem*. 1992, *70,* 612.

Stewart G. W., Henis J. M. S., Gaspar P. P., *J. Chem. Phys*. 1973, *58*, 890.

Tacke R., Heinrich T., Kornek T., Merget M., Wagner S. A., GrossJ., Keim C., Lambrecht G., Mutschler E., Beckers T., Bernd M., Reissmann T., *Phosphorus, Sulfur, Silicon*, 1999, *150*, 69-87.

Tacke R., Linoh H., *In the Chemistry of Organic Silicon Compounds*, Part 2, Patai S. Rappoport Z., Eds.; Wiley: Chichester, U. K., 1989, 1143-1206.

Tacke R., Merget M., Bertermann R., Bernd M., Beckers T., Reissmann T., *Organometallics* 2000, *19*, 3486-3497.

Tacke R., Wagner S. A., *In the Chemistry of Organic Silicon Compounds*, Vol 2, Part 3; Rappoport Z., Apeloig Y., Eds.: Wiley: chichester, U.K., 1998, 2363-2400.

Teramae H., *J. Am. Chem. Soc.* 1987, *109*, 4140.

Thomas J. R., Deleeuw B. J., Vacek G., Schaefer H. F., *J. Chem. Phys.* 1993, *98*, 1336.

Thomas J. R., Deleeuw B. J., Veck G., Crawford T. D., Yamaguchi Y., Schaefer H. F., *J. Chem. Phys*. 1993, *99*, 403.

Triniquier G., *J. Am. Chem. Soc.* 1991, *113*, 144.

Trinquier G., Malrieu K., *J. Am. Chem. Soc.* 1991, *113*, 8634.

Tuggle R. M., Weaver D. L., *Inorg. Chem*. 1971, *10*, 1504.

von Barth U., Hedin L., *Phys. Rev.* 1979, *A20*, 1693.

Vosko S. H., Wilk L., Nusair M., *Can. J. Phys.* 1980, *58*, 1200.

Wachters A. J. H., IBM Technol. Rept. RJ584, 1969.

Wachters A. J. H., *J. Chem. Phys*. 1970, *52*, 1033.

Wadt W. R., Hay P. J., *J. Chem. Phys.* 1985, *82*, 284.

We thank the National Computational Science Alliance (NCSA) for allotting the computational time on an SGI/GRAY Origin 2000 supercomputer (Grant No. CHE000018N).

Weinbauer G. F., Nieschlag E., *Peptides in Oncology I* (Ed.: K. Höffgen), Springer, Heidelberg, 1992, 113-136.

Windus T., Gordon M. S., *J. Am. Chem. Soc*. 1992, *114*, 9559.

Wong M. W. and Radom L., *J. Am. Chem. Soc.* 1993, *115*, 1507.

Wong M. W., Rdom L., *J. Am. Chem. Soc.* 1993, *115*, 1507.

Woo T., Folga E., Ziegler T., *Organometallics* 1993, *12*, 1289.

Ziock K., Basic Quantum Mechanics, Wiley: New York, 1969.